

OPTIMISING SHAFT PRESSURE LOSSES THROUGH COMPUTATIONAL FLUID DYNAMIC MODELLING

WILLIAM JAMES KEMPSON

Presented as fulfilment for the degree

PhD (Mining Engineering)

**IN THE FACULTY OF ENGINEERING, BUILT ENVIRONMENT AND INFORMATION
TECHNOLOGY**

DEPARTMENT OF MINING ENGINEERING

UNIVERSITY OF PRETORIA



January 2012



DECLARATION

I hereby declare that this dissertation is my own unaided work. It is being submitted for the degree PhD (Mining Engineering) at the University of Pretoria, Pretoria. It has not been submitted before for any degree or examination in any other University.

A handwritten signature in black ink, appearing to read 'William James Kempson', written over a horizontal line.

William James Kempson

Dated this 5th day of March 2012

UNIVERSITY OF PRETORIA**FACULTY OF ENGINEERING, BUILT ENVIRONMENT AND INFORMATION TECHNOLOGY****DEPARTMENT OF MINING ENGINEERING**

The Department of Mining Engineering places great emphasis upon integrity and ethical conduct in the preparation of all written work submitted for academic evaluation. While academic staff teaches you about systems of referring and how to avoid plagiarism, you too have a responsibility in this regard. If you are at any stage uncertain as to what is required, you should speak to your lecturer before any written work is submitted.

You are guilty of plagiarism if you copy something from a book, article or website without acknowledging the source and pass it off as your own. In effect you are stealing something that belongs to someone else. This is not only the case when you copy work word-by-word (verbatim), but also when you submit someone else's work in a slightly altered form (paraphrase) or use a line of argument without acknowledging it. You are not allowed to use another student's past written work. You are also not allowed to let anybody copy your work with the intention of passing it off as his/her work.

Students who commit plagiarism will lose all credits obtained in the plagiarised work. The matter may also be referred to the Disciplinary Committee (Students) for a ruling. Plagiarism is regarded as a serious contravention of the University's rules and can lead to expulsion from the University. The declaration which follows must be appended to all written work submitted while you are a student of the Department of Mining Engineering. No written work will be accepted unless the declaration has been completed and attached.

I (full names) William James Kempson

Student number 24552242

Topic of work Optimising Shaft Pressure Losses Through Computational Fluid Dynamic Modelling

Declaration

I understand what plagiarism is and am aware of the University's policy in this regard.

I declare that this dissertation is my own original work. Where other people's work has been used (either from a printed source, internet or any other source), this has been properly acknowledged and referenced in accordance with departmental requirements.

I have not used another student's past written work to hand in as my own.

I have not allowed, and will not allow, anyone to copy my work with the intention of passing it off as his or her own work.

Signature





LANGUAGE EDIT

I, Beverlie Margaret Davies, Member of the Professional Editors' Group, hereby declare that I performed an English language edit on the final version of this project report.

A handwritten signature in black ink, appearing to read 'Bm Davies'.

6 March 2012

Signature

Date

ABSTRACT

Optimising Shaft Pressure Losses Through Computational Fluid Dynamic Modelling

WJ Kempson

Supervisor: Professor R.C.W. Webber-Youngman
Co-Supervisor: Professor Josua P Meyer
Department: Mining Engineering
University: University of Pretoria
Degree: PhD (Mining Engineering)

As a result of the rising electrical energy costs in South Africa, a method was sought to reduce the overall electrical consumption of typical shaft systems. A typical shaft configuration was analysed and the primary energy consumers were identified. The ventilation fans for this system were found to consume a total of 15% of the total energy of the shaft system. It was calculated that more than 50% of this energy is consumed by the shaft itself, more specifically by the pressure losses that occur in the shaft as the ventilation air passes through it.

It was recognised that there was therefore an opportunity to achieve an energy savings and therefore a costs savings in the total cost of operating a shaft system by reducing the overall resistance of the equipped downcast shaft. However, before any work could continue in this regard, the results noted above required validation. This was achieved through the comprehensive evaluation of the Impala #14 Shaft system. This system was tested and the pressure losses noted in the calculations were verified.

In order to ensure that the theory being used was accurate, the next step was to evaluate a number of shafts both from a theoretical perspective by measuring the real shaft pressure losses against time. This was done and a total of five shafts were instrumented and the actual pressure losses over the shaft plotted against time. These shafts were then subjected to a theoretical evaluation using the theory as described by McPherson in 1987.

Finally, in order to ensure a thorough understanding of the behaviour of the ventilation air in shaft systems, the systems were simulated using computational fluid dynamic (CFD) techniques.

On the whole there was not a good correlation between the tests and either the theoretical calculations or the

CFD simulations. This was attributed to the general imperfections in the shaft and the difficulty in obtaining exact values for the drag coefficients of the buntons. These differences highlight the difficulty in modelling the non-homogenous physical environment and providing a factor that can be used to ensure that the theoretical designs are aligned with the physical reality. This factor is approximately 30%.

There were also significant discrepancies between the theoretical analysis and the CFD simulation during the initial comparisons. This discrepancy reduced as the complexity of the CFD models increased, until, when the complete shaft was modelled using the full buntons sets, the pipes and the flanges, the difference between the theoretical evaluation and the CFD simulation was small.

This result demonstrates that the theory is insufficient and that the inter-related effect of the buntons and fittings has not been fully appreciated. The current theory however has been developed using drag coefficients and interference factors for the buntons sets which have been taken from measurements of similar configurations. This does account for the relative accuracy of the current theory in that there is little difference between the CFD result and that of the theory. However, as the shaft parameters are changed to reflect new layouts and scenarios, it is unlikely that theory will continue to prove accurate.

The final phase of the work presented here was to evaluate the cost-effectiveness of using different bunton shapes and shaft configurations. It is shown that:

- The increase in the pressure losses and therefore the direct operating costs of the shaft can vary by as much as 80%, depending on the bunton configuration chosen.
- The placement of the piping in the shaft can increase the pressure losses and therefore the direct operating costs of the shaft by as much as 12%, depending on the placement of the piping in the shaft; this effect includes the use of flanges.
- The use of fairings on a large cage can reduce the resistance that the cage offers to the ventilation flow by as much as 30%. This, however, does not translate into a direct saving because as the cage moves through the shaft, the overall effect is transitory.

The savings discussed above can be significant when the items highlighted in this work are applied correctly.



ACKNOWLEDGEMENTS

I wish to express my appreciation to the following organisations which made this project report possible:

Impala Platinum for the allowing me access to the various shafts to complete the testing phase of this work.

Hatch for the financial assistance in the completion of this work.

The following people are gratefully acknowledged for their assistance during the course of the study:

James Janse van Rensburg

Lister Sinclair

Karel Rossouw

Professor R.W.C. Webber-Youngman, my supervisor, and Professor Josua P. Meyer, my co-supervisor, for their guidance and support.



TABLE OF CONTENTS

ABSTRACT	V
ACKNOWLEDGEMENTS.....	VII
TABLE OF CONTENTS	VIII
LIST OF FIGURES	XIV
LIST OF TABLES.....	XVI
LIST OF SYMBOLS AND ABBREVIATIONS.....	XVII
CHAPTER 1 INTRODUCTION.....	1
1.1 OVERVIEW	1
1.2 RELEVANCE OF THE MINING INDUSTRY	1
1.3 ELECTRICAL ENERGY SUPPLY.....	3
1.3.1 Increases in Energy Costs	6
1.3.1 General Discussion	7
1.4 EVALUATION OF ENERGY CONSUMPTION IN DEEP-LEVEL MINES.....	8
1.4.1 General Parameters	8
1.4.2 Initial Evaluation.....	8
1.4.2.1 Winding maximum power requirement	10
1.4.2.2 Compressed air	11
1.4.2.3 In-stope rock handling.....	12
1.4.2.4 Pumping requirement	12
1.4.3 Evaluation of Ventilation and Refrigeration.....	13
1.4.3.1 Demand side management.....	14
1.4.3.2 General remarks	14
1.4.4 Calculation and Verification Data.....	16
1.4.4.1 Verification of the shaft pressure losses identified	17
1.5 PROJECT BACKGROUND.....	22
1.5.1 Evaluation of Costs Associated with the Sinking, Equipping and Operation of Shafts.....	22
1.5.2 Components Contributing to the Present Shaft Resistance and Subsequent Pressure Losses.....	25
1.5.2.1 Parameters used for designing a shaft	25
1.5.2.2 Shaft configuration and analysis techniques	26
1.5.3 Justification of Additional Work	27
1.6 PROBLEM STATEMENT AND PURPOSE OF STUDY.....	28
1.7 OBJECTIVES.....	29



1.7.1	Literature Study.....	29
1.7.2	Evaluation of Current Shaft Configurations	29
1.7.3	Detailed Analysis	30
1.7.4	Installation, Maintenance and Costing.....	30
1.7.5	Conclusions	30
1.8	METHODOLOGY	31
1.8.1	Literature Study.....	31
1.8.2	Evaluation of Current Shaft Configurations	31
1.8.3	Detailed Analysis	31
1.8.4	Conclusions	32
1.8.5	Outline of the Study	32
1.9	SUMMARY AND CONCLUSIONS – CHAPTER 1	32
1.9.1	Summary	32
1.9.2	Conclusions	33
CHAPTER 2	LITERATURE STUDY	34
2.1	INTRODUCTION	34
2.2	MEASUREMENT	34
2.2.1	Efficacy of the Use of Scale Models	35
2.2.2	Measured Data Discussions, Results and Conclusions.....	36
2.2.3	Significance of Available Data	48
2.2.4	Methods of Testing Shaft Pressures.....	49
2.3	DESIGN CONSIDERATIONS	52
2.3.2	General Discussion	53
2.3.3	Significance of Available Data	59
2.4	COMPUTATIONAL FLUID DYNAMICS.....	59
2.4.1	General Discussion	60
2.4.2	Significance of Available Data	62
2.5	SUMMARY AND CONCLUSIONS – CHAPTER 2	62
2.5.1	Measurement.....	62
2.5.2	Design.....	63
2.5.3	CFD	64
CHAPTER 3	METHOD OF EXPERIMENTATION AND ANALYSIS.....	65
3.1	INTRODUCTION	65
3.2	THEORY FOR ANALYSIS OF SHAFT RESISTANCES	65
3.2.1	Static Resistance of Shafts.....	65
3.2.1.1	Chezy-Darcy friction factor	66



3.2.1.2	Atkinson calculations.....	67
3.2.1.3	Rational resistance	69
3.2.2	Shaft Friction Resistance	70
3.2.2.1	Friction resistance of shaft	71
3.2.2.2	Resistance offered by shaft fittings	71
3.2.2.3	Resistance offered by shaft cages	75
3.2.3	Accuracy Limits of the Theory	79
3.2.3.1	Accuracy of calculation for friction resistance of shaft.....	79
3.2.3.2	Accuracy of calculation for resistance offered by shaft fittings.....	79
3.2.3.3	Accuracy of calculation for resistance offered by shaft cages.....	80
3.2.3.4	General comments on the accuracy of the theory	80
3.3	VALIDATION OF EXISTING THEORY AND INITIAL SHAFT TESTS.....	80
3.3.1	Test Methodology	81
3.4	TESTS USED TO VALIDATE THEORY.....	82
3.4.1	Test Methodology	82
3.4.1.1	Main downcast shaft test procedure.....	82
3.4.1.2	Test procedure in the rest of the mine shafts	83
3.4.1.3	Accuracy and repeatability of test data.....	85
3.4.1.4	Ideal test methodology.....	86
3.4.2	Results of Tests.....	86
3.4.3	Conclusion and Recommendations.....	88
3.4.4	Innovative Testing Methodology	88
3.5	TESTS CONDUCTED ON SHAFTS	89
3.5.1	Equipment Used.....	89
3.5.1.1	Environmental instrumentation	89
3.5.1.2	Winder measurements.....	91
3.5.1.3	Velocity measurements.....	94
3.5.2	Data Collection and Collation.....	94
3.5.2.1	Data collection.....	94
3.5.2.2	Data collation	95
3.5.3	Results and Conclusion.....	96
3.5.4	Accuracy of Data Collation Instrumentation	96
3.6	COMPUTATIONAL FLUID DYNAMICS.....	99
3.6.1	Mesh Generation	99
3.6.2	Fluid Model Selection.....	101
3.6.3	Boundary Conditions.....	102
3.6.4	Simulation Runs.....	102
3.6.5	Simulations Completed for this Analysis.....	102
3.6.5.1	T01 – Shaft barrel pressure losses	102



3.6.5.2	T02 – Shaft barrel and one buntion across the shaft.....	102
3.6.5.3	T03 – Shaft barrel and two buntions across the shaft.....	103
3.6.5.4	T04 – Shaft barrel and full buntions set	103
3.6.5.5	T05 – Shaft barrel and pipes at pipe diameter	103
3.6.5.6	T06 – Shaft barrel and pipes at flange diameter	103
3.6.5.7	T07 – Shaft barrel and pipe including flanges.....	103
3.6.5.8	T08 – Shaft barrel and buntions and pipes at pipe diameter	103
3.6.5.9	T09 – Shaft barrel and buntions and pipes at flange diameter	104
3.6.5.10	T10 – Shaft barrel and buntions and pipe including flanges	104
3.6.5.11	T11 – Shaft barrel and buntions and pipe including flanges and skip 1	104
3.6.5.12	T12 – Shaft barrel and buntions and pipe including flanges and skip 2	104
3.6.5.13	T13 – Shaft barrel and buntions and pipe including flanges and man cage 1	104
3.6.5.14	T14 – Shaft barrel and buntions and pipe including flanges and man cage 2	104
3.6.5.15	T15 – Shaft barrel and buntions and pipe including flanges and service cage.....	104
3.7	ECONOMICS.....	105
3.7.1	Shaft Modifications	105
3.7.2	Shaft Equipping	105
3.7.3	Shaft Conveyances	105
3.7.4	Operating Costs.....	106
3.8	SUMMARY OF METHOD OF EXPERIMENTATION AND ANALYSIS	106
CHAPTER 4	RESULTS AND EVALUATION OF SHAFT TESTS	108
4.1	RESULTS OF SHAFT TESTS.....	108
4.1.1	Tests on No. 14 shaft.....	108
4.1.1.1	Shaft details and installation of equipment.....	108
4.1.1.2	Environmental loggers.....	110
4.1.1.3	Rotary encoders	110
4.1.1.4	Summary of data from tests on No. 14 shaft.....	110
4.1.2	Tests on No. 11 shaft.....	113
4.1.2.1	Shaft details and installation of equipment.....	113
4.1.2.2	Environmental loggers.....	114
4.1.2.3	Rotary encoder	115
4.1.2.4	Summary of data from tests on No. 11 shaft.....	115
4.1.3	Tests on No. 1 shaft.....	116
4.1.3.1	Shaft details and installation of equipment.....	116
4.1.3.2	Environmental loggers.....	118
4.1.3.3	Rotary encoder	118
4.1.3.4	Summary of data from tests on No. 1 shaft.....	119
4.1.4	Tests on No. 11C shaft.....	121
4.1.4.1	Shaft details and installation of equipment.....	121

4.1.4.2	Environmental loggers.....	122
4.1.4.3	Rotary encoder	122
4.1.4.4	Summary of data from tests on No. 11c shaft.....	123
4.1.5	Tests on No. 12N shaft	124
4.1.5.1	Shaft details and installation of equipment.....	124
4.1.5.2	Environmental loggers.....	126
4.1.5.3	Rotary encoder	127
4.1.5.4	Summary of data from tests on No. 12N shaft.....	127
4.2	SUMMARY OF AND CONCLUSIONS FROM THE SHAFT TEST RESULTS	128
4.2.1	Accuracy of the Results	128
4.2.2	Summary of the Various Shaft Tests	129
4.2.2.1	Summary of results from the No. 14 shaft tests.....	129
4.2.2.2	Summary of results from the No. 11 shaft tests.....	130
4.2.2.3	Summary of results from the No. 1 shaft tests.....	130
4.2.2.4	Summary of results from No. 11C shaft	131
4.2.2.5	Summary of results from No. 12N shaft	131
4.2.3	Summary and Conclusions from the Shaft Test Results.....	131
4.2.3.1	Accuracy of the data.....	131
4.2.4	Conveyances Moving in the Shaft	133
4.2.5	Conclusions from the Results and Evaluation of Shaft Tests	134
CHAPTER 5	RESULTS AND EVALUATION OF CFD ANALYSIS	136
5.1	RESULTS OF CFD ANALYSIS	136
5.1.1	CFD Simulation No. 1 (Shaft Barrel)	136
5.1.2	CFD Simulations Nos T02, T03 and T04.....	138
5.1.3	CFD Simulation Nos T05, T06 and T07	142
5.1.4	CFD Simulations Nos T08, T09 and T10.....	146
5.1.5	CFD Simulations Nos T11, T12, T13, T14 and T15	150
5.2	SUMMARY AND CONCLUSIONS FROM THE CFD SIMULATION RESULTS	154
5.2.1	Conclusions from the CFD Simulation Results.....	157
CHAPTER 6	COLLATION OF ALL RESULTS	158
6.1	GENERAL	158
6.2	SUMMARY AND CONCLUSIONS.....	161
CHAPTER 7	ECONOMIC EVALUATION OF SHAFT OPTIONS.....	162
7.1	SUMMARY OF OPTIONS.....	162
7.2	SUMMARY OF RESULTS.....	164
7.2.1	Bunton Shapes	164



7.2.2	Piping Arrangements.....	165
7.2.3	Coefficient of Fill and Cage Configurations	166
7.3	SUMMARY AND CONCLUSIONS	167
CHAPTER 8	SUMMARY, CONCLUSIONS AND RECOMMENDATIONS	168
8.1	SUMMARY	168
8.2	CONCLUSIONS	170
8.2.1	Conclusions from Perusal of the Test Data	170
8.2.2	General Conclusions from the Analysis.....	171
8.2.3	Conclusions from the Economic Evaluation	174
8.2.3.1	Buntons	174
8.2.3.2	Pipes	174
8.2.3.3	Cages	174
8.3	SUGGESTIONS FOR FURTHER WORK.....	175
CHAPTER 9	REFERENCES.....	176
APPENDICES	183
	APPENDIX A: CALCULATIONS FOR THE 'MODEL' MINE.....	184
	APPENDIX B: INITIAL TEST METHODOLOGIES	185
	APPENDIX C: VERIFICATION OF RESULTS OF THE QUOTED PAPERS	186
	APPENDIX D: RESULTS OF TESTS FOR 14 SHAFT	187
	APPENDIX E: RESULTS OF TESTS FOR 11 SHAFT	188
	APPENDIX F: RESULTS OF TESTS FOR 11C SHAFT.....	189
	APPENDIX G: RESULTS OF TESTS FOR 1 SHAFT	190
	APPENDIX H: RESULTS OF TESTS FOR 12N SHAFT.....	191

LIST OF FIGURES

Figure 1-1:	Summary of overall mineral sales contribution in South Africa (Statistics South Africa, 2011a)...	2
Figure 1-2:	Total quantity of electricity available for distribution in South Africa (Statistics South Africa, 2011b)	4
Figure 1-3:	Comparison of annual percentage change in available electricity and GDP (Statistics South Africa, 2011c)	5
Figure 1-4:	Consequence of increases with respect to operating costs.....	7
Figure 1-5:	Summary of mine installed electrical energy consumption requirements	9
Figure 1-6:	Summary of mine installed electrical energy consumption requirements (as % total installed consumption capacity).....	9
Figure 1-7:	Typical winder cycle	11
Figure 1-8:	Schematic of ventilation layout.....	16
Figure 1-9:	Schematic of mine shafts tested	18
Figure 1-10:	Configuration of No. 14B downcast shaft bottom	21
Figure 1-11:	Estimated cost of shaft sinking per linear metre	23
Figure 1-12:	Shaft decision cost criteria	24
Figure 2-1:	Chezy-Darcy friction factors for Harmony No. 2 and No. 3 shaft scale model tests	39
Figure 3-1:	Conveyance shock loss estimation for conveyances.....	77
Figure 3-2:	Pitot tube attachment bracket on rope above cage	84
Figure 3-3:	Pitot tube attachment bracket (above cage)	84
Figure 3-4:	Testing instrumentation – Pitot tube, barometer and whirling hygrometer	85
Figure 3-5:	EASYLog 80CL	91
Figure 3-6:	PLC, interface and GSM module for rotary encoder	92
Figure 3-7:	Rotary encoder.....	93
Figure 3-8:	Rotary encoder connection on winder side shaft	93
Figure 3-9:	Kestrel 4000 environmental logger.....	94
Figure 3-10:	Typical graph of collated results (including environmental data and winder data).....	96
Figure 3-11:	Schematic of meshed shaft arrangement	101
Figure 4-1:	Cross-section of No. 14 shaft	109
Figure 4-2:	Cross-section of No. 11 shaft	114
Figure 4-3:	Cross-section of No. 1 shaft	118
Figure 4-4:	Cross-section of No. 11C shaft	122
Figure 4-5:	Cross-section of No. 12N shaft.....	126
Figure 5-1:	Velocity profiles for simulation T01 – Shaft barrel pressure losses	137
Figure 5-2:	Velocity profiles for simulations T02, T03 and T04	141
Figure 5-3:	Velocity profiles for simulations 5, 6 and 7	145

Figure 5-4: Velocity profiles for simulations 8, 9 and 10..... 149

Figure 5-5: Velocity profiles for simulations 11, 12, 13, 14 and 15 154

Figure 5-6: Velocity profiles for simulations T04, T07 and T10 156

Figure 7-1: Typical cross-section 163

LIST OF TABLES

Table 1-1:	Summary of ventilation power requirements for mine analysed	17
Table 1-2:	Summary of ventilation pressure losses	19
Table 2-1:	No. 2 shaft (7.92 m (26 ft) diameter)	37
Table 2-2:	Pioneer shaft bunton shape changes	41
Table 2-3:	Tests on downcast shafts	45
Table 3-1:	Summary of drag coefficients of elongated bodies of infinite span (McPherson, 1987)	73
Table 3-2:	Impala No. 14 shaft – details of tested shafts	87
Table 3-3:	EASYlog 80CL specifications	90
Table 3-4:	Evaluation of Accuracy of Temperature Measurements on the Overall Results	97
Table 3-5:	Evaluation of Accuracy of Pressure Measurements on the Overall Results Typical)	98
Table 3-6:	Evaluation of Accuracy of the Velocity Measurements on the Overall Results Typical)	98
Table 3-4:	Mesh refinement evaluation	100
Table 4-1:	No. 14 shaft test results – Data	111
Table 4-2:	No. 14 shaft test results – Service cage	111
Table 4-3:	No. 14 shaft test results – Rock skip	112
Table 4-4:	No. 14 shaft test results – Man cage	112
Table 4-5:	No. 11 shaft test results – Data	115
Table 4-6:	No. 11 shaft test results	116
Table 4-7:	No. 1 shaft test results – Data	120
Table 4-8:	No. 1 shaft test results	120
Table 4-9:	No. 11C shaft test results – Data	123
Table 4-10:	No. 11C shaft test results	124
Table 4-11:	No. 12N shaft test results – Data	127
Table 4-12:	No. 12N shaft test results	128
Table 4-13:	Summary of shaft test results	132
Table 5-1:	CFD simulation No. T01 – Shaft barrel pressure losses	136
Table 5-2:	CFD simulations Nos T02, T03 and T04	138
Table 5-3:	CFD simulations Nos 5, 6 and 7	142
Table 5-4:	CFD simulations Nos 8, 9 and 10	146
Table 5-5:	CFD simulations Nos 11, 12, 13, 14 and 15 T15	150
Table 6-1:	CFD simulation No. T10 – Shaft barrel and buntons and pipes including flanges	158
Table 6-2:	CFD simulations Nos T11, T12, T13, T14 and T15	159
Table 7-1:	CFD simulation for piping placement	164
Table 7-2:	CFD simulation for piping arrangements	165
Table 7-3:	CFD simulation for varying cage fill factors	166

LIST OF SYMBOLS AND ABBREVIATIONS

μ	kg/(ms)	lb.s/ft ²	slugs/fts	Absolute/dynamic viscosity of air
A_{B1}	m ²	ft ²		Frontal area of buntons
A_{B2}	m ²	ft ²		Frontal area of secondary buntons
A_{B3}	m ²	ft ²		Frontal area of tertiary buntons
A_{BF}	m ²	ft ²		Total frontal area of all buntons
$A_{CS\text{ Shaft}}$	m ²	ft ²		Cross -sectional area of shaft
A_{FS}	m ²	ft ²		Free cross-sectional area of shaft
A_{Conv}	m ²	ft ²		Frontal cross-sectional area of the conveyance
BC	m			Below collar
BIC	-			Bushveld Igneous Complex
BS	m	ft		Spacing between buntons
C_D	-			Coefficient of drag
C_{D1}	-			Coefficient of drag for the primary buntons
C_{D2}	-			Coefficient of drag for the secondary buntons
C_{D3}	-			Coefficient of drag for the tertiary buntons
C_{DF}				Final coefficient of drag, average on total frontal area contribution
C_f	-			Coefficient of fill
c_p	J/(kgK)			Specific heat at constant pressure
CPI	-			Consumer Price Index
DN	-			Diameter nominal (of pipe)



DSM	-		Demand side management
$E_{l(\text{meas})}$	J/kg		Energy loss (based on measured data)
f	-		Chezy-Darcy Friction factor
f_{B1}			Chezy-Darcy Frictional resistance of the bunton set 1 (primary bun tons set)
f_{B2}			Chezy-Darcy Frictional resistance of the bunton set 2 (secondary bunton set)
f_{B3}			Chezy-Darcy Frictional resistance of the bunton set 3 (tertiary bunton set)
$f_{B\text{Total}}$			Chezy-Darcy Overall frictional resistance of the bunton sets
f_{Shaft}			Chezy-Darcy Friction factor of the shaft
f_{Total}			Chezy-Darcy Total friction factor of the shaft
G	kg/s		Mass flow rate
g	m/s^2		Gravitational constant
GDP	-		Gross Domestic Product
H	m		Height
h_{ai}	J/kg		Enthalpy of dry air (inlet)
h_{ao}	J/kg		Enthalpy of dry air (outlet)
h'_{wi}	J/kg		Enthalpy of water vapour
h'_{wl}	J/kg		Enthalpy of liquid water
h'_{wo}	J/kg		Enthalpy of water vapour
k	kg/m^3	Ns^2/m^4	Atkinson friction factor



$k_{\text{Buntons Total}}$	kg/m^3	Ns^2/m^4		Total Atkinson friction factor of buntons
KIC	-			Key Industry Consumer
k_{shaft}	kg/m^3	Ns^2/m^4		Atkinson friction factor for shaft
k_{Total}	kg/m^3	Ns^2/m^4		Atkinson friction factor for total shaft
ktpm	tonnes			Thousands of Kilotonnes per month
L_{B1}	m	ft		Length of the primary buntion support
L_{B2}	m	ft		Length of the secondary buntion support
L_{B3}	m	ft		Length of the tertiary buntion support
L_{s}	m	ft		Length of shaft
P	Pa	Bar (mm Hg)	in. WG	Pressure
P_{ws}	Pa			Saturated vapour pressure
P_{Bar}	Pa			Barometric pressure
P_{FS}	m	ft		Resultant perimeter of shaft (from free cross-section)
PGM	-			Platinum Group Metals
$P_{\text{L (Atkinson)}}$	Pa			Pressure loss calculated in accordance with Atkinson friction factor
$P_{\text{L (Darcy)}}$	Pa			Pressure loss calculated in accordance with Darcy-Weisbach formula using the Chezy-Darcy friction factor
$P_{\text{L (meas)}}$	Pa			Measured pressure loss
$P_{\text{L (Rational)}}$	Pa			Pressure loss calculated in accordance with rational theory
P_{SC}	Pa			Pressure loss as a result of the stationary cage

P_{MC}	Pa		Pressure loss as a result of a moving cage
$P_{MC (Max)}$	Pa		Maximum pressure loss of a moving cage (moving against airflow)
$P_{MC (Max)}$	Pa		maximum pressure loss of a moving cage (moving with airflow)
Power	W		Measurement of power
Per	m	ft	Perimeter of shaft
P_{Static}	Pa		Static pressure
P_{Tot}	Pa		Total pressure
P_w	Pa		Vapour pressure
Q_F	m^3/s		Volumetric flow rate
R	J/(kgK)		Rydberg constant
r	kg_{water}/kg_{air}	g/lb	Moisture content
r_0	kg_{water}/kg_{air}		Moisture content of saturated air at t_{wb}
SD	m	ft	Shaft diameter
SD_{FS}	m	ft	Resultant diameter of shaft (from free cross-section)
T	°C	°F	Temperature
T_{DB}	°C	°F	Dry bulb temperature
T_{WB}	°C	°F	Wet bulb temperature
U	m/s	Fpm	Velocity of air in the shaft
V	m/s		Velocity
V_{FS}	m/s		Ventilation air flow in free area of shaft
V_p	Pa		Velocity pressure



VRT	°C	Virgin rock temperature		
V_{Conv}	m/s	Velocity of moving conveyance		
W	m	Width		
w_1	m	inches	Average width of the main buntions	
w_{b2}	m	inches	Average width of the secondary buntions	
w_{b3}	m	inches	Average width of the tertiary buntions	
w_{bf}	m	inches	Average width of all buntions (from total frontal area)	
WWB	-	West Wits Basin		
ΔP	Pa	Pressure difference		
$\Delta P/m$		Pressure difference per metre of shaft length		
ϵ	m	Roughness (shaft wall)		
λ	-	Frictional resistance in shaft		
ν	m^2/s	Kinematic viscosity		
ρ	kg/m^3	lb/ft^3	$slugs/ft^3$	Density
Γ_{B1}		Rational resistance of buntion set 1		
Γ_{B2}		Rational resistance of buntion set 2		
Γ_{B3}		Rational resistance of buntion set 3		
Γ_{BTotal}		Overall rational resistance of buntions		
Γ_{Shaft}		Rational resistance of shaft		
Γ_{Conv}		Rational resistance of conveyance		
Γ_{Total}		Calculated total rational resistance		

CHAPTER 1

INTRODUCTION

1.1 OVERVIEW

This chapter highlights the importance of the mining industry to South Africa and introduces the challenges facing the industry with respect to the energy it consumes. Once these parameters have been defined, the problem statement and purpose of the study are given, after which the methodology used is presented. Lastly, an outline of the study in terms of the chapter content is given.

1.2 RELEVANCE OF THE MINING INDUSTRY

The mining industry is one of the mainstays of the South African economy. This is borne out by the figures quoted by the Chamber of Mines of South Africa's Annual Report (2009–2010) (Chamber of Mines, 2010), which contains the latest data available. The information quoted below illustrates the loss to the South African economy if the mining sector were to be 'removed' from the economy.

If mining were temporarily removed from the South African economy, the economy would lose:

- 19% of GDP (8.8% directly)
- In excess of 50% of merchandise exports (primary and beneficiated exports)
- 1 million jobs
- 18% of gross investment (10% of direct investment)
- Approximately 30% of capital inflows into the economy (via the financial account of the balance of payments)
- 33% of the market capitalisation of the Johannesburg Stock Exchange
- 93% of the country's electrical generating capacity
- 30% of the country's liquid fuel supply
- 20% of direct corporate tax receipts

South Africa has a wide assortment of minerals available for exploitation. These resources have been effectively exploited and this has given rise to the dominant position in which mining finds itself in the South African economy. This exploitation has been facilitated by the relative accessibility of these minerals.

Historically, one of the most important commodities mined in South Africa has been gold. This has recently been matched and exceeded by the resurgence of platinum and the majority of more recent capital investments have been in this, the platinum sector. The importance of these two sectors is shown by the figures published by Statistics South Africa in their report of 2011 (2011a). These figures have been summarised in Figure 1-1.

It can be seen from these figures that the Platinum Group Metals (PGMs) earn the most revenue. The next highest revenue-generating mineral is coal, closely followed by gold. Coal, however, is not evaluated here as these mines tend to be very shallow by comparison and employ mining methods that are substantially different from the hard rock mining methods use in the platinum and gold mines.

The data represented in Figure 1-1 summarise the total value of mineral sales according to mining divisions, mineral groups and minerals. These data are collated by the Minerals Bureau and cover all mining establishments operating in the South African economy (Statistics South Africa, 2011a).

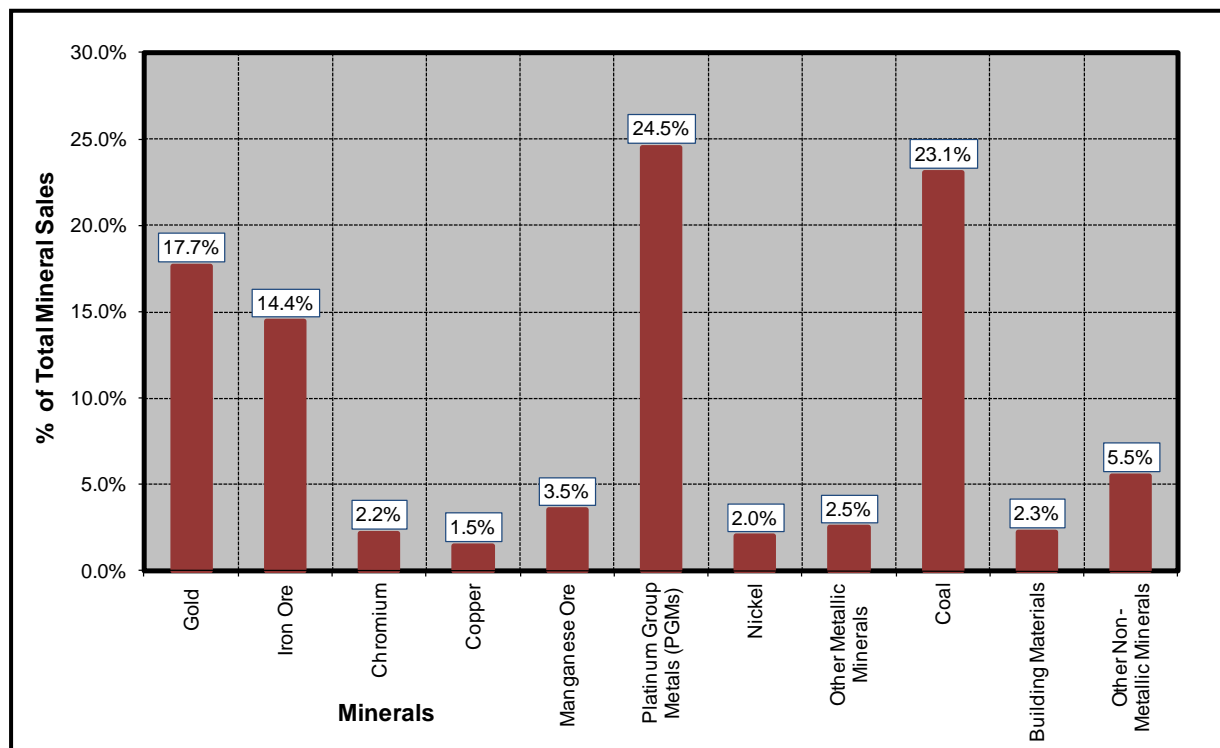


Figure 1-1: Summary of overall mineral sales contribution in South Africa (Statistics South Africa, 2011a)

As a result of the figures shown in Figure 1-1, the emphasis in this thesis is placed on relatively deep mines as are found in the platinum and gold industries. Both of these minerals are generally mined from depth, with both the platinum and gold mining industries having to go deeper in order to access additional reserves. It should, however, be noted that, generally speaking, the mines

developed for gold mining are deeper (maximum depth is in excess of 4 000 m) than those for platinum mining (maximum depth in excess of 2 000 m). Both of these industries face similar challenges primarily as a result of the differences in the geothermal gradients found in the regions in which these minerals are mined.

Relatively deep-level platinum mines in South Africa are found in the Bushveld Igneous Complex (BIC). This region has some unique geophysical properties, one of which is that the temperature gradient increase with depth is approximately twice as severe as in the West Wits Basin (WWB), where the deep-level gold mines are generally situated. The geothermal gradient of platinum mines in the BIC is typically 2.2°C per 100 m (Hustrulid and Bullock, 2001), which is more than double the typical gradient of 1.1 °C per 100 m (Hartman et al., 1997) found in gold mines in the WWB.

This poses some challenges with respect to heat dissipation within mines: the virgin rock temperature (VRT) of 40 °C is realised at a depth of 650 m in the BIC, as opposed to a depth of 1 800 m in the WWB (Biffi et al., 2006). This difference must be borne in mind when discussing or comparing deep-level platinum mines with their gold counterparts.

1.3 ELECTRICAL ENERGY SUPPLY

The mining industry in South Africa faces particular challenges at present, primarily in the area of electrical energy consumption. During 2007, South Africans faced increasingly stringent load shedding of the electrical supply. In January 2008 Eskom took the unprecedented step of informing its key industry consumers (KICs) that it could no longer guarantee its supply to them. This announcement resulted in the temporary closure of all the deep-level mines associated with the large mining houses (i.e. Anglo American, Gold Fields, etc.) as a result of safety concerns if the power did indeed fail.

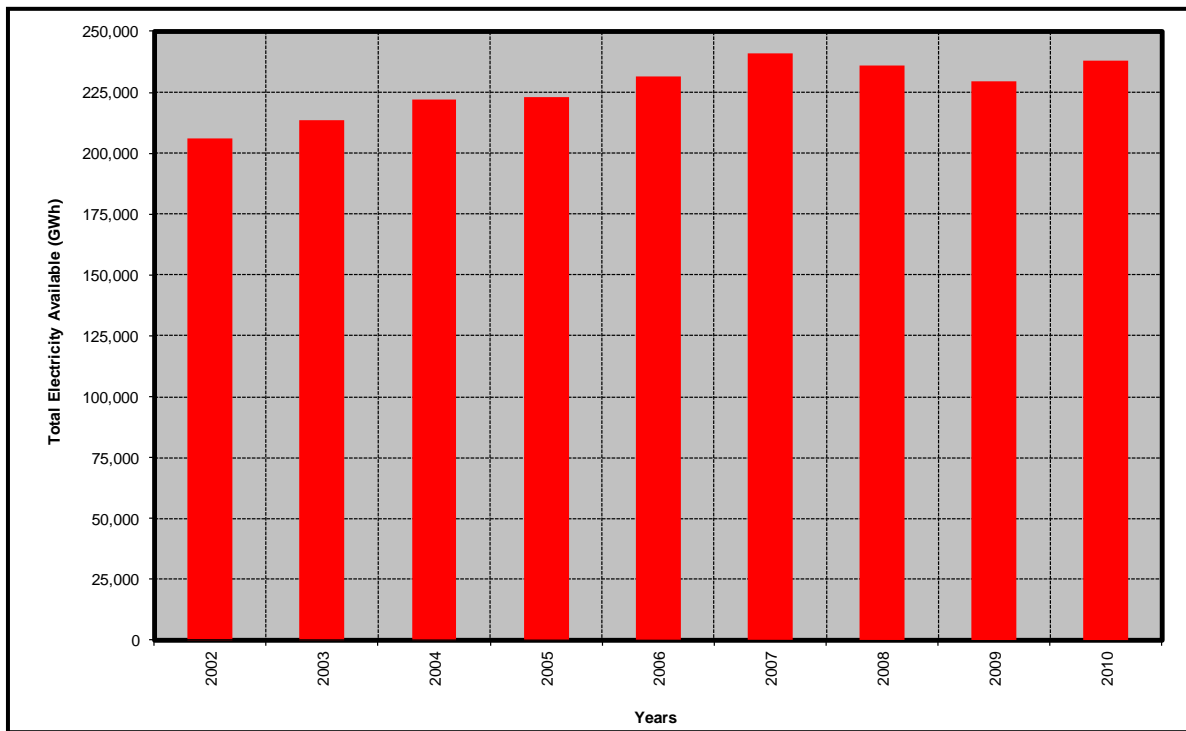


Figure 1-2: Total quantity of electricity available for distribution in South Africa (Statistics South Africa, 2011b)

Figure 1-2 shows the electricity that has been generated by Eskom over the past number of years. This graph shows that the overall generation capacity for the last five years has been reasonably consistent. This has resulted in a number of years of cheap and consistent electrical power supply. There has been a small increase in the total indicated capacity supplied by Eskom since 2002 of an average of 1.6% per annum (Statistics South Africa, 2011b). During the same period, however, the South African economy grew on average 3.7% per annum (Statistics South Africa, 2011c). It is obvious from these statistics that the economic growth of the country has not been matched by a commensurate increase in Eskom's capacity.

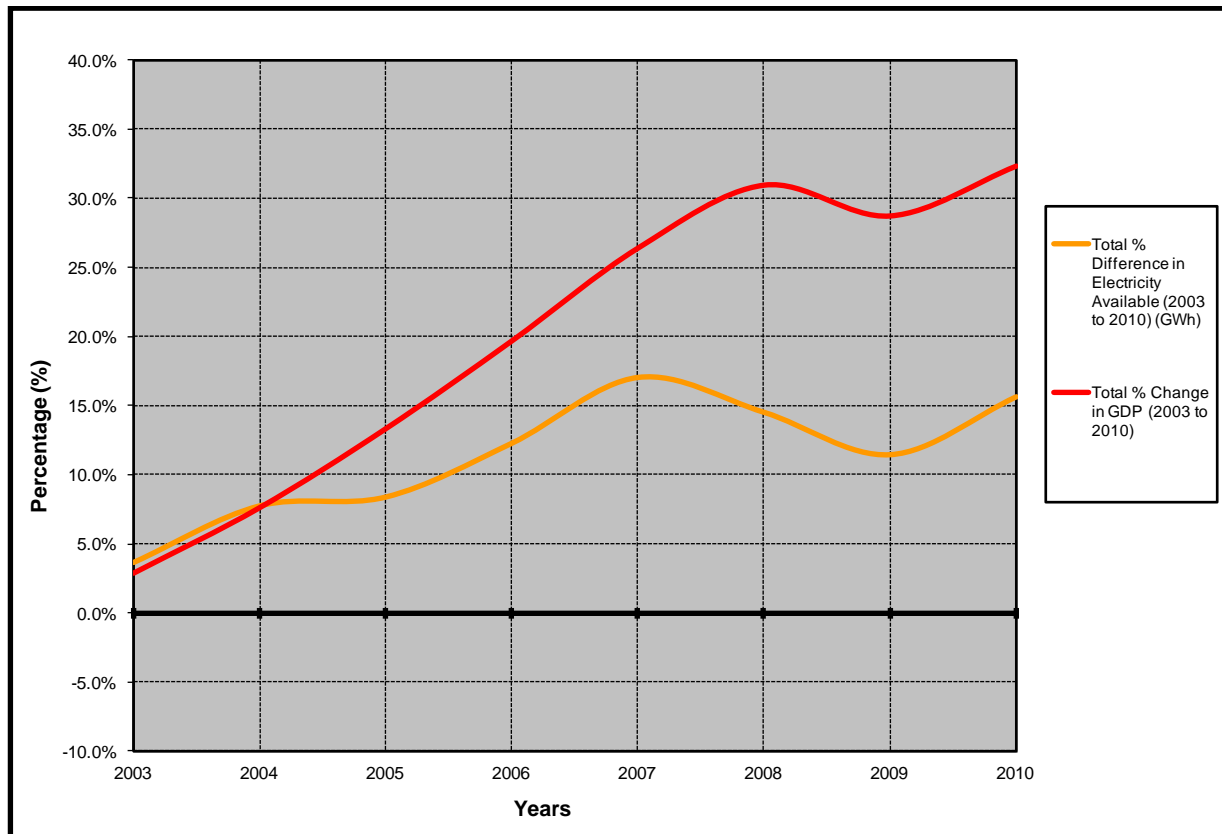


Figure 1-3: Comparison of annual percentage change in available electricity and GDP (Statistics South Africa, 2011c)

Eskom noted in its 2010 Annual Report that the current maximum generating capacity was approximately 40 870 MW, as opposed to 40 503 MW in 2009 and up from an estimated 38 747 MW in 2008. It was, however, noted in the 2010 Annual Report that demand had returned to the 2007 level by March 2010. However, it was also noted that if energy efficiency measures were not put in place by the winter of 2010, the power system would be under pressure beyond the winter of 2010 and in 2011 the risk of interruption would increase.

Eskom has improved its reserve margin since 2008 when it was 5.6 to 10.6% in 2009 and 16.4% in 2010. The reserve margin is the difference between the net system capability and the maximum load requirement. The 2009 margin is in line with internationally required margins which are generally in the region of 10 to 15% and the 2010 margin is in excess of this requirement.

This margin was in part achieved as a result of the small growth in sales that Eskom achieved in 2008, namely 2.9% (4.9% was forecast), and the negative growth in sales it experienced in 2009, namely -4.3%, and again a small growth in 2010 of 1.3% (Eskom, 2008, 2009, 2010). Nevertheless, Eskom has embarked on a substantial programme to ensure that the load shedding experienced in 2007 and 2008 does not happen again. In addition, the future needs of the country need to be taken into

account.

To provide an example of the state of South Africa's electrical generating capacity, a comparison is made between the growth in South Africa's Gross Domestic Product (GDP) and the increase in available electricity over the same period. These figures are shown in Figure 1-3. It should be noted that the period used for this comparison is from 2003 to 2010. During this period the cumulative growth of the GDP was above 32%, while the increase in the country's electrical generating capacity was 15.6%. This means that South Africa is not increasing its electrical supply capacity concomitantly with the rate at which it is growing.

1.3.1 Increases in Energy Costs

In December 2007, the National Energy Regulator of South Africa (NERSA) awarded Eskom a revised price increase of 14,2% for the 2008/2009 evaluation period ending in March 2009. Although this increase was well in excess of the country's CPI, it was well below the 60% that Eskom requested. This request by Eskom resulted in the urgent call for Nedlac to convene a 'national energy summit'. The meeting was in response to a call by the African National Congress (ANC) and other stakeholders for further consultation and explanation of the request by Eskom for the tariff increase. The summit raised the point that electricity tariffs should ensure the sustainable development of industry, but that it must avoid imposing unacceptable costs to the poor and an excessive shock to the economy.

In response to this request, NERSA announced on 18 June 2008 an additional increase in the electricity tariff of 13,3% for the year ending March 2009 which resulted in a 27.5% average increase year-on-year. NERSA also ruled that the price increase to 'poor' residential customers should be limited to 14,2%.

In the following year, Eskom also requested an increase of 34% for the 2009/2010 period. NERSA granted a tariff increase of 31.3% for the last nine-month portion of this period (ending on 31 March 2010). This increase did, however, include a new levy from the government on generating electricity from non-renewable resources. Thus, the 31.3% increase resulted in a real increase of 24.1%, which was again substantially below the requested increase.

Once again in 2010, Eskom requested an increase in tariffs of 35%. This was again refused by NERSA, which allowed an annual increase of only 24.8%.

The future increases determined by NERSA were defined in its 2010 Annual Report (NERSA, 2010), as follows:

- 1 Year 2010–2011: 24.8%
- 2 Year 2011–2012: 25.8%

3 Year 2012–2013: 25.9%

1.3.1 General Discussion

As the requirement for additional energy in South Africa drives the development of additional sources of electrical energy, the cost of this energy will increase. Eskom has already requested increases in the amount it charges for electricity well above inflation, primarily to allow it to source the capital required for the building of additional power stations. To demonstrate the effect that these increases could have on the operating costs of a mine, a number of alternatives were evaluated. The results of this analysis are shown in Figure 1-4. The baseline cost of 10% of the monthly production costs was increased by the indicated amount as indicative of the energy costs. The production costs themselves were increased by an estimated 6% to account for inflation. The overall increase in the percentage of the monthly costs was calculated, and this is the percentage increase shown in the graph.

The best-case scenario shows that the energy costs will increase to become a total of 20% of the monthly cost by 2015; the worst case shows this to be 40% of the monthly cost by 2015.

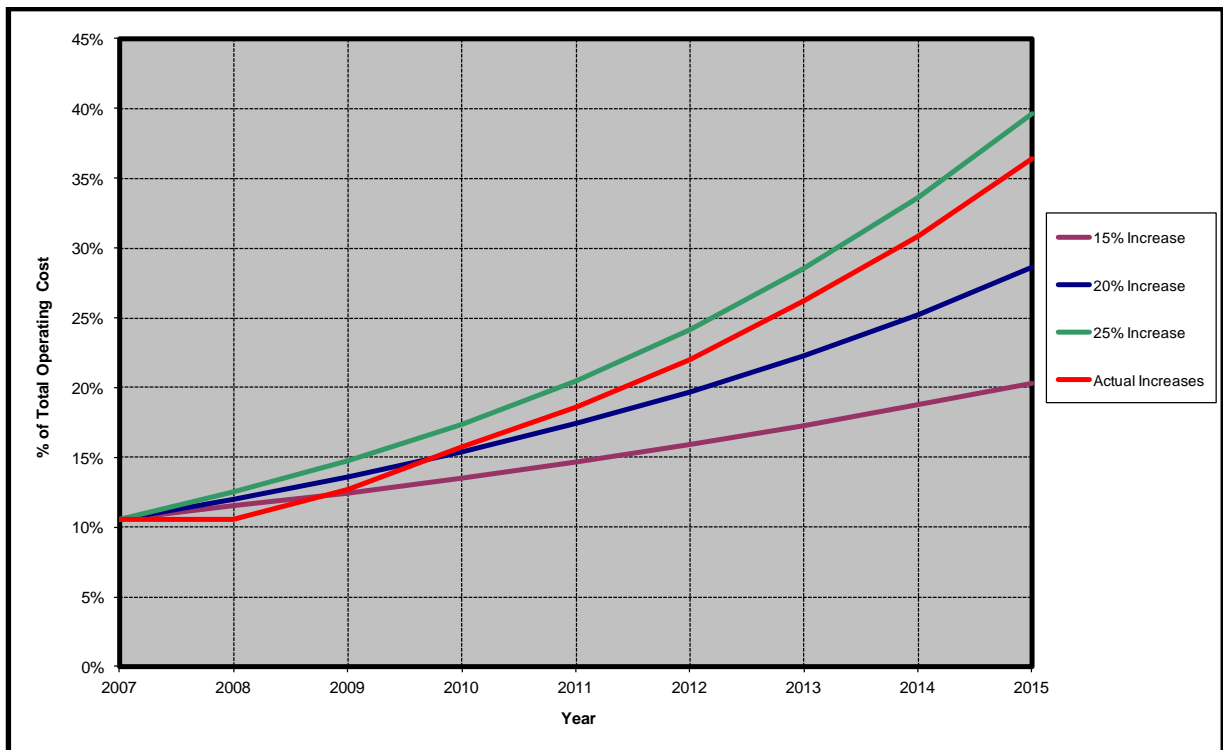


Figure 1-4: Consequence of increases with respect to operating costs

In order to ensure that they are able to operate effectively in this environment of increasing energy costs and reduced energy availability, the mining industry must optimise the manner in which it uses the available energy. This evaluation and optimisation provide the primary thrust of the work

presented in this thesis and therefore the data presented in the graph are quantified more fully as the work progresses.

1.4 EVALUATION OF ENERGY CONSUMPTION IN DEEP-LEVEL MINES

The purpose of the work presented in this section is to quantify the actual electrical energy used in a typical mine and to highlight the largest consumers. This analysis will allow us to determine the area of the mine that will benefit most from additional analysis.

1.4.1 General Parameters

To ensure a meaningful analysis of the electrical energy consumed by a typical deep-level mine, the basic parameters of the study must be quantified. In this instance only underground deep-level mining operations are considered, i.e. mines that are serviced using vertical shafts and declines as part of an access strategy.

1.4.2 Initial Evaluation

To evaluate the electrical energy consumption of deep-level mines, the various primary electrical energy consumers in the mine must be understood. Calculations were done for the design of an underground platinum mining operation. The results of these calculations show the installed electrical energy consumption capacity for the various areas in a standard underground mining operation. These results are shown in Figure 1-5. The 'model' mine was designed with a shaft depth of approximately 1 000 m and a decline system originating at the bottom of the shaft was used to access the ore body. Figure 1-5 shows the total use energy calculation for each of the appropriate sections, Figure 1-6 shows these figures as a percentage of the total expected energy use. The general parameters for the mine analysed are:

i	Total design tonnage	:	± 185 kilotonnes per month (ktpm)
ii	Main shaft diameter	:	8.5 m
iii	Main shaft depth	:	1 048 m
iv	Ventilation shaft diameter	:	6.5 m
v	Anticipated airflow	:	± 650 kg/s
vi	Mining method	:	Scattered breast
vii	Panel length	:	30 m

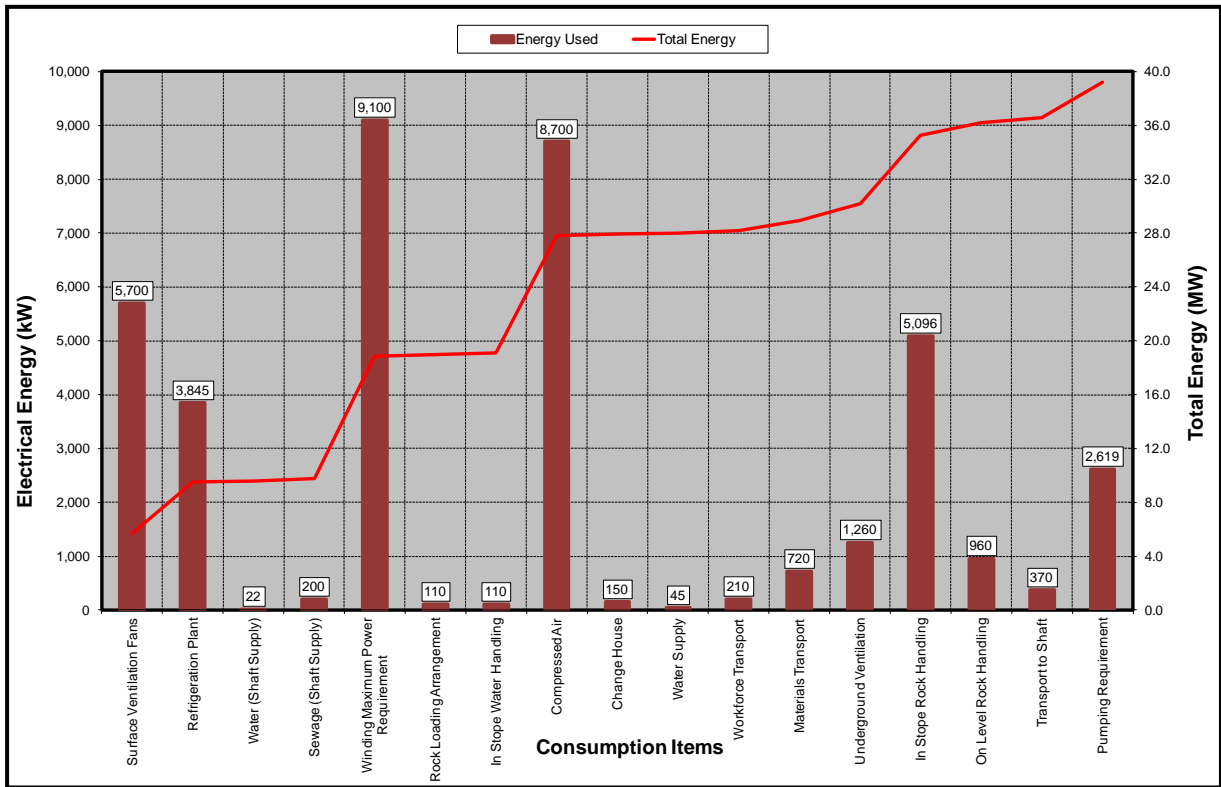


Figure 1-5: Summary of mine installed electrical energy consumption requirements

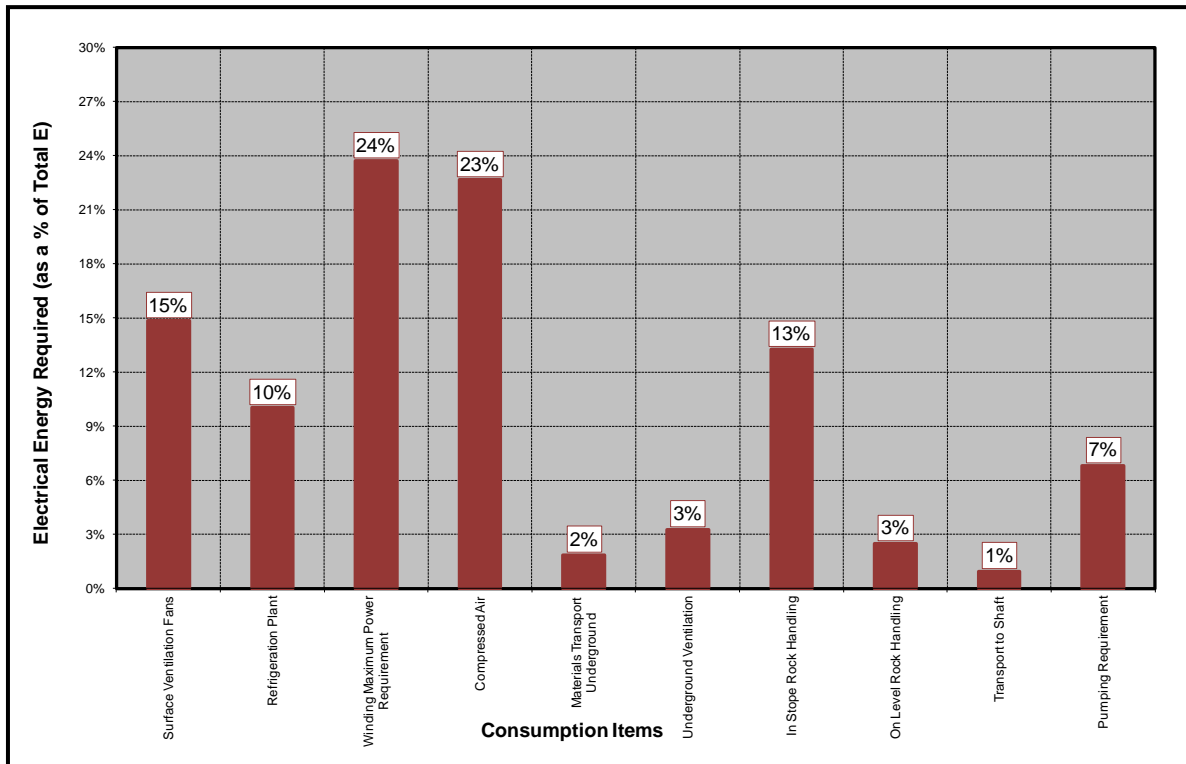


Figure 1-6: Summary of mine installed electrical energy consumption requirements (as % total installed consumption capacity)

The results of this analysis are useful in that they allow us to see explicitly which of the electrical energy users in the mine potentially consume the most energy. These primary users and their total contribution to the energy consumed are listed below:

- 1 Winding maximum power requirement (24%)
- 2 Compressed air (23%)
- 3 Surface ventilation fans (15%)
- 4 In-stope rock handling (13%)
- 5 Refrigeration plant (10%)
- 6 Pumping requirements (7%)

These are the users that consume up to 92% of the total energy required for effective operation of the mine. It must be borne in mind during this analysis, that the total installed capacity does not necessarily mean that a particular item consumes the most electrical energy. Comment is added in the various sections discussed below as to whether this is the peak or the average installed electrical consumption capacity

An overview of the winding requirement, compressed air requirement, in-stope rock handling and pumping requirements is presented here. The remaining ventilation and refrigeration requirements provide the primary thrust for this research and are discussed in more detail in Section 1.4.3.

1.4.2.1 Winding maximum power requirement

The winding requirement of the shaft is the highest peak consumer of electrical energy for the shaft system analysed. It consumes 24% of the total energy requirement, a total of 9.1 MW. The motor size and therefore peak electrical power required for winding is based on the power needed to accelerate the mass to the travelling velocity and cooling requirement of the motor. The motor is therefore sized to accommodate the peak power requirement and does not represent a steady-state consumption. The actual electrical power requirement is considerably less, especially when it is considered that winding systems are generally balanced, either with a counterweight or an empty skip counterbalancing the transporting cage or skip respectively.

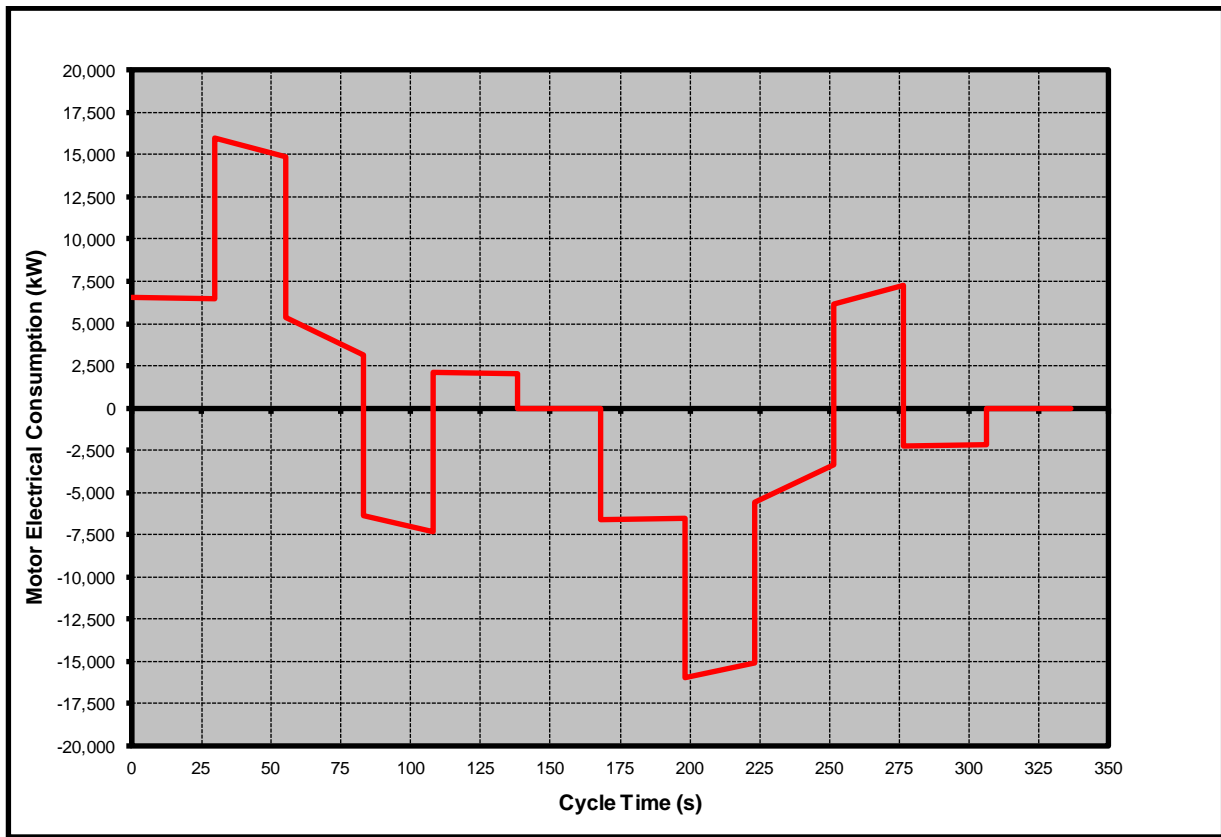


Figure 1-7: Typical winder cycle

Figure 1-7 represents a typical winder cycle. The total electrical power required peaks as the load is accelerated and quickly drops as the conveyance reaches its constant transport velocity. This requirement is then reversed for the deceleration portion of the wind and the cycle is then repeated.

The working of winders and the associated men and material transport is well understood and are therefore not considered in detail here. It should, however, be noted that there could be a small decrease in the total electrical energy consumed here as a result of changes to the shaft and cage configuration; these are included in the final analysis.

1.4.2.2 Compressed air

One of the primary consumers of electrical energy on the mine is the compressed air required for powering the rockdrills. In a conventional compressed air system as was used for the analysis depicted above, the compressed air generation equipment accounts for a total of 23% of the total energy requirement. This amounts to a total of 8.7 MW (Figure 1-6). The use of these rockdrills is generally cyclical and therefore the electrical energy is not consumed 24 hours a day. However these rockdrills are generally required to be used during the “peak” electrical supply period and as such are expensive to operate. In addition, a certain “base load” of compressed air is required to maintain the compressed air pressure in the system when the rockdrills are not being use.

There are a number of alternatives to the pneumatic rockdrills considered above, specifically hydraulic drills using high-pressure water (hydropower), as well as electric rockdrills. All of these systems have varying efficiencies and operational flexibilities. They have been examined in detail in other studies and are not considered further in this work.

Additional information on hydropower and electric rockdrill systems can be obtained in the papers by Wills (2008) and Petit (2006).

The various drilling systems and their advantages, disadvantages and efficiencies are well understood and therefore do not form part of the scope of the work reported in this thesis.

1.4.2.3 In-stope rock handling

This refers to the transport of the broken rock at the panels in the stopes to the box holes such that it is ready to be taken to the central ore passes before it is removed from the mine. The technique used in the analysis above is based on using face scrapers in the face and scrapers in the raise line to transfer the broken rock to the box holes. The calculation from the example shows a use of 13% of the total electrical energy or 5.0 MW (Figure 1-6). None of these scrapers requires a significant quantity of electrical energy. However, the mine-wide face-cleaning requirement results in a number of these systems being used in parallel for the cleaning shift of the mine, leading to a significant cumulative use of electrical energy.

There are a number of alternatives to traditional face scraping as used in the example above, primarily using water jet-assisted techniques (i.e. another application for hydropower). Additional information on hydropower equipment alternatives for the stopes can be obtained in the paper by Du Plessis et al. (1989).

The various stoping equipment suites and the techniques used for cleaning the panels and stopes are well understood and have been researched and reported on in numerous other papers. They therefore do not form part of the scope of the work reported in this thesis.

1.4.2.4 Pumping requirement

The pumping requirement for various mines can differ significantly, depending on the fissure water within the mine and on the mining method. The analysis completed in the example used for the initial evaluation came from a mine with very little fissure water. There are some mines that have a significant quantity of fissure water to contend with and the overall electrical energy required to dewater these mines will be larger than the total electrical energy calculated here. This analysis showed that the pumping will consume approximately 6% of the mine's total electrical energy requirement, or 2.6 MW during the pumping shift.

There are a number of alternatives to the traditional pumping systems used in the example, primarily using energy-regeneration techniques such as the chamber pump system. Additional information on more energy-efficient pump systems can be obtained from the paper by Fraser and Le Roux (2007).

The evaluation, control and removal of water from mines has been well researched and reported on. This topic is therefore well understood and the associated systems have been examined in detail in other studies. It is not considered further in this work.

1.4.3 Evaluation of Ventilation and Refrigeration

The ventilation and refrigeration requirements for a mine must always be considered together. The primary requirement of the ventilation in a stoping arrangement is the provision of adequate air velocities at the face. This quantity of air can, however, be affected by the cooling requirement. It is common practice to cool the air before it is taken into the mine and to use it as the cooling medium underground. This can, however, have an effect on the total air quantity required if the heat requiring dissipation in an area results in higher airflow rates through that area than are required by ventilation concerns alone. There are a number of areas in a typical ventilation analysis that could benefit from a more detailed evaluation. These are discussed in more detail here.

The ventilation component of the analysis used for this comparison is some 15% of the total electrical energy requirement in the mine or 5.7 MW (Figure 1-6). This is required for the main ventilation fans. While it is possible to “turn the fans down” during periods where the mine has fewer personnel underground, it is never recommended that the ventilation flow to the mine be stopped altogether. The refrigeration component of the analysis used for the comparison of the electrical energy consumption in mines is some 10% of the total electrical energy requirement in the mine or 3.8 MW (Figure 1-6). Together these two considerations total 25% of the total electrical energy consumed. The objective of this discussion is to examine these areas and determine whether any of these areas could benefit from additional investigation. It must be noted again here that the refrigeration requirement is not considered directly in this report but, as discussed above, must be considered in conjunction with the ventilation of the mine. The refrigeration requirement will therefore be affected by changes in the efficiency with which the ventilation air can be delivered to the mine’s workings.

A number of areas have been investigated with respect to the demand side management (DSM) of ventilation and cooling systems. These are discussed in more detail in the next section. It must be noted though that DSM differs from energy efficiency in that it deals with the use of the currently installed systems to specifically reduce the cost of operating them through the optimisation of the different times of use. The emphasis of the work reported here is on the reduction of the total

electrical energy requirement of the mine at the design stage, thus increasing the overall energy efficiency of the system while it is being constructed.

1.4.3.1 Demand side management

Marx et al. (2008) deal with the DSM of ventilation and cooling systems on mines. In this paper they evaluate two areas, namely fan control and thermal storage and present a summary of the DSM projects currently under way in South Africa.

The fan power required to move air through a mine is proportional to the cube of the volume of flow for that fan. Thus reducing the airflow by, for example, 15% will, in theory, reduce the fan power by approximately 38%. This theoretical power reduction is possible, but in reality there are a number of factors that change and reduce this benefit, e.g. the potentially lower power factor, the motor efficiency and the aerodynamic changes of the fan (Du Plessis and Marx, 2007). This paper reviews the three basic methods for the control of mine ventilation fans, i.e. the outlet dampers, fan speed and inlet guide vanes. In addition they emphasise the need for an efficient and robust communication, monitoring and control infrastructure. These systems are useful for retrofitting on existing mines and indeed have been successfully implemented in some cases.

Thermal storage systems are not new techniques. This system is based on generating ice or cold water at times during the day when the cost of electrical energy is at its cheapest and preserving this cooling capacity until it is required during the mine's busiest period of the day. Deep-level gold mines have used large chilled water dams located on surface to provide thermal storage for mine cooling systems in the past. This technique is also commonly used in air-conditioning systems in North America and Europe (Wilson et al., 2003).

The technologies discussed above, as well as others not discussed here, which can provide significant electrical energy savings in South African mines, are available and their application is well understood. These technologies are based on the efficient use of the systems in place and control of the ventilation and cooling systems such that the times when the electrical energy is used is optimised with respect to the overall load on South Africa's power grid, and that the load is timed to limit the overall consumption during periods of peak electrical demand.

1.4.3.2 General remarks

In addition to the generation and optimisation systems described in the preceding sections, there is also the question of the distribution of the required cooling capacity. The usual technique is to cool the air used for the ventilation of the mine and to distribute it throughout the mine. This method has the advantage that the air that is required to provide a safe working mine can also be used for cooling. However, in deep-level mines, the driving factor is not the distribution of sufficient air, but

rather the distribution of the cooling medium. This can result in an increase in the air quantities being distributed to the workings as a result of the need to distribute cooling, rather than meeting the actual ventilation requirement, with a commensurate increase in the power required for the distribution of this ventilation and cooling.

It should also be noted at this point that although there is a drive to use the concept of ‘cooling power’ as a more adequate indication of the working environment’s ability to provide the necessary cooling capacity, this has not been fully accepted as yet (Biffi et al., 2006). The adoption of this standard could result in the reduction of the overall quantity of air being required.

In some instances where significant cooling is required, it becomes inefficient and, in specific cases, impossible to transport the required cooling using the ventilation air. The “process of gravitational compression, or autocompression in downcast shafts produces an increase in the temperature of the air. This is independent of any frictional effects and will be superimposed upon the influence of any heat transfer with the surrounding strata that may occur across the shaft walls.” (McPherson, 1993). If the shaft is sufficiently deep, this can result in the air becoming a heat source instead of a cooling medium.

These factors must be considered in association with the general ventilation and cooling requirement of the mine. It was noted by Biffi et al. (2006) that one of the most important methods available to reduce the energy consumption of a mine is the integration of the ventilation system design as a fully fledged component of the overall mine design.

The importance of integrating the ventilation design with the mine design and the design of the various mine components cannot be over emphasised. The technique of designing mines in modular form, with extensions being managed as additions to these modules, is also important. This integration must also be seen in the context of the drive to make mines more operationally flexible. If this flexibility is met with increasingly costly ventilation and cooling costs, the benefit of having a flexible system will be offset by these costs.

This mine flexibility requirement can come in two forms. In the first instance it is the operating flexibility to deal with changes in the economy and the price being offered on the market for the commodity. Macfarlane (2005) emphasises the importance of flexibility in the mine plan by arguing that “where flexibility to deal with changing economic cycles has not been created, reactive planning has to be undertaken, which is value destroying”.

In the second instance, if operating flexibility is regarded as the ability to move the mining operation swiftly to different production faces when issues of grade control or unpredicted geological structures require it, then the mine’s resource can be managed effectively to allow it to control the production of its resource while ensuring that the maximum portion of ore reserve is exploited

(Musingwini et al., 2006).

1.4.4 Calculation and Verification Data

To highlight the areas of the ventilation system that require the most electrical energy, the example mine discussed in Section 1.4.2 needs to be shown in more detail. A schematic of the arrangement is shown in Figure 1-8. The refrigeration requirement was not analysed separately as in this example the cooling capacity required by the mine is distributed using the bulk air cooler on surface to chill the air. No additional cooling was required. The quantities of air noted in Section 1.4.2 (page 9) of this thesis provide the cooling requirement needed by the mine.

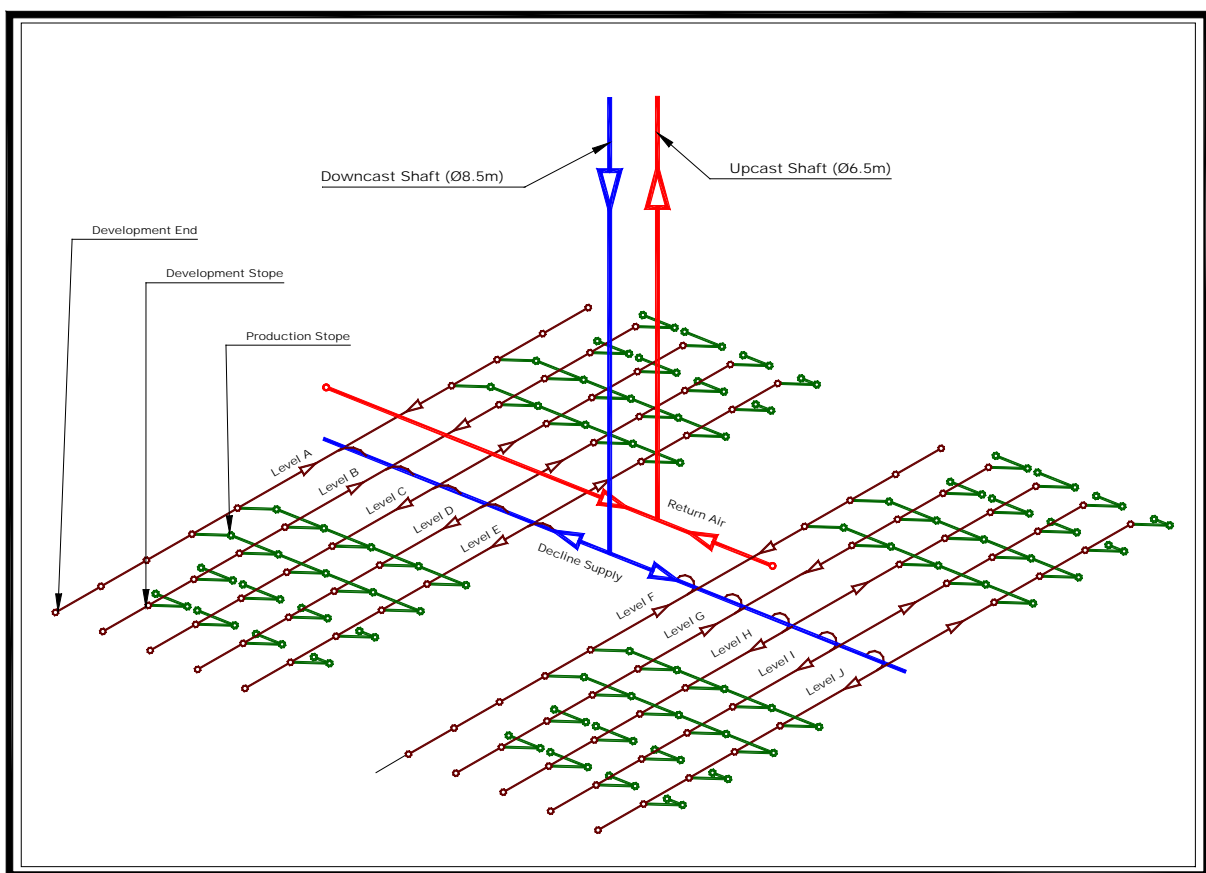


Figure 1-8: Schematic of ventilation layout

The electrical energy required to move air around the mine is based on the quantity of air in a section as well as the pressure required to move this air to that section. In this regard the main ventilation airways and the resistance to the airflow quantities needed must be carefully considered. For the 'model' mine under examination here, the sections shown in Table 1-1 have been identified and shown in more detail to highlight the areas which require the most energy to move the required air through them. The details of this calculation can be found in Appendix A.

Table 1-1: Summary of ventilation power requirements for mine analysed

Item	Description	ΔP (Pa)		Q (kg/s)	Power (kW)	
		Value	%		Value	%
1	Primary intake configuration (downcast)	1,793	35%	703	1,261	54%
2	Main intake systems	645	13%	150	97	4%
3	Haulage intakes	634	12%	70	44	2%
4	Stope configuration	90	2%	70	6	0%
5	Stope return configuration	379	7%	70	26	1%
6	Main return airway	656	13%	340	223	10%
7	Return shaft (exhaust)	951	18%	703	669	29%

Note:

The flows and changes in pressure shown here are of the of mine ventilation system and are a selection of the worst-case scenarios in certain areas to allow evaluation of the efficiency of the overall system and to provide a guide as to the areas that will benefit most from an optimisation exercise.

It follows from this analysis that the two areas resulting in the high pressure changes and therefore requiring the most power and from the main ventilation fans during operation are the downcast and upcast shafts. These two areas consume 83% of the total power supplied by the fans in this configuration. This power requirement translates directly to an increased requirement for electrical energy.

This high percentage indicates that this could be an area of worthy of additional analysis. To achieve this, the ventilation manager at Impala Platinum Mines was approached. The specific request to this department was to allow access to a shaft to do measurements that would confirm the high pressure drops in the shaft and potentially to optimise the shaft design to optimise these pressure drops, resulting in an overall reduction in the energy required to operate mines.

1.4.4.1 Verification of the shaft pressure losses identified

Impala Platinum Mines Management was approached with the request to allow testing on their various shafts in their mining group, primarily as there are a number of shafts available for testing

with easy reach of each other.

Impala Platinum Mines agreed to allow the initial shaft pressure loss tests to be conducted on one of their shafts. Impala No. 14 shaft was chosen as this shaft consists of two downcast and two upcast shafts, all of which were accessible. A schematic of the shaft configuration is shown in Figure 1-9.

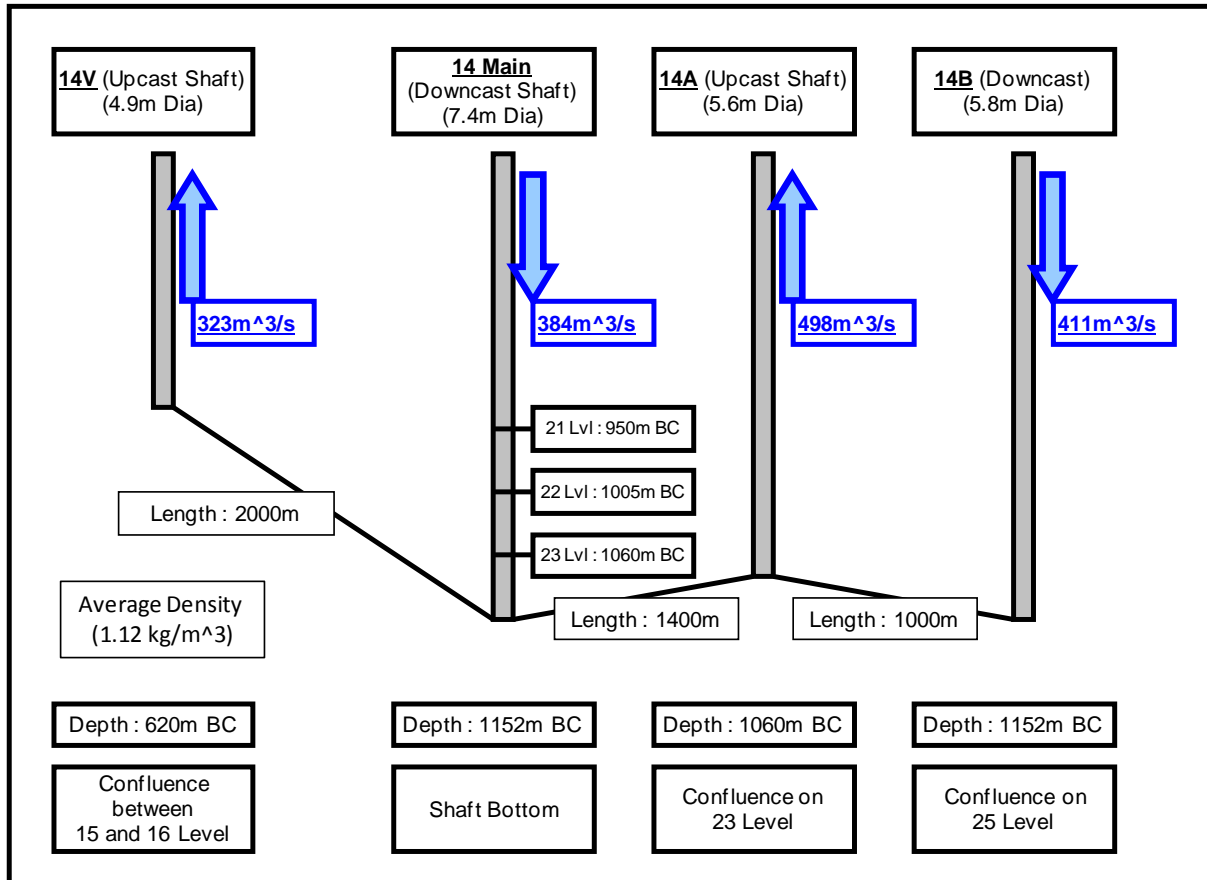


Figure 1-9: Schematic of mine shafts tested

It should be noted from the schematic depicted in Figure 1-9 that there is a discrepancy between the total downcast quantity of air and the total upcast quantity of air measured ($795 \text{ m}^3/\text{s}$ as opposed to $843 \text{ m}^3/\text{s}$, i.e. some 6% difference). This difference is attributed to the experimental error primarily as a result of the complex shapes shown at the bottom of the upcast shafts. In addition, the mine does experience some additional ventilation inflow from neighbouring shafts, the exact quantity of which is not known. The details of these data and the subsequent calculation can be found in Appendix B of this thesis.

The initial tests were designed to ascertain, on a broad perspective, the pressure losses in the shaft systems as a whole. In the equipped downcast shaft, it was possible to take measurements at various points in the shaft. This was not possible for the unequipped ventilation shafts, so on these shafts measurements were taken as close to the shaft as possible try to limit the interference from

shock entrance and exit losses. The indirect pressure survey method used for these calculations is the barometric survey method laid out in the Mine Ventilation Society of South Africa's Handbook (1989). Sufficient data were required to allow the pressure drop of the shaft to be calculated in accordance with this method. In this regard the following measurements were taken:

- 1 Wet bulb temperature
- 2 Dry bulb temperature
- 3 Static pressure
- 4 Velocity pressure (or dynamic pressure)

The specifics of the test methodology can be found in Appendix B. The results of this analysis are listed in Table 1-2.

Table 1-2: Summary of ventilation pressure losses

Impala No. 14 shaft (downcast) (384 m³/s)		
918 Pa	Measured	19% Difference
748 Pa	Calculated	
Impala No. 14V shaft (upcast) (323 m³/s)		
1 302 Pa	Measured	31% Difference
902 Pa	Calculated	
Impala No. 14A shaft (upcast) (520 m³/s)		
694 Pa	Measured	7% Difference
642 Pa	Calculated	
Impala 14B No. shaft (downcast) (411 m³/s)		
1 021 Pa	Measured	15% Difference
1 175 Pa	Calculated	

Total pressure for fan 1 (14A Upcast Shaft)	
4 088	Pa
Total pressure for fan 2 (14V Upcast Shaft)	
3 202	Pa
<p>54% of the total fan pressure available from the main fans is used to overcome the pressure drop experienced as a result of air moving through the shafts.</p> <p>Notes:</p> <ul style="list-style-type: none"> i The percentage difference noted in the measurements of the No. 14 Downcast and the No. 14A upcast shaft are consistent with the percentage difference noted in the overall quantity of air measured in the shaft and presented in Figure 1-9. ii The percentage difference noted in the measurements of the No. 14V upcast and the No. 14C downcast shafts is significantly higher. This increase in the experimental error is a result of the increasingly complex ventilation distribution shape at the bottom of these shafts. In addition, the mine has an unknown quantity of air being entrained from neighbouring shafts. iii The detailed calculation and schematics used to calculate the above figures can be found in Appendix A. 	

The calculations from the initial shaft configuration are borne out by the measurements. These indicate that the pressure losses in both of the vertical shaft complexes absorb most of the pressure supplied by the ventilation fans.

A comparison was also made between the measurements taken and the current theory available. These showed some correlation in some areas. It should be noted, though, that when the shaft configuration became more complicated (i.e. when station take-off occurred or multiple entry ways were noted in the ventilation configuration), the correlation between the measured and calculated data was not in close agreement. This is particularly apparent in the No. 14B downcast shaft configuration shown in Figure 1-10. To obtain the final flow through this shaft, the velocity in each of the four openings was measured and the total quantity of air that would be entrained in this shaft was summed. The normal experimental error in this configuration would thus also be summed. This

was mitigated by ensuring that the testing was done in strict accordance with good experimental procedure.

The real-life complexity of the systems being measured and the associated differences between the calculated data and the measured data can give rise to discrepancies. However, another reason for these discrepancies could be the inadequate nature of the basic calculations used to verify the measured data. Although this is undoubtedly not true for the classically derived formulae (i.e. the pipe friction flow model), there is perhaps room for improvement in the empirically derived data, particularly for the calculation of ‘shock’ losses and losses associated with partially obstructed airways.

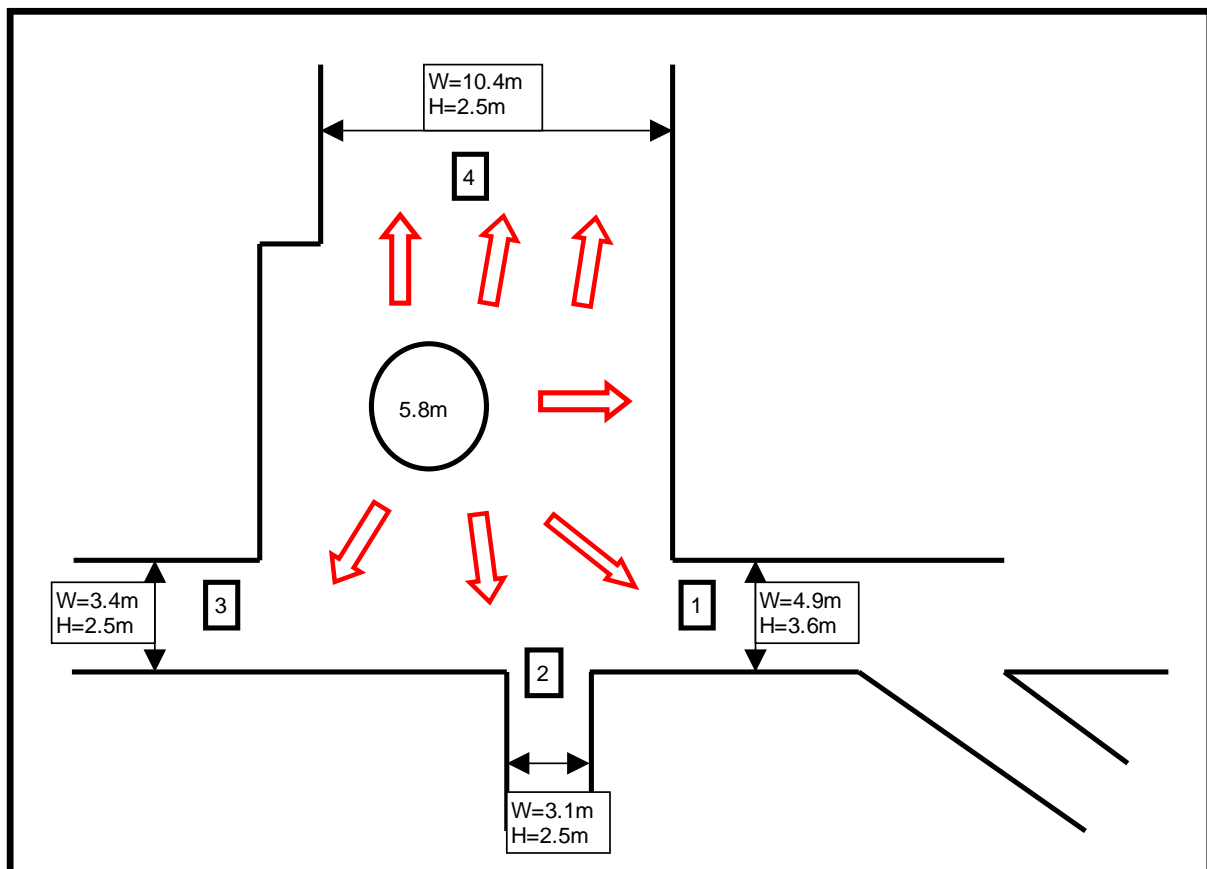


Figure 1-10: Configuration of No. 14B downcast shaft bottom

Despite the above errors, the quality of the data collected and the subsequent analysis allows us to draw some conclusions. These are:

- 1 Ventilation fans must supply a significant amount of energy to the ventilation air to overcome the frictional resistance in shaft systems.

- 2 The theory associated with the prediction of these pressure losses potentially requires additional investigation.

The primary reason for this recommendation is that the relationship between the power required by a fan (and therefore the electrical energy) to move air against a resistance which would result in pressure loss is directly proportional. This is governed by the relationship of the power required by a fan equals the product of the pressure required and the flow rate (if compressibility effects are ignored).

It should also be noted that the measurements discussed here were taken in an equipped shaft from a stationary conveyance. The shaft resistance and therefore the pressure drop will increase if the main cage or any of the cages and/or skips in the shaft are moving against the airflow of the shaft.

1.5 PROJECT BACKGROUND

This section describes the process undertaken to complete a shaft design, the process of costing these shafts and the difficulties encountered in this costing. Finally, the status of the current theory used for the analysis of shaft systems is evaluated and potential areas of investigation highlighted.

1.5.1 Evaluation of Costs Associated with the Sinking, Equipping and Operation of Shafts

To evaluate the potential costs and savings from modifications to the shaft systems, it was necessary to identify the parameters of the resistance within the shaft systems that could influence the pressure losses associated with it. It must be noted that while this analysis is normally done in conjunction with the overall mine, in this instance our interest is specifically in the shaft itself.

As the size of an airway increases, its resistance, and therefore operating costs, will decrease for a given airflow. However, the capital costs of excavating the airway increase with its size. The total combination of capital and operating costs is the total cost of owning and ventilating the airway. The most economical or optimum size of the airway and its associated fitting occurs when this total cost is a minimum (McPherson, 1993).

Determining accurate costs for the sinking of shafts is difficult when they are used as a basis for comparison. However, for this exercise, to provide a consistent basis for comparison, it has been assumed that the shaft-sinking company will supply all the temporary works and will sink the shaft. An example of the increasing costs associated with sinking shafts of various diameters is shown in Figure 1-11.

Generally, it is noted that a significant long-term reduction in costs will be required in order to justify

the immediate increase in the capital costs. The increases in energy costs noted in Section 1.3.1 make the potential savings more significant and, potentially, where the economic saving would not have been significant in the recent past, these savings could now provide the basis for re-evaluation of the shaft-sinking costs.

A financial model was introduced by Barenbrug (1961) to evaluate the effectiveness of changes in shaft design. This model is still used today in various guises and was used by McPherson (1993) to demonstrate the evaluation required to calculate the total cost for a shaft. An example of this model is shown in Figure 1-12.

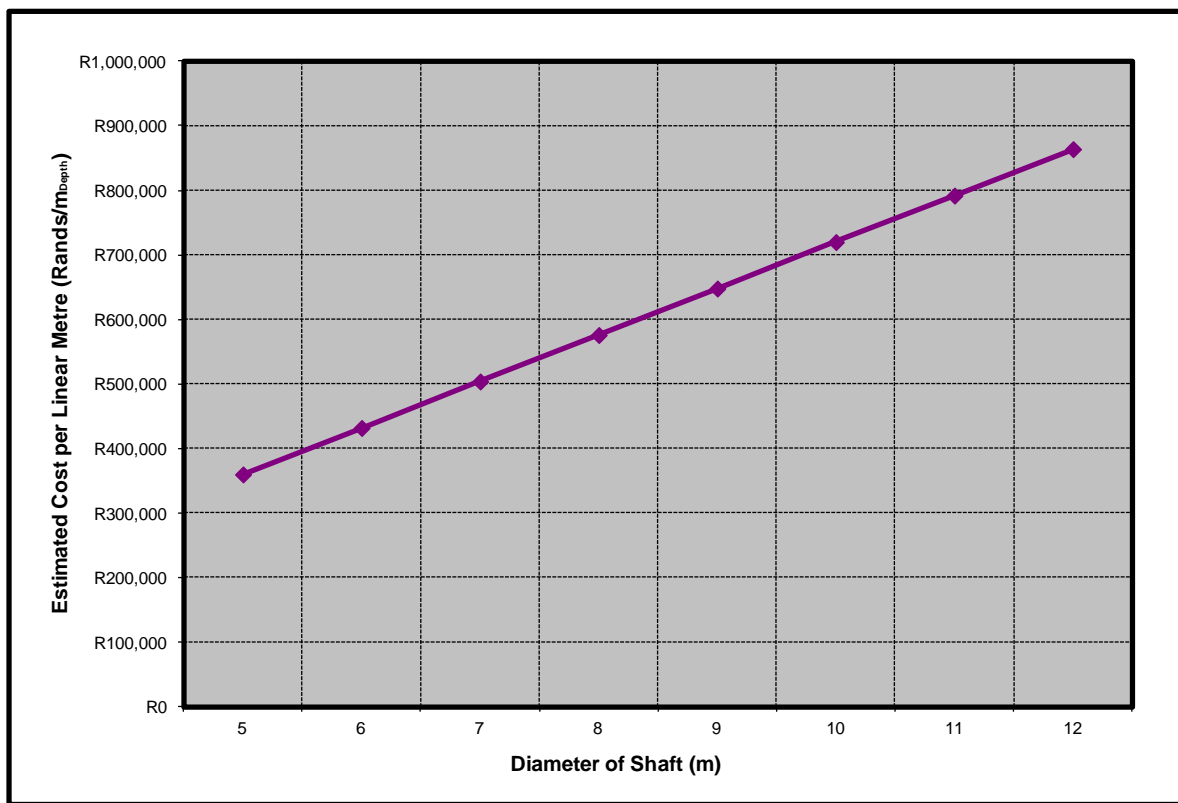


Figure 1-11: Estimated cost of shaft sinking per linear metre

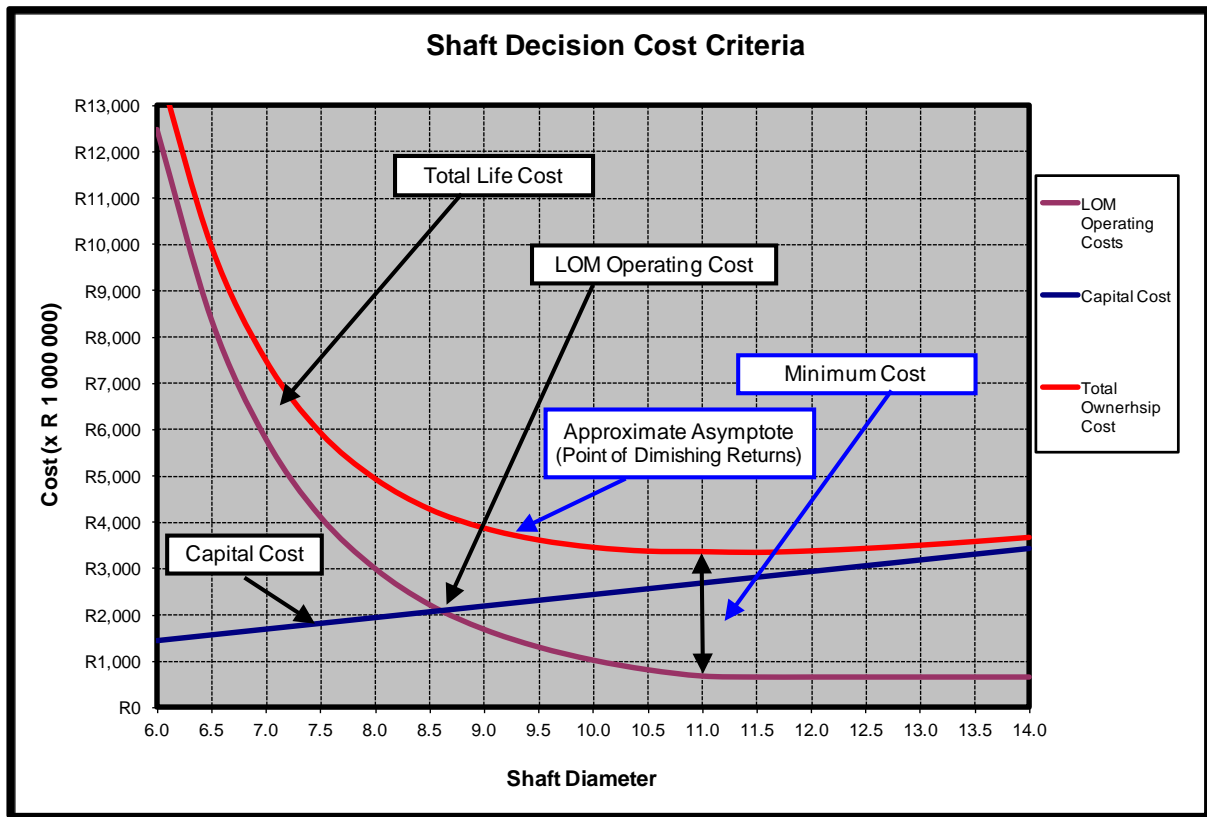


Figure 1-12: Shaft decision cost criteria

Figure 1-11 and Figure 1-12 provide the basis for the evaluation of the shaft diameter with respect to operating costs. These parameters are well understood and used extensively. The emphasis of the work reported on this in this thesis will therefore be on comparing the overall lifecycle cost of different equipping options and the associated capital costs in order to elicit a total cost for the life of mine (LOM). This decision was made when discussions with sinking professionals highlighted that fact that the costs for equipping and maintaining the various shaft steelwork options are sufficiently similar to make delineation very difficult.

The comparison will be based on a period of 20 years at a lower-than-anticipated electrical tariff increase of 12% per annum. In order to derive an accurate cost, the cash flows should also be discounted such that the time value of money is also taken in to account. This allows a net present value to be determined which provides a realistic cost to compare the various savings. All future savings were discounted by 7% per annum.

When evaluating the cost effectiveness of the different options, the entire capital cost of the shaft was not considered. Only the areas affected by the changes were evaluated, these included the operating costs for the fans (but no capital costs which could accrue as a result of the reduced pressure requirement). The costs for the buntons and guides were included, where appropriate, as

well as other equipment associated directly with the shaft, as appropriate.

1.5.2 Components Contributing to the Present Shaft Resistance and Subsequent Pressure Losses

This section gives the background to the specific area of interest and provides some insight into the status of work being conducted in this area of research.

1.5.2.1 Parameters used for designing a shaft

To understand the parameters contributing to the shaft resistance and the subsequent pressure losses, we will first broadly define the steps (McPherson, 1993) that are generally taken to design a typical equipped downcast shaft from the perspective of the ventilation requirement of the mine:

- 1 Determine the duties required for
 - i rock hoisting
 - ii personnel transport
 - iii mass, dimensions and frequency of materials and equipment
- 2 Analyse the above with respect to the conveyance sizes and required hoisting speeds.
- 3 Conduct the ventilation analysis:
 - i The primary requirement for ventilation will be based on the mine design, the layout and the distribution of the workings over the LOM.
 - ii Standard factors will be used for estimating the shaft resistance and other significant contributors to the overall pressure drop in the mine.
- 4 Assess the dimensions of proposed shaft fittings. This will include:
 - i Shaft fittings (i.e. buntions and guides)
 - ii Services (i.e. pipes, cables, etc.)
- 5 Conduct an optimisation exercise to find the size of shaft that will pass the required airflow at the minimum combination of operating costs and capital expense.
- 6 Review the free air velocity of the ventilation requirement to ensure that it is within accepted limits. (Generally, the velocity in an equipped downcast shaft should be approximately 10 m/s and that in the unequipped upcast shaft should not exceed 20 m/s.) (The free air velocity is calculated by taking the volumetric flow rate of the air and dividing it by the area of the shaft available to allow the air to flow (ie the total shaft area minus

- the area of the pipes, buntun and other shaft fitting (excluding the conveyances)).
- 7 Review the coefficient of fill of the conveyances to ensure that they are within accepted limits. (If this exceeds approximately 30% for two or more conveyances or 50% for a single conveyance, then the dimension of the conveyance should be reviewed.)
 - 8 Calculate the maximum relative velocity between the airflow and the largest conveyance. (If this exceeds approximately 30 m/s, then additional precautions should be taken to improve the stability of the conveyance.) This relative velocity should not exceed 50 m/s.
 - 9 Assess the air velocities at all the loading/unloading stations.
 - 10 Determine the total resistance of the shaft using ventilation network analysis techniques.
 - 11 Complete the overall ventilation network analysis with the established shaft resistance in order to determine the final fan pressures required.

The specific area of interest is the design of the shaft system itself and the effect that the equipment within the shaft has on the overall resistance offered to the ventilation air flowing through it.

1.5.2.2 Shaft configuration and analysis techniques

Mine shafts, specifically downcast shafts, that are used as primary ventilation routes are different in their airflow characteristics from other subsurface openings because of the aerodynamic affects of the various shaft fittings, i.e.

- i guide rails
- ii buntuns
- iii pipes, cables and ropes
- iv conveyances (shape, size and velocity)

McPherson (1987) noted that shafts contribute heavily to the overall resistance of a mine ventilation circuit. This was borne out by the measurements discussed in the preceding sections.

The most recent theoretical work analysing these particular areas of shaft systems was carried out initially by McPherson (1987). It was based on the work carried out by Bromilov in 1960. In turn, both of these papers relied heavily on work carried out by Stevenson (1956). These papers will be discussed in more detail in CHAPTER 2. Suffice it to note here that a large portion of the analyses presented in this thesis is based on work published in 1956, 1960 and 1987.

The accuracy of these equations was verified by Deen (1991). In this analysis, using the modified technique described by McPherson (1987), he achieved accuracies of 5 to 12% when comparing the overall measured shafts resistances with the resistances calculated theoretically.

In this regard, a survey was undertaken by Wallace and Rogers (1987) to collate the actual installations of a number of shafts. The data from a total of 37 shafts were evaluated and the various factors for each shaft were collated. The details of these results will be discussed more fully in CHAPTER 2. A summary of these findings is as follows:

- i The coefficient of fill should not exceed 30% for shafts with two or more conveyances, and an upper limit of 50% is suggested for a single conveyance.
- ii A free air velocity of 10 m/s is considered to be acceptable, with a maximum relative velocity of 30 m/s.
- iii As shafts increase with depth, the coefficient of fill should decrease.
- iv It is recommended that air bypasses or enlarged shaft stations be installed to minimise high airflow resistances.

Evaluation of the overall calculation technique highlights the significant contribution that the buntons make to the overall resistance of the shaft. The data obtained from the Impala shaft indicate that 80.9% of the total resistance factor is a result of the buntons. The remaining 19.1% comes from the roughness of the shaft walls and the contribution of the shaft fittings to reducing the overall free area of the shaft.

The buntons at Impala No. 14 shaft are oval in shape and therefore have a low coefficient of drag, which is used in calculating the resistance offered by the buntons. In spite of this, they still offer a significant resistance when compared with the remainder of the shaft.

Regarding the question of the bunton shape, scale shafts have been tested by a number of researchers and these experimental data have been used in the design of specific shaft systems. Most of this work is also circa 1960, and it was used by Bromilov (1960) to verify the results he obtained from the theoretical analysis. These papers and their results will be discussed in more detail in Chapter 2. Suffice it to note here that the primary purpose of these papers was to analyse the effect on the shaft resistances of circular shafts vs. rectangular shafts, as well as to evaluate the shape of the buntons being installed in shafts. The overall conclusion of all the tests was that the more streamlined the bunton section, the less its contribution to the overall shaft resistance. This work also reviewed shafts that were being built at that time and does not examine what the best shaft configuration would be for a particular shaft system.

1.5.3 Justification of Additional Work

The general analysis of shaft systems and the techniques currently being used have been discussed. The validity of these analysis techniques has been verified both by testing in the field and by

research work describing the specific verification of the technique (Bromilov, 1960).

The primary aim of the work discussed here was to determine what can be done to reduce the operating costs in shafts significantly as these systems still consume the largest portion of pressure supplied by the main ventilation fans.

As was noted in Section 1.4.4, the most significant portion of the pressure drop occurs as a result of the buntons themselves. However, the one parameter that was not included in the initial analysis was the movement of the cages themselves. The analysis technique does provide guidance as to how these should be treated and a detailed evaluation of this is provided in CHAPTER 2. It should be noted here that the theory shows that this movement can increase the overall resistance of the shaft by more than 30%, depending on its configuration and the hoisting speed.

The following specific areas were investigated:

- 1 *Buntons and guides:* This analysis includes evaluation of the buntons' resistance based on the obstruction they place in the path of the airflow. No work has previously been done on optimising the actual configuration of the buntons in their situation when compared with the obstruction offered by the sidewall or the support of shaft services.
- 2 *Cages:* This analysis includes evaluation of the cages, once again based on the obstruction they place in the path of the airflow. No work has previously been done on the potential for streamlining these conveyances specifically in conjunction with the buntion configuration. In addition, the potential for reducing the resistance by having various conveyances moving at different intervals has not been quantified.
- 3 *Services (pipes, cables, etc.):* This analysis includes evaluation of the obstruction offered by these services based on the amount they reduce the overall shaft cross-section. McPherson (1987) also noted that these services may indeed reduce the overall resistance of the shaft based on the obstruction they offer and the resultant potential reduction in the swirl of the ventilation flow. No work has previously been done on the preferred placement of these services and the specific configuration that would optimise this effect.

1.6 PROBLEM STATEMENT AND PURPOSE OF STUDY

The current theory for the definition of shaft resistances allows us to evaluate shafts and to predict the overall resistance they offer to the ventilation air flowing through them. This theory, however, does not allow us to optimise the shaft cross section layout specifically to reduce this resistance by the moving of conveyance travel zones and varying the placement of buntons, guiders and services within the shaft. The deficiencies in the theory are highlighted in the thesis. The purpose of this

study is to minimise the shaft resistance by varying the actual layout of the shaft and the placement of the shaft buntons, guides and services.

1.7 OBJECTIVES

Several objectives were set for this study, and these are detailed in the following sections.

1.7.1 Literature Study

A detailed literature review was undertaken with the following specific objectives:

- Identify all the aspects pertaining to the resistance that shaft systems offer to the ventilation air passing through them. This includes the fittings in the shaft, the stations and associated steelwork, as well as the entrance and exit effects experienced by the ventilation air.
- Identify modelling work completed on shaft airway analysis with the specific purpose of understanding and collating the appropriate parameters to ensure that any modelling work undertaken for the current analysis will be accurate.

1.7.2 Evaluation of Current Shaft Configurations

During this phase of the work, the resistances of different shafts were measured. The specific objective of this phase was to ensure that the current shaft design trends are understood, as well as the resistance these configurations offer to the ventilation air flowing past them.

The data obtained from these measurements are subjected to a theoretical analysis based on the current techniques available in order to ensure that the strengths and limitations offered by these techniques are understood and incorporated into the next phase of the work.

The following specific parameters are noted:

- 1 Shaft
 - i Diameter
 - ii Lining
- 2 Shaft fittings
 - i Buntons
 - ii Guides
 - iii Pipes

- 3 Conveyances
 - i Type and Number of conveyances
 - ii Speed of conveyance

1.7.3 Detailed Analysis

During this phase of the work, the results of the evaluation described in Section 1.7.2 were subjected to a theoretical analysis. This analysis consists of two parts:

- 1 Analysis of the shaft systems evaluated with respect to the current available theory.
- 2 Analysis of the shaft systems evaluated with the use of a computational fluid dynamics (CFD) model.

1.7.4 Installation, Maintenance and Costing

The output of the detailed analysis provides parameters for the design of shaft systems in a manner that will limit the resistance of the shaft. These design parameters must, however, be evaluated against the following specific requirements:

- 1 *Installation:* The system must be able to be installed with ease. In this instance preference was given to the completion of upfront work to limit the actual time taken for the installation as far as is practically possible.
- 2 *Maintenance:* The proposed system must be maintenance friendly. The specific parameter against which this was evaluated is that it must be possible to complete all maintenance work effectively during the weekly shaft inspection shift.
- 3 *Cost:* The overall cost of any proposed design must be such that the any capital cost requirement is mitigated by the reduction in operating costs. These costs will be evaluated in Section 3.7.

1.7.5 Conclusions

The specific objective of all the preceding work is to define the design requirements and systems of deep-level shaft systems such that these shafts offer as little resistance as possible to the ventilation flow around them.

1.8 METHODOLOGY

1.8.1 Literature Study

A review of all the work undertaken with respect to the analysis of shaft resistances was undertaken. Each of the particular areas discussed in Section 1.7 was subjected to the following procedure:

- 1 *Assemble information:* Various search tools and library facilities were used to find as much information as possible on each of the subjects in question.
- 2 *Review information:* All the assembled information was reviewed, analysed and collated with respect to pertinence to the current research and its applicability.
- 3 *Presentation:* CHAPTER 2 presents the results of the literature study.

1.8.2 Evaluation of Current Shaft Configurations

During this phase of the work as many shafts as possible were examined and the pressure drops over the shaft were measured. This was done in conjunction with Impala Platinum Mines. The one requirement Impala placed on this work was that it must in no way affect the production of any shaft. Therefore all the measurements were taken in periods when the shafts were being maintained or not being used at all.

The shaft measurements were taken at a time when the conveyances in the shaft were limited in their movement in order to obtain results that are not overtly affected by these conveyances. Once the initial measurements had been completed, the winders and the various levels within the shaft were measured over a number of shifts to ascertain whether there were any pressure spikes in the system when the shaft is operating at a steady state.

The above data were evaluated against the current theory such that any strengths and weaknesses of the theory could be confirmed and used in the subsequent analysis. This evaluation also provided an initial check to ensure the quality of the measured data. The analysis was completed immediately after each test so that if additional measurements were required, they could be taken immediately.

1.8.3 Detailed Analysis

During this phase of the work, the results of the evaluation in Section 1.7.2 were subjected to a theoretical analysis. This analysis consisted of two parts:

- 1 Analysis of the shaft systems evaluated with respect to the current available theory
- 2 Analysis of the shaft systems evaluated by means of a computational fluid dynamics (CFD) model

1.8.4 Conclusions

The conclusions on the specific design considerations are drawn in a manner that will allow any future design work to include the recommendations from this work.

In addition, potential areas of difficulty are highlighted and the area that will make the most significant difference to the shaft resistance is defined.

Finally, recommendations are made as to what direction future work in this regard should take.

1.8.5 Outline of the Study

This chapter has described the background to the work and its specific objectives. Chapter 2 provides an overview of the literature available on this subject, without commenting on work not directly associated with the stated objectives.

CHAPTER 3 presents the experimental procedure and the specific analysis techniques used in the evaluation. The results of this evaluation and analysis are in CHAPTER 4 and CHAPTER 5. The final chapters give the conclusions drawn from the analysis and comment on the economic evaluation of the shafts.

1.9 SUMMARY AND CONCLUSIONS – CHAPTER 1

1.9.1 Summary

As a result of the rising electrical energy costs in South Africa, a method was being sought to reduce the overall electrical consumption of typical mine shaft systems. To achieve this, the first step was to analyse a typical shaft system and to determine what areas required the most energy to operate.

A typical shaft configuration was analysed and the primary energy consumers were identified. The ventilation fans for this system were found to consume 15% of the total energy of the shaft system. More than 50% of the energy supplied to an equipped downcast shaft to move the ventilation air through the shaft was calculated to be consumed by the shaft itself, more specifically by the pressure losses that occur in the shaft as the ventilation air passes through it. This area was deemed worthy of additional evaluation.

This evaluation took the form of completing a series of static tests on the shaft to determine the actual pressure losses of the systems and comparing these losses with those predicted by the current available theory. No. 14 shaft at Impala Platinum was used for these tests.

No. 14 shaft consists of two downcast and two upcast shafts. The pressure losses in each of these were measured and compared against the theory. It was found that there was a difference of

approximately 20% between the theory and the measured results. More importantly, it was noted that 54% of the electrical energy consumed by the ventilation fans was used to overcome the pressure losses within the equipped downcast shaft. The remainder of the work presented here was conducted in order to reduce this percentage by as much as possible.

To complete the analysis, the objectives of the work were defined and the manner in which these were achieved was laid out. The following steps were identified as being required:

- 1 Literature study
- 2 Definition of the objectives
- 3 Evaluation of current shaft configurations
- 4 Detailed analysis
- 5 CFD simulation of the shaft system
- 6 Economic evaluation

1.9.2 Conclusions

The following conclusions can be drawn from this chapter:

- 1 The increase in electrical energy costs in South Africa requires that the electrical energy consumed by shaft systems be reduced by as much as is practically possible.
- 2 One of the primary electrical consumers is the ventilation fans, most of whose electrical energy is required to overcome the pressure drops experienced in transporting air down the equipped shaft.

CHAPTER 2 LITERATURE STUDY

2.1 INTRODUCTION

Chapter 1 of this thesis described the need for the investigation. The specific objectives of this work were defined and the general areas of investigation were detailed with regard to the requirement for finding ways to increase the energy efficiency of shafts in the design phase of projects. With respect to improving this efficiency, the energy losses resulting from the flow of air through shafts were highlighted as being worthy of further investigation.

To ensure that these areas were effectively evaluated, a literature review was undertaken. This review concentrated on the following general topics:

- 1 *Measurement*: The various measurements that have been undertaken are discussed and the results are evaluated against current theory.
- 2 *Theory*: The theory currently available for the evaluation of the pressure drops in shaft systems is evaluated and its efficacy is commented on.
- 3 *Computational fluid dynamics*: The efficacy of using this analysis technique for further evaluation is commented on.

2.2 MEASUREMENT

A comprehensive search of the available literature on the actual resistance of shafts was completed and the pertinent papers are discussed here. Most of these tests were completed circa 1960. At this time the shape of shafts was in the process of changing from rectangular to circular. One of the primary drivers for this change was the increased difficulty being experienced by engineers in ensuring that sufficient ventilation was supplied to the mine workings. It is intriguing to note that the primary driver for the tests was to confirm that the pressure losses would still allow ventilation to be distributed and not specifically to ensure that the overall shaft complex operated efficiently.

It will also be noted that while some shafts were themselves measured, a number of the tests were carried out using scale models of shafts. It is therefore prudent first to evaluate the efficacy of using scale models to draw conclusions on the resistance of shaft systems.

2.2.1 Efficacy of the Use of Scale Models

The use of scale models depends primarily on the use of dimensional analysis in order to understand the importance of certain parameters in the system being considered. A definition was supplied by Pankhurst (1964): “The dimensions of physical quantities can be manipulated algebraically and the results can be interpreted to provide a great deal of information about the physical processes involved in the situation considered.”

Unless the geometry of the systems has no effect on the physical situation to be evaluated, the first requirement of a scale model is that it should be geometrically similar to the actual system being evaluated, i.e. the distance between any two points in the modelled system must bear a constant ratio to the distance between the corresponding two points in the original system. This constant ratio is called the ‘geometrical factor’.

Similarly, we define the kinematic similarity (i.e. when velocities are involved) by the condition that the velocity at any point in the one system bears a constant ratio to the velocity at the corresponding point in the other system. This is called the ‘velocity scale factor’.

Various other factors, such as elastic similarity, thermal similarity, etc., are all defined in a similar fashion but are not pertinent to this discussion.

The limitations of this technique must also be highlighted. Although this technique is powerful and allows a meaningful comparison of scale models with full-scale systems, it must be emphasised that this is only valid as long as the system does not require extrapolation beyond the ranges of the dimensionless parameters defined in the tests. Within these ranges, the dimensional analysis provides the required scale factors, but it provides no information whatsoever about the way in which a given non-dimensional coefficient varies with the dimensionless parameter on which it depends. As a result the specific parameters are allowed to vary and those to which the scale factors will apply must be chosen with care.

As will be discussed below, a number of the measurements carried out and used in the evaluation of shaft resistances were done on scale models (Chasteau, 1962). The two models generally referred to are the 1.981 m (78 inch) model and the 0305 m (12 inch) scale models which were operated by the CSIR. These models were constructed in the horizontal plane and were both configured to allow the flow in them to achieve a fully developed profile before the typical shaft obstructions interrupted this flow. Care was taken to ensure that the mechanical scaling factors for the models and shafts were carefully correlated before tests began. However, as a result of practical limitations, the maximum airflow achieved in these models was half of that generally found in a typical shaft configuration. This had a direct effect on the Reynolds number used in the tests and raises some concern as to the extrapolation of the results.

In order to try and define the extent to which the data from this scale model could be used, various shaft configurations were tested by Chasteau (1962) and the results compared. These tests showed little correlation. In the 0.305 m (12 inch) model, the test showed little agreement even to standard pipe values. The tested values were lower than expected and the results showed that the test flow was potentially not fully developed.

The results also showed that it is perhaps generally better to use direct drag measurements to determine the effect of the resistance of buntons than to use the pressure drop. This has the advantage of removing the pipe wall roughness considerations from the overall measurements. When compared with full-scale shafts, the scaling up of the Reynolds number may be an inaccurate procedure even if the effect of wall roughness can be taken into account. The differences between the two scale models seems to be primarily a result of the difference in wall friction effects. The direct drag measurements do correlate satisfactorily.

In spite of these shortcomings, which show that direct correlation of the results may yield inaccurate results upon calculation, the tests completed are sufficient to demonstrate the empirical direction that should be taken to reduce shaft resistances.

2.2.2 Measured Data Discussions, Results and Conclusions

In 1957, scale model tests were carried out on the configurations being included in the design of Harmony Gold Mining Company's No. 2 and No. 3 shafts (Martinson, 1957). These tests were undertaken at the time specifically because the shafts in question were installing equipment that was novel. It was therefore decided that to obtain an accurate result for the resistance each of the shafts offered to the air flowing through them, it would be necessary to subject the arrangement to scale model tests. These tests went further than the standard measurement of the shaft configuration. To gain an understanding of the overall effect of each of the pieces of equipment that were to be installed in the shaft, tests were conducted as equipment was added to the scale model.

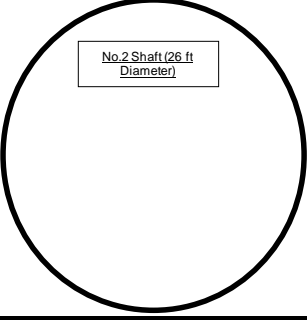
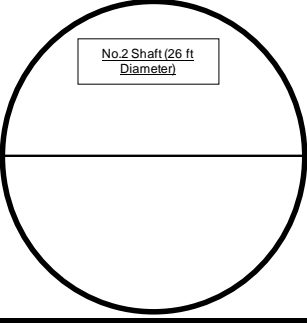
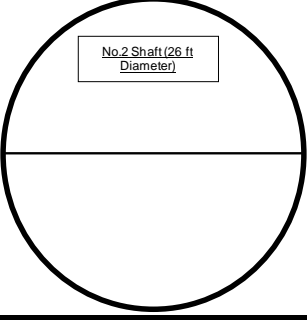
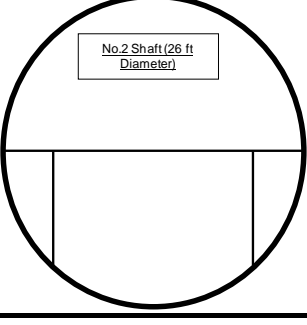
The basic requirements for scale models were adhered to:

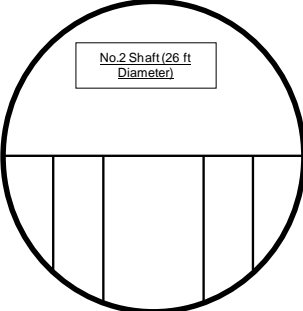
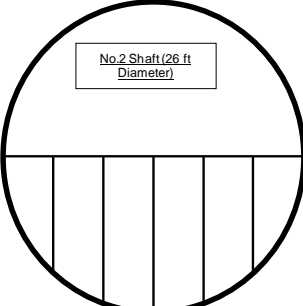
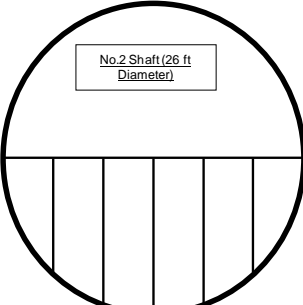
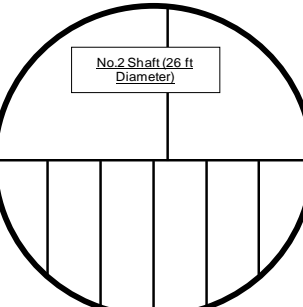
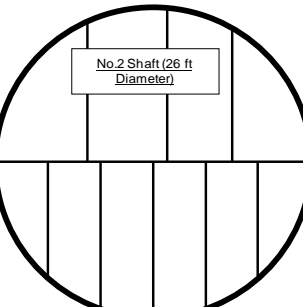
- 1 The scale model must be geometrically similar to the original shaft for which it is being used to predict losses.
- 2 Dynamically similar conditions between the flow conditions in the model and the shaft must exist, i.e. the air velocity in the model duct must be equal to the air velocity in the full-size shaft, multiplied by the chosen scale ratio.

The scale factors that were used are 1:12.9 for the No. 2 shaft and 1:12 for the No. 3 shaft. The details of these calculations can be found in Appendix C. A summary of the various tests completed for the Harmony No. 2 shaft is given in Table 2-1. This table shows the various shaft configurations

that were tested in the scale model. The Chezy-Darcy friction factor that was calculated from the measurement of these models is shown for both shafts in Figure 2-1.

Table 2-1: No. 2 shaft (7.92 m (26 ft) diameter)

	<p style="text-align: center;">Test Number 1</p> <p style="text-align: right;">No buntons</p> <p style="text-align: right;">No buntons</p>
	<p style="text-align: center;">Test Number 2</p> <p style="text-align: right;">Buntion at 9.144 m (30 foot) centres</p>
	<p style="text-align: center;">Test Number 3</p> <p style="text-align: right;">Buntions at 4.572 m (15 foot) centres</p>
	<p style="text-align: center;">Test Number 4</p> <p style="text-align: right;">Buntions at 4.572 m (15 foot) centres</p>
<div style="border: 1px solid black; height: 50px;"></div>	

	<p>Test Number 5</p> <hr/>	<p>Buntons at 4.572 m (15 foot) centres</p>
	<p>Test Number 6</p> <hr/>	<p>Buntion at 9.144 m (30 foot) centres</p>
	<p>Test Number 7</p> <hr/>	<p>Buntions at 4.572 m (15 foot) centres</p>
	<p>Test Number 8</p> <hr/>	<p>Buntions at 4.572 m (15 foot) centres</p> <p>Plus all the guides on the dividers</p>
	<p>Test Number 9</p> <hr/>	<p>Buntions at 4.572 m (15 foot) centres</p> <p>Plus all the guides on the dividers</p>

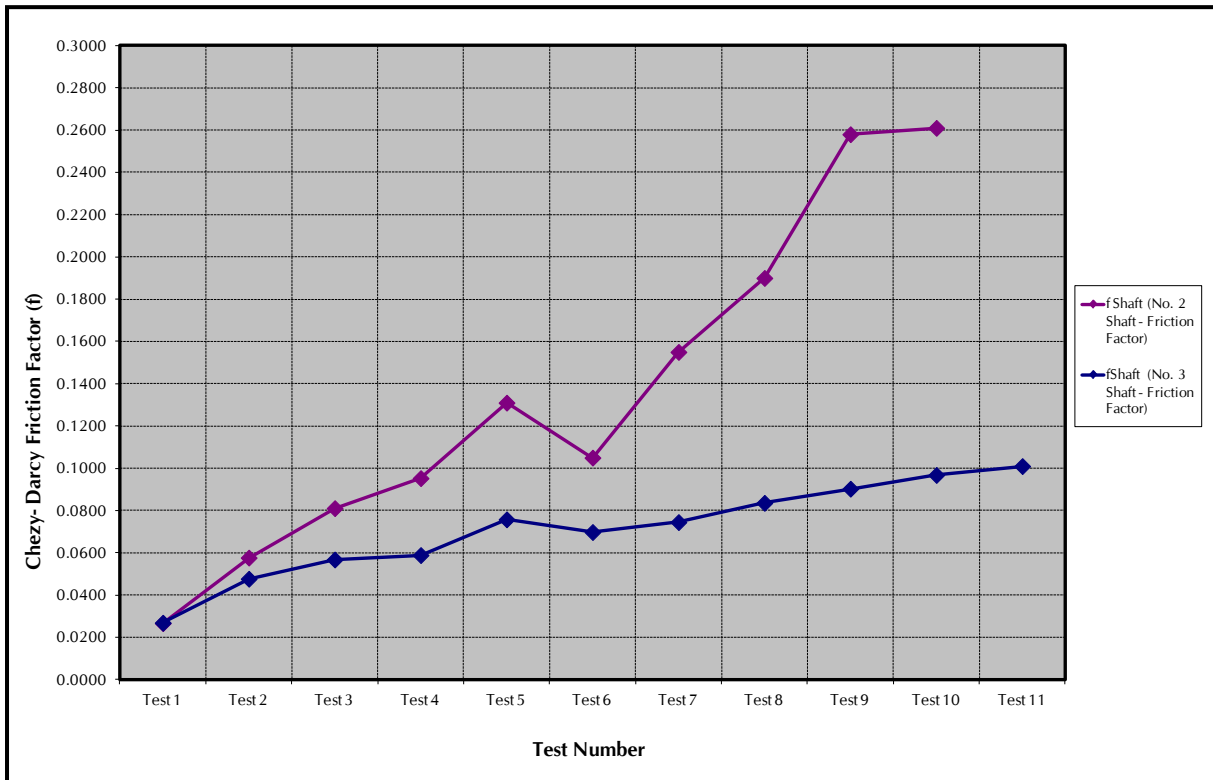
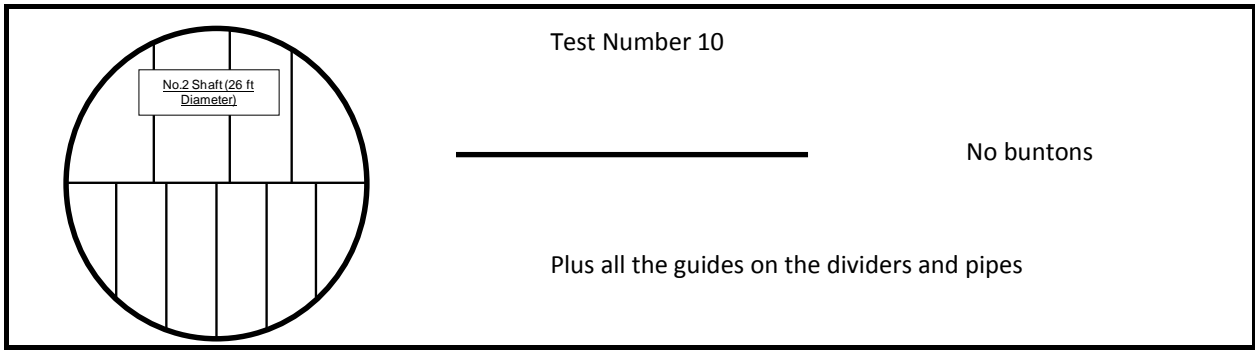


Figure 2-1: Chezy-Darcy friction factors for Harmony No. 2 and No. 3 shaft scale model tests

The tests with this scale model were carried out with Reynolds numbers between 500 000 and 900 000. There are some anomalies in the data. The following general comments are applicable to the data evaluated here:

- 1 The inconsistencies remarked on are particularly apparent for the resistance values obtained for the individual members in No. 2 shaft. The differences in the profiles do not appear to account for the variations in the measured resistances. It was postulated by the author that the changes are due to changes in the velocity profile in the shaft as additional members were added to the shaft cross-section. These differences were also

noted in the test results from No. 3 shaft. It would therefore be advisable to treat the individual resistance values with caution if they are to be applied to other shafts.

- 2 The few longitudinal spacing tests carried out do not provide sufficient data with which to establish any relationship between the shaft resistance and the spacing of the shaft supports. Although these data do demonstrate that increasing the distance between bunton centres has an effect on the shaft resistance, this also asymptotes at approximately 4.572 m (15 foot) centres for the one bunton configuration tested.
- 3 These tests did confirm that the Chezy-Darcy friction factor is largely independent of the Reynolds number, which is as expected.
- 4 The data measured from this experiment were analysed in accordance with current theory. The results of this analysis can be found in Appendix C. The calculations show that there is some correlation with the current theory for the prediction of pressure losses in shafts, but this agreement is not consistent. The difference between the calculated resistance and the measured resistance is consistently approximately 30%. This may be attributed to a number of factors:
 - A number of the parameters need to be assumed from standard tables (e.g. the drag coefficients, the velocity profile of the test section, etc.).
 - There is limited knowledge on the actual scaled system used for the tests other than the broad description. Thus ensuring that the correct values were used for the required parameters was challenging.

This was the first recorded instance of the use of a scale model to test the resistance of a shaft and it is thus expected that there will be some anomalies that will require clarification. The test did, however, achieve its goal in that the shafts in question were shown to be able to support the required ventilation and this proved to be correct.

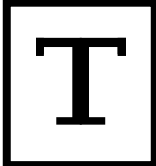






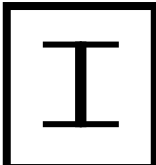
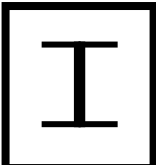
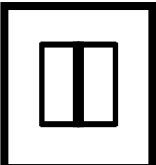
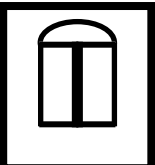
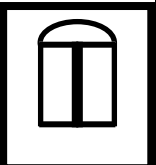
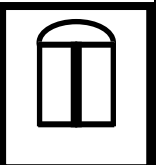
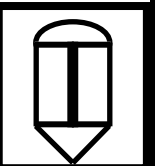
In 1959, Chasteau conducted some basic tests on the Pioneer Shafts of the Buffelsfontein Gold Mine. In this instance some measurements were taken on the shaft itself and these were compared with the results obtained using a scale model test rig. It was a horizontal test rig 1.9812 m (78 inches) in diameter, which resulted in scale ratio of 1:4. The steelwork was manufactured from plywood, including the radii of the buntons. The tests were conducted at relatively low Reynolds numbers. The results from the scale test did not compare favourably with those from the shaft itself. This difference was attributed to the particularly difficult conditions encountered in the shaft during the tests. These comparisons were made with the final test configurations.

However, the scale test did evaluate the different bunton shapes. These were changed sequentially

for the different tests and allowed meaningful comparisons to be made. The initial bunton shapes were standard RSJ sections and modified T sections. These were modified until the overall shape being evaluated was similar to a streamlined bunton connection. These bunton shape changes are depicted in Table 2-2.

The measured results were compared with current theory; the details of these calculations can be found in Appendix C. These calculations showed varying correlation with the measured results. These differences are in some part attributed to the assumptions that were made of the drag coefficients for the various bunton shapes. The tests showed clearly that the streamlined bunton sections offered approximately half the resistance offered by the un-streamlined sections.

Table 2-2: Pioneer shaft bunton shape changes

Primary bunton shapes						
Test 1	Test 2	Test 3	Test 4	Test 5	Test 6	Test 7
						
Secondary bunton shapes						
						
Measured friction resistances of the shaft configuration for the various tests						
0.381	0.255	0.210	0.198	0.168	0.159	0.152
<p>Note</p> <p>Each test considers the primary and the secondary buntions together.</p>						

The following general comments should be noted on the tests conducted for Pioneer shaft.

- i The actual free air velocity measured was very low in comparison with the velocities usually found in shafts.
- ii The general analysis of the system is only to depict how best to reduce the friction of the

shaft; in this it was successful. However, the data are insufficient to draw more than general conclusions about the behaviour of the airflow around the buntions.

- iii The correlation between the measured and calculated figures is strongly dependent on the complexity of the buntion shape being considered.

These two initial tests showed the way forward with respect to both potential shaft layouts and the shape of the buntion to be used for the shaft steelwork. Neither of the papers (Martinson, 1957; Chasteau, 1962) dealt with the placement and efficacy of the services within the shaft or the overall effect of the cage movement within the shaft. In addition, while these results provide general guidance as to the layout and the buntion shapes, neither of these parameters can be used in more than general terms for the analysis of additional shafts.

Graves (1961) noted that before the 1960s, all shafts were rectangular and were designed for the transport of men and materials alone. However, when the energy costs became important and it became increasingly difficult to move ventilation air underground, the shaft resistance to the ventilation air was considered. Graves felt this was worth highlighting in order to emphasise the importance of changing only one parameter at a time in order to obtain the best results. In this instance significant savings were accrued from modifications to the buntions, as well as the use of round shafts. The extent to which each of these changes contributed to these reductions was never ascertained.

In this regard (i.e. the evaluation of rectangular shafts) the effect of changing the equipment in a rectangular shaft was monitored Botha and Taussig (1961). The equipment in this shaft was changed in the following ways:

- 1 Old worn timber sets were replaced with steel sets.
- 2 Existing steel ventilation piping was used to facilitate the carrying of additional downcast air in a timbered rectangular shaft.
- 3 The effect of placing half-round caps on the buntions was evaluated.
- 4 The effect of removing some of the buntions in a shaft was evaluated. This was possible as the hoisting speed was reduced.
- 5 The Chezy-Darcy friction factors for wood, smooth steel and galvanised iron piping in vertical shafts was evaluated.

The shafts were tested but not in detail due to the limited shaft time available. The emphasis was put on getting enough data of sufficiently good quality which could be used on a relative basis.

The following particulars were noted from the tests:

- i It was noted that replacing old timber in shafts with un-streamlined buntons had no beneficial effect.
- ii The large-diameter smooth pipe did help to increase the air-carrying capacity of the shaft without increasing the power consumption.
- iii The half-round caps that were placed on the buntons in the concrete-lined shafts did reduce the shaft resistance by approximately 30%.
- iv It was possible to remove every second or third bunton and this reduced the shaft resistance by between 25 and 40%. The original bunton spacing was 3.048 m (10 ft).

All the changes discussed here are strongly dependent on the velocity of the ventilation air and therefore the required outcome for a specific shaft may require different methodologies and analyses. The nature of the tests was such that the data presented could not be relied on for detailed analysis, but it was hoped they would provide a useful summary. The overall reduction effect is consistent with those found in other shafts.

The next test took the understanding of the resistances shafts offer to ventilation air to another level. In this instance, the resistance that the Vaal Reefs No. 1 shaft offers to the air flowing through it was measured by Quilliam et al. (1961). This is a dry shaft divided into five compartments. Various tests were conducted in the shaft and on the levels to obtain measurements that would allow the calculation of the shaft resistance. However, the details of the tests and the observations made were not included in the paper. It was stated that during the tests the ventilation fans were baffled in order to vary the velocity of the air in the shaft. These variations in velocity showed that there was a significant difference in the resistance in the lower Reynolds number range, but that this difference was reduced once the higher Reynolds numbers were used.

Once the above tests had been completed, Chasteau (1961) set up the scale model to be similar to the Vaal Reefs shaft in order to verify the measured data. The same scale arrangement was used as for the Pioneer shaft discussed above. In addition to this, a 1.981 m (78 inch) wind tunnel and the 0.305 m (12 inch) wind tunnel were used. These tunnels had scale ratios of 1:1,393 and 1:24 respectively. Once again, as the scale models were equipped, the buntons were increasingly streamlined and the differences measured. In both of these models the data showed significant scatter when lower Reynolds numbers were used for the testing. Although the resistance at these lower velocities was also noted to be lower, this scatter was attributed to the inadequacies of the instrumentation used. At high Reynolds numbers, i.e. 1.2×10^5 for the 1.981 m (78 inch) model and 2.5×10^5 for the 0.305 m (12 inch) model, the Chezy-Darcy friction factor calculated from the data became constant. In addition, in the sections of the wind tunnel that had no 'equipment' installed, it

was noted that the results were very similar to those of the full-scale shaft measured.

The data were also plotted against the mean air velocity in the scale models. This showed a much better correlation to the shaft measurement than the Reynolds number, prompting speculation from the author that this was perhaps a better way to depict the results. It was also recommended that, in order to understand the air flow in the mine shaft more fully, the turbulence characteristics of the models and the mine shaft needed to be better correlated. In spite of this there was good agreement between the shaft test results and those of the scale model.

These tests and comparisons provided additional insight into the working of the shaft system. However, there are a number of questions that the tests still did not consider:

- i An increase in the turbulence of the scaled systems from 1% to 3% resulted in an increase in the drag coefficient from 1.27 to 1.33. This highlighted the individual nature of shafts as the majority of the turbulence experienced by the shaft ventilation air is induced by the structure within the shaft. It also emphasised the importance of ensuring the accuracy of the various coefficients used for the theoretical evaluation. (in this instance, the intensity of turbulence encountered is measured by the non dimensional number N, where

$$Re = \frac{\rho D U}{\mu} = \frac{\rho D U}{\rho l v} = N$$

Where:

Re	-	Reynolds Number
ρ	-	density
D	-	diameter
μ	-	dynamic viscosity
l	-	mixing length
v	-	component of turbulent velocity at right angles to the mean speed U
N	-	non dimensional number for turbulent flow equivalent to the Re number in laminar flow

- ii The results from the two wind tunnels agreed reasonably well for Reynolds numbers of 400 000, but this agreement was closer for buntons that were further apart.
- iii The resistance of the shaft only was evaluated, and of the shaft and the equipment in it. No attempt was made to evaluate the effect that the age of the shaft and the age of the skips might have on the resistance of the shaft.

- iv The aim of the general analysis of the systems was only to depict how best to reduce the friction of the shaft; in this it was successful. However, the data are insufficient to draw more than general conclusions about the behaviour of the airflow around the buntons.
- v There seems to be a linear relationship between the increase in the bunton spacing and the resistance of the shaft.

The measured results were compared with current theory and the details of these calculations can be found in Appendix C. These calculations showed varying degrees of correlation with the measured results, with one measurement showing a significant difference. The average percentage difference is approximately 50%. It is thought that these differences are a result of the assumptions made for the drag coefficients for the various bunton shapes that had to be estimated. This is thought to be one of the primary reasons for the discrepancies between the calculations and the measured results. However, as was noted by Chasteau (1961), perhaps some portion of these differences could be accounted for by the lack of adequate instrumentation, especially where the lower Reynolds numbers were used.

At this stage of the progress in determining the actual resistances of shaft systems, we have a number of scale model tests, none of which were verified with field tests. Graves (1962) helped to fill this gap by testing three shafts to determine their actual resistance to airflow. The basic characteristics of each of these shafts are listed in Table 2-3.

Table 2-3: Tests on downcast shafts

Description	Shaft No. 1	Shaft No. 2	Shaft No. 3
Name	President Brand No. 3	Vaal Reefs No. 2	Western Deep Levels No. 3
Bunton type	AirSave	Squashed pipe	Squashed pipe
Coefficient of drag	$C_D = 1.55$	$C_D = 1.25$	$C_D = 1.25$
Shaft depth	1 219.2 m	1 493.2 m	1 592.9 m
Bunton spacing	4.572 m	6.10 m	6.10 m
Velocity of air in shaft (free air velocity)	12.93 m/s	10.19 m/s	10.10 m/s

All the shafts had pipes and cables in them, but not in significant quantities. All the cages being used in the shaft were parked on the bank during the tests and the air was entrained in the shaft below this level, resulting in the measurement of an unobstructed shaft.

The results of these tests were tabulated and conclusions were presented by the author (Chasteau, 1961). These are:

- 1 The resistance of the slim (0.102 m (4 inch) wide) hexagonal buntions is appreciably less than that of the rather thicker (0.152 m (6 inch) wide) rounded buntions.
- 2 The wider vertical spacing of the buntion sets results in a reduction of the shaft resistance.
- 3 The 0.152 m (6 inch) squashed pipe buntions used show a lower resistance than the semi-streamlined buntions.
- 4 It is concluded that the streamlined buntions do in fact reduce the airflow resistance by some 50% over the standard I sections.

The measured results were compared with current theory. The details of these calculations can be found in Appendix C. These calculations again showed varying amounts of correlation with the measured results, with one measurement showing a significant difference. The average percentage difference is approximately 50%. It is thought that these differences are a result of the assumptions that were made in determining the drag coefficients for the various buntion shapes. In addition, no information was made available about additional inclusions in the shaft, such as levels and intermediate pump station levels, all of which would have an effect on the measured shaft resistances.

Although this paper does not deal with the dynamic aspects of the resistance losses and does not evaluate actual shaft configurations, up to this time this was the most complete set of results that had been compiled for the evaluation of shaft resistance. However, the measurements were only taken at the top and bottom of the shaft and no attempt was made to identify the progressive resistance of the shaft. This could also be one of the factors that resulted in the difference between the theoretical calculations and the results from the research work, as none of the effects of the station steelwork or the stations themselves was taken into account.

Nevertheless, the data presented here once again provide empirical evidence as to the validity of the design of shaft systems using more streamlined buntion sets. Martinson (1962) notes that as a result of the work completed on the resistance of shafts, the use of RSJ as buntions and dividers in shafts had been scrapped. This scrapping was matched by an increase in the buntion spacing for the same reason, namely to reduce the resistance of the shaft. He also noted that both the 'airsave' buntion and the 'squashed pipe' buntion significantly reduced the resistance of the shaft, but

cautioned against the statement that the actual resistance of the 'airflow' bunton was higher than that of the 'squashed pipe' version, as this statement was based on observations made on two different shafts without an effective evaluation of other variables. He recommended that these buntions should first be tested in similar conditions before such statements were made.

In an attempt to quantify the actual effect of the various systems in the shaft, Chasteau and Kemp (1962) conducted a series of tests on a scale model. The initial tests showed that the increased streamlining of buntions reduced the shaft resistance. Although this was not new, additional variations in the shaft configuration also showed that streamlining the central portion of the shaft cross-section had the most significant effect on the overall shaft resistance. It was noted as well that the most significant reduction occurred when I sections were converted to streamlined sections. There was, however, little difference when tails were added to this configuration.

These tests were also the first to consider the contribution made by the cables and pipes to the resistance of the overall shaft. Removing the cables resulted in a reduction of 10% and removing the pipes and the associated brackets an additional 11%. Lambrechts and Deacon (1962) built further on this work by testing the changes in shaft resistance in a shaft while it was being rehabilitated, i.e. with the rough wall smoothed and the bunton and guides in the shaft removed. In this instance, the shaft resistance was reduced by 87% when the buntions, guides and associated connections were removed. An additional 50% reduction in the shaft resistance was noted once the rough wall had been smoothed.

Casati and Martinson (1962) also added to this growing database by using a model to measure the effect that bunton spacing had on the overall resistance of the shaft. This test showed that the resistance of the shaft equipment was significantly higher than that of the shaft wall. The test also showed a reduction in the shaft resistance as the bunton spacing was increased.

Casati and Martinson (1962) also did tests on a different model. In this instance the No. 4 shaft at City Deep Mine was modelled. This is a circular shaft. One result of interest from this test was that the lined portion of the shaft showed a resistance of approximately 40% less than that of the unlined portion. Another interesting result was that the addition of various pipes and cables decreased the resistance of the shaft. No reason was proposed for this anomaly and no additional investigations were made at this time. Once again no effort was made to evaluate the effect of the shaft cages on the shaft resistance.

In this regard some anomalies were noted in ventilation pressure and energy surveys at Freddie's Consolidated Mine Limited (Unsted and Benecke, 1978). There were large variations in absolute pressure, sometimes accompanied by airflow reversals. These reversals were traced back to the passage of the large cage in the downcast shaft at No. 3 shaft.

To establish how this occurred, barometers were placed at the bank of No. 3 and No. 1 shafts and on 53 level of the same shaft. It was noted that the barometric pressure was considerably lower when the cage was below the observation point than when above it. In addition, the barometric pressure fluctuations at No. 1 and No. 3 shafts were 'in phase' and these phases were linked to the position of the cage in No. 3 shaft. No. 1 and No. 3 shafts are approximately 4 500 m apart and these pressure variations were instantaneously transmitted throughout the ventilation system. This was due partly to the high velocities present in these shafts. An air flow velocity of 18.9 m/s was present in No. 3 shaft and this increased to approximately 25.4 m/s when the cage was in the shaft.

In order to effectively evaluate the response of the ventilation flow in a shaft to cages moving through the shaft a study was undertaken by Ruglen and Wilson (Ruglen and Wilson, 1978). In this paper various shaft and haulage configurations were evaluated, including the effect of conveyances on ventilation flow in a shaft. One of the most significant findings was the large effect that the inclusion of ribs had on the overall resistance that the conveyance offered to ventilation flow through the shaft. The importance of keeping the cages doors closed while moving the conveyance through the shaft was also noted. While little data was included in this report, it was noted that reduction in the losses around the cage could be reduced by as much as 50% for a cage with a shaft blockage of 30%, but that this reduced to 40% for the blockage of 50%. The optimum size of fitting size of fairing was found to be between 0.3 and 0.35 times the width of the cage.

2.2.3 Significance of Available Data

All these tests provide valuable empirical data, as well as valuable direction as to the way in which the design of shaft systems should proceed. There is a definite trend towards the following criteria for shaft design at this point:

- i Buntions and guides should be streamlined.
- ii Shaft walls should be lined.
- iii Buntions should be spaced as far apart as possible.
- iv In addition, it is important to ensure that the velocity profile in any test section is as close to that of the shaft as possible.

Up to this point, however, no definitive data are available on the actual manner in which the above systems should be designed. This is primarily a result of the difficulty in measuring the actual resistances of installed shafts and, once measured, of the high requirements in terms of time and cost to adapt their configuration for additional tests. This led to the use of scale models. The accuracy of such models and concerns surrounding their use and results have been described.

In addition, there is no reference to the quantification of the results in accordance with the procedure presented by Bromilov (1960). The calculations performed during this research project are based on the work presented by Bromilov (1960) and latterly McPherson (1987), and there is little correlation between these and the tests carried out.

Finally, although the manner in which the various measurements were taken is recorded, little information is available from the actual data measured and, other than the reference by Chateau (1961) to the accuracy of the instrumentation and its placement, no comment is made on this.

One of the objectives in reviewing these papers was to try and find additional data to calibrate a computational model. In this instance the difficulties associated with the measurement of shaft resistances were highlighted, particularly with regard to ensuring that sufficient time is allowed in the shaft to complete such measurements.

It was also noted that the horizontal test chamber (Chateau, 1962) showed little reduction in the shaft resistances when pipes and cables were introduced. Other papers to note this was that presented by Casati and Martinson (1962). This reduction was also noted by Bromilov (1960) and this highlights the danger of using scale models without fully understanding their ramifications.

The effects of the uniqueness of each shaft layout, the resultant effect on the turbulence of the shaft and its effect on the measured coefficient of drag were also highlighted by Chateau (1961). As a result of the general lack of information available on the shafts and models being tested, the various methods available for testing shaft resistances accurately are discussed below.

The investigation of fairings on the shaft conveyance is worthy of investigation as these can also result in reductions in the overall losses experienced by the shaft.

2.2.4 Methods of Testing Shaft Pressures

The actual manner in which the measurements were taken for the various tests should be considered when evaluating the current results. The shaft measurements discussed above used different techniques for measuring the pressure and free air velocity at various points in the shaft. Three recognised techniques are used to evaluate the resistance of a shaft:

- 1 Density method
- 2 Full volume–Reduced volume method
- 3 Trailing hose method

Bareza and Martinson (1961) commented on the efficacy of using these methods for the measurement of shaft systems and these comments are discussed here to highlight the fact that when systems with large vertical differences (i.e. shaft systems) are tested, there are often

parameters that normally would not cause concern but that suddenly become very important to control if accurate measurements are to be achieved.

- 1 *Density method:* The pressures at the top and bottom of the shaft are measured. The pressure at the bottom of the shaft is then compared with the calculated pressure that should occur at the shaft bottom, assuming the shaft was frictionless. This method requires some calculation and it is therefore an indirect method of measurement.
- 2 *Full volume–Reduced volume method:* This is based on the fact that the pressure loss in any given section of an airway is a function of the flow rate and of the mean density only. This method is useful because of its simplicity, but to obtain good results it is better used in areas where the difference in the flow rate is large. This is also an indirect method of measurement.
- 3 *Trailing hose method:* When this method is used, density correction must be applied to obtain the correct value (Barenbrug, 1962). If this is not done, the error can become significant when pressure is evaluated over the length of a shaft. This is, however, a direct measurement system, albeit one given to inaccuracy due to the long vertical differences between each of the measurement points.

Density method

In order for this method to apply, it is assumed that the density of the fluid varies linearly with the elevation. This assumption is of particular importance when evaluating the theoretical term over large elevation differences where the assumption of linearity may not apply.

An examination that was conducted by Hemp (1975) showed that the assumptions noted above did provide reasonably accurate results but that there were also a number of cases where this was not true. To try and achieve better accuracies, Hemp suggested a two-pronged: approach:

- i Recognise the assumption that conditions along an airway are perhaps not valid.
- ii Use a method for correcting the pressure survey results to allow for departure from the assumption.

A method is supplied to test the accuracy of the calculations, but this has not gained general acceptance. In order to ensure, as far as is practically possible, the accuracy of the planned tests, this calculation must be completed for steady-state tests to verify the testing procedure. However, the act of correcting data could also corrupt the reason for the measurement, which is to ascertain the extent of the pressure losses that occur during the dynamic conditions of the cage movement, and it will thus not be used once the procedure has been confirmed.

Suffice it to say that when the experimental procedure is designed it must take cognisance of these

potential inaccuracies and ensure that the requirements to avoid them are met. Although it should be noted that there are problems associated with this indirect measurement method, these problems can be overcome by proper design of the survey.

Full volume–Reduced volume method

This survey method involves measuring the barometric pressure, as well as the wet bulb and dry bulb temperatures at the two ends of the survey. These measurements are taken during the full flow condition and during the reduced flow condition.

This method has advantages. However, to be able to calculate the pressure drop over an operating shaft, it is not possible to reduce the volume of air flowing through it without affecting the production of the shaft. This method will therefore not be considered further here.

Trailing hose method

The principle of this method is straightforward. A hose is laid along the length of the airway and a suitable pressure differential measuring device is attached to either end. If the airway is horizontal, then the differential pressure is equal to the friction pressure loss. In a vertical airway this is not identical, but calculations can be used to find the friction pressure loss.

This method has its advantages and disadvantages, all of which can be corrected. For example, care must be taken to ensure that the psychrometric properties in the hose are the same at different elevations. This is most easily taken care of by ensuring that there is no moisture in the hose and that the conditions are such that condensation does not occur. This method has one primary disadvantage, namely the physical length of the hose and the logistics of laying a trailing hose in a shaft more than 1 000 m long. This method will therefore not be considered further here.

Kemp (1962) investigated these methods of measurement and commented specifically on the use of the trailing hose method of resistance measurement. He noted that the use of the trailing hose resulted in error owing to the differences between the density of the air in the shaft and the air in the manometer tubes. This effect increases as the length of the trailing hose increases. This concern can be overcome by ensuring that the air in the manometer is at the same temperature as the shaft air. In addition, the hose should be well ventilated with the shaft air to ensure consistent moisture content before the tests are started.

2.3 DESIGN CONSIDERATIONS

Any discussion on the design of shaft systems and their evaluation with respect to the resistance they offer would not be complete without discussing the work contributed by Bromilov (1960). Bromilov separated the resistances for the various items in a shaft system in order to evaluate each of these items separately. The sum of the resistances offered by each of these items listed below results in the calculation of the total shaft resistance:

- 1 Shaft walls
- 2 Shaft fittings (buntons, guides, pipes, etc.)
- 3 Cages and/ or skips

The base assumption of this work is that the resistance offered by each of these items is independent of the resistance offered by the others. In the context of the work produced by Bromilov, each of these will be discussed separately because the analysis techniques for each differ.

Shaft walls

The resistance of the shaft wall is calculated using factors available for standard pipe theory for skin Chezy-Darcy friction factor of the wall or the duct wall. These Chezy-Darcy friction factors allow the calculation of the resistance of this item based on its size, the roughness expected of the wall and the flow of air through it. The limitation of this theory is that it can give conservative results when very rough walls are included in the calculation.

Guides, pipes and cables

It was noted that fittings such as these may actually reduce the resistance in a shaft. Nevertheless, the resistance they offer is estimated by subtracting the area of these fittings from the area of the shaft to obtain an increased air velocity. To calculate the resistance offered by fittings such as flanges, the free area used for the calculation of the increased velocity is reduced by the amount that the flanges reduce the overall area available.

It should be noted that no attempt is made to quantify the potential decrease in the shaft resistance as a result of the inclusion of these items or to quantify the additional turbulence that would occur as a result of the inclusion of discontinuities such as the flanges. It was, however, postulated that the reduction in resistance is based on the reduction of the swirl in the shaft.

Buntons

The calculation of the resistance that the buntons offer the airstream is based on the drag that the buntion would experience. This drag is defined as follows (McPherson, 1987): “A body placed in an airstream is acted on by forces due to the movement of the air past it. The force on the body that is parallel to the airstream is known as the drag and is proportional to the approach velocity to that body and of the air and frontal area of the body presented to the airflow”.

One of the limiting assumptions for this theory to apply is that the airflow past a set of buntons is not affected by the presence of the buntons upstream. To estimate this effect, the calculation includes for the use of an interference factor, which is calculated based on the distance between subsequent sets of buntons.

Cages and skips

The calculation of this is based on work by Stevenson (1956). Stevenson used a horizontal duct of circular cross-section in which he placed cages of various configurations and sizes, and measured the response of the airstream to these. The resistance that these offer to the airstream has been included in Bromilov’s calculation via the use of various factors applied to the cage based on its shape, size and length.

It was interesting to note that Stevenson also investigate the use of fairings. The judicious use of these resulted in the measured resistance of the cage reducing, in some instances by more than half. The application of this work does, however, assume that the cages are sufficiently far apart such that any disturbances they apply to the airflow will not affect the other conveyances.

2.3.2 General Discussion

At the time, Bromilov’s work was the first attempt to calculate the actual resistance offered by shaft systems. Following this work, Van Wyk (1961) presented a paper which discussed the design requirements of shaft systems with the respective resistances a shaft would be expected to offer. Van Wyk did not refer to Bromilov’s work, but the conclusions reached were similar. He produced a table comparing the unit cost of each of the buntion shapes with the resistance they offered to the flow of air in the shaft. However, before one can have a meaningful discussion on the most cost-effective system to be installed in a shaft, it is necessary to have a better understanding of the current shaft steelwork design theory of shaft systems.

The current design theory and understanding of the ideal buntion and guide connection holds that shaft system should be designed so that the buntons are as flexible as possible and the guides as rigid as possible. This arrangement offers the best configuration for the support of the conveyances as they move in the shaft and the constraint of the conveyances within their travel paths. This

requirement is fortunate as the more slender buntons have a significant advantage for the flow of ventilation, and the cross-section of the guides that is generally presented to the flow is minimal.

Rope guides should also be considered in the design of shaft systems as they present the smallest cross-section to the airflow. However, the large space requirements between the conveyances in such a shaft and between the conveyances and the sidewall are such that a large shaft is required to accommodate a number of conveyances. There is also the complication in multi-level mines that each of the conveyances to be used must be constrained at each of the levels that the cage serves. This generally requires construction of a system that will protrude into the shaft, thus creating a potential safety risk to the operators of the shaft. Any constraint in this regard will also have an effect on the cycle times of the conveyances.

In shallow mines, the portion of total capital cost apportioned to shaft sinking is relatively small. This cost increases substantially as the shafts are sunk to deeper levels. It is therefore important to utilise this capital expenditure as efficiently as possible. This means that a shaft must be designed to permit maximum hoisting while still allowing the maximum ventilation through the shaft. There are basically three ways to reduce the resistance of the shaft during the design phase. These are:

- 1 Improve the aerodynamic shape of the obstructions.
- 2 Reduce the frontal area of the obstruction.
- 3 Increase the space between the obstructions.

A fourth way will be examined in this thesis, and that is optimising the layout of the cages, skips, guides and services in such a way as to minimise the overall resistance offered by the shaft.

Knowing the interaction between these options is important, and Van Wyk's paper highlights some of the more significant concerns in this regard.

Once the aerodynamics have been considered, the only other methods left for reducing the shaft resistance are to reduce the frontal area of the shaft fitting and to increase the spacing between the buntons. These methods must be considered in conjunction with the alignment of the shaft. If the shaft can be correctly aligned, then it is possible to reduce the strength the buntons needed and the number of buntons can be reduced.

With regard to increasing the bunton spacing, it must be noted that with the improvement of the aerodynamics of the buntons, the effect of increasing the bunton spacing becomes less pronounced (Martinson, 1962). The use of these buntons must, however, be considered in conjunction with the complications they introduce, with respect to both the installation and maintenance of the shaft. Once these criteria have been optimised, the auxiliary services become important.

In conclusion, Van Wyk felt that the contribution of the shape of the bunton to the shaft resistances

had reached a point where it could now be considered fully developed. He proposed that the emphasis now be placed on the design considerations.

In this paper, Van Wyk highlighted the specific design concerns that the shaft engineer had to consider. However, no theory other than the broad terms described above was included. In addition, all the comments he made were with respect to static installed systems. He did not comment on the resistance offered by the cages or the specific placement of the services and how these placements could affect the shaft resistance.

Bromilov's (1960) work was further built on by McPherson (1987). In this work McPherson simplified and metricated the calculation of shaft resistances. He also introduced the concept of 'rational resistance'. In this representation the resistance depends only upon the airway geometry and roughness, and is independent of air density.

In addition, he proposed the use of the Colebrook-White equation for the derivation of the shaft Chezy-Darcy friction factor. This equation is based on the Moody chart for the Chezy-Darcy friction factor and is consistent with the work Bromilov presented. The use of this equation does allow the mathematical evaluation of the shaft lining in the more conventional manner.

The theory used in McPherson's paper was consistent with that proposed by Bromilov. He also evaluated the results from Stevenson's tests and included these in the evaluation of the resistances offered by conveyances in the shaft. In this paper McPherson did not add significantly to the store of knowledge available for the calculation of shaft resistances, but he did simplify its application.

In conjunction with the work by McPherson, Wallace and Rogers (1987) conducted a survey of the shafts currently being used around the world and how they were configured. In this survey, questionnaires were sent to various mining companies. A total of sixteen mining operations participated in the survey with a total of 37 shafts. In this survey the following information was supplied:

- 1 *Coefficient of fill (C_f):* This is the percentage of area that a conveyance occupies in a shaft.
 - 23 shafts had a C_f of less than 20%.
 - 8 shafts had a C_f greater than 50%, all of which were men and materials downcast shafts with a single conveyance.

The trend is therefore that men and materials shafts have a greater C_f while hoisting shafts have a lower C_f . In addition, it was generally noted that as the shafts became deeper, the C_f was lower.

- 2 *Free air velocity:* This is the velocity of the ventilation flow in the free area of the shafts.
 - The most common free air velocity was 5 to 7.5 m/s. (Approximately half of the

men and material shafts were in this range.)

- The highest free air velocity was 17.85 m/s.

The modified theory put forward by McPherson (1987) was evaluated by Deen (1991). Deen's specific aim was to define the resistances of shafts and to validate these calculations based on the theory. The shafts chosen for this study varied in size, shape, depth and general fitting arrangements. This work included the review of a rectangular shaft. Deen achieved very good accuracy when comparing his calculated resistances with those calculated using the current theory. The accuracy on three of the shafts was to less than a 5% difference and the difference was 11.8% for the final shaft.

In this exercise, the comparison showed good congruity between the theory and the results. Unfortunately, no information was supplied on how the tests were done, or the assumptions used for the basis of the calculation or the detailed comparison of the results.

In the evaluation of the theory discussed above, all the calculations require that a good database be available for evaluation of the various resistances. In this regard, Fytas and Gagnon (2008) compiled a database of ventilation factors obtained from various mines in the Quebec province of Canada. The reason for undertaking this exercise was increasing concern that the current Atkinson friction factors were based on historical factors obtained from old workings. It was argued that these factors were no longer applicable as a result of advances in mining layouts and techniques. In the compilation of these figures, 137 Atkinson friction factors were measured in 10 underground mines. Unfortunately, no shaft resistances were measured. However, good data were supplied from current mining operations and it was possible to compare the resultant Atkinson friction factors with the historical data. These data showed that small reductions in the measured Atkinson friction factors were possible when compared with the older data.

Fytas and Gagnon's (2008) paper did highlight the importance of ensuring that the Atkinson friction factors used in any evaluation are appropriate to that application.

The design of any system must, however, be undertaken with full cognisance of the capital and operating cost ramifications of any decision. In this regard, there are several costs that influence the size and equipping of shaft systems, namely:

- The total ventilation air that the shaft is required to accommodate
- The cost of the shaft and its equipment
- The limitation of the velocity of the air passing through the shaft
- The size of the equipment to be carried through the shaft (i.e. skips, services, cages, etc).

The general operating costs for ventilation systems have not changed. Barenbrug (1961) noted that:

“As is often the case in engineering plants, a high capital outlay could result in low operating costs, or low capital outlay in high operating costs and in the ventilation of mine, the same principles hold good. Large diameter shafts with large capital outlay usually result in smaller fan power requirements whilst for the same volume small diameter shafts require large fan power because of the high resistance to airflow. There is thus for a certain volume of air a size of shaft which will give the lowest total cost”.

In this regard he noted that the operating costs with respect to a shaft are dependent on

- 1 the volume and mass of the air transported
- 2 the density of that volume
- 3 the length of the shaft
- 4 the perimeter of the shaft
- 5 the area of the shaft
- 6 the overall Chezy-Darcy friction factor of the shaft
- 7 the mean density of air in shaft
- 8 the power cost per unit
- 9 the fan efficiency and the maintenance cost of the fans.

Prince (1961) noted particularly that the shaft is a wasting asset and that for the increase in capital to be used in the sinking of a shaft to be useful, it should be evaluated against the borrowed capital rate to evaluate the actual return on capital. Uhlmann (1961) noted that a more correct criterion for the most economical size (of shaft) is that point at which the percentage return on increased capital expenditure is equal to the rate of interest that the client can obtain on alternative investments or which he would have to pay for borrowing the extra capital. This point must be noted as the overall requirement for the sinking of a shaft is to make a gain on the overall capital investment. This is entirely consistent with the approach suggested by McPherson (1993).

Wells (1973) also emphasised the importance of incorporating the operating costs of the shaft with the overall capital required to build the shaft. The specific emphasis of the design to reduce the resistance of the shaft is correctly based on the fact that the cost of power to overcome the internal resistance to the flow of air through a shaft will live with the mine for its full lifespan. In this regard Wells recommended that the design of shaft parameters that affect the resistance of the shaft should be very carefully considered when designing the internal configuration of a shaft. The additional expense incurred in the construction stage is generally negligible when compared with

the benefits that will accrue for the rest of the life of the mine. Some of the more important parameters are listed below:

- Arrangement of shaft steelwork
- Spacing of buntons
- Streamlining of buntion cross-section
- Alternative methods of guiding conveyances (i.e. stub buntions, rope guides, etc.)
- Smooth concrete lining
- Widening of shaft at station elevations
- Bank bypass (independent ventilation inlet)
- Long narrow conveyances
- Scientifically designed ventilation inlets or outlets from the shaft (i.e. splitter blades)
- Fairings to streamline conveyances
- Evase design

This requirement to design efficient shafts goes hand in hand with the requirement to contain the operating costs of the mine. To contain these costs it is necessary that the ventilation engineer on the mine should understand fully the resistance factor within that mine. Once this is achieved, specific steps can be taken to control and improve the overall resistance. Krishna (1992) noted that it is of vital importance that the mine ventilation planning be integrated with the overall mine production and layout planning. This is especially true of the shaft system as decisions affecting this system can have a significant effect on the overall power consumption of the mine. Although deficiencies in the design of these systems can be easily overcome by increasing the pressure that the main ventilation fan can accommodate, this pressure is dissipated in the shaft system and cannot be used to ventilate the mine. It should also be borne in mind that the relationship between power and airflow is cubic, and the cost of these increases is substantially more than the linear value of the increase.

Seeber (2002) also emphasised this point. He noted that through the generation of the Atkinson friction (K) factor, mine operators have a viable means of assessing the impact that ventilation costs have on their operations. The relationship between the pressure drop in the system and the energy required to overcome that pressure drop is a simple mathematical process, providing the mine operator has a good understanding of a ventilation system's resistance characteristics.

2.3.3 Significance of Available Data

The theory described in this section allows for the complete mathematical design of a shaft system with respect to the resistance that the shaft will offer to air flowing through it, but some critical questions regarding this analysis remain unanswered. These concerns are:

- 1 As the duty required of shafts increases and they are used to transport more services underground, the actual effect of the shaft fittings needs to be quantified. This is especially applicable when it is considered that both Bromilov (1960) and McPherson (1987) commented on the potential decrease of the shaft resistance through the judicious placement of these. In addition, the effect of the connections of the fittings (i.e. pipe flanges, cable brackets) needs to be evaluated so that an explicit solution can be derived.
- 2 The effect that conveyances have on the resistance of the shaft needs to be more explicitly quantified. This is especially important when the behaviour of large conveyances is considered, with respect to both the forces they apply on the shaft steelwork and the resistance they offer to the ventilation air.
- 3 The effect that the shaft steelwork has on the ventilation air has been quantified based on the drag resistance it offers to the airflow. In addition, it is noted that the further away the buntons are from each other, the better. Although this had been proven, the actual effect of these on each other required quantification.

The maintenance of shaft systems must be optimised such that it takes as little time in the shaft as possible. In the evaluation of these systems cognisance should also be taken of more recent trends in shaft system design, specifically the general increases in design air velocities. Biffi et al. (2006) noted that although equipped shafts inherently present a higher frictional resistance to airflow, they are also designed for higher air velocities.

The free air velocities in equipped shafts may be as high as 12 m/s and air velocities of up to 22 m/s may be tolerated in unequipped shafts, although some of the free air velocities in South African shaft are higher. These velocities are higher than those recommended by McPherson and are indicative of the requirement to make capital assets such as the shaft work as hard as possible to service the mine's general requirements.

2.4 COMPUTATIONAL FLUID DYNAMICS

Computational fluid dynamics (CFD) was proposed as a method to help further the understanding of shaft resistances. The first instance of the use of this technique in mining was by Wala et al. (1993). One of the objectives of this paper was to show how CFD simulations can be used to study the

airflow across the main airways of a mine ventilation system. In particular, the flow through the transition zone between the upcast shaft and the main fan ductwork was investigated.

2.4.1 General Discussion

Although CFD has many advantages, it does not completely eliminate the need for experimental results, which are still needed to validate numerical solutions. The transition piece was developed and the results collated with tests conducted on site. In this regard favorable comparisons between simulations and measurements supported the use of the software package CFD2000 as a tool for the design and planning of fan ductwork configurations. This is one of the few applications of CFD to design and verify practical ventilation problems. Wala et al.'s (1997) study showed good correlation between the modeled data and that which was measured. The CFD technique used in this instance was therefore validated.

In a similar vein, Meyer and Marx (1993) used CFD to evaluate the design of a fan drift–mine shaft intersection. In this work, Star-CD was used to create a CFD model of this intersection. A number of options were evaluated with respect to the geometry of this intersection. The results of the analysis demonstrated that savings could be achieved by adhering to certain ratios when defining the fan drift geometry. The finite volume mesh for this model was created using the SIMPLE algorithm and the turbulent model used was k–epsilon. The economics of the potential reduction in pressure losses were also evaluated.

This work and that described above was found to be some of the earliest work using CFD to resolve engineering issues on mines.

In 1995, Brunner et al. described a number of problems they had solved using advanced CFD techniques. The most useful was their finding that the mesh generation at this point had developed to the extent of allowing relative movement of the meshes, enabling the simulation of multiple moving bodies. In these examples, trains moving through openings were evaluated and the specific geometry of the opening through which they were moving was evaluated. These models were created using the Fluent software. The models assumed incompressible fluid, and radiation and heat conduction were neglected in their evaluation. The result of this analysis showed the importance of ‘flaring’ the opening in order to reduce the pressure losses through these openings.

To explore the potential for using CFD modelling in mines, Wala et al. (1997) used CFD techniques to model the flow of air between a shaft and the main ventilation fans of a mine. These modelled results were compared with those from work completed in 1995 on measuring the flow characteristics between these points. The model assumed incompressible airflow and specified steady-state, turbulent, single-phase flow. The effects of body forces and heat transfer were

considered to be small and were not taken into consideration. This exercise showed favourable comparisons between the data and the measured results.

Additional work was done by Graig (2001) on the CFD evaluation of the drag coefficient on buntons of various shapes. A number of different geometries were evaluated using a 2D model generated using Fluent v5.5 software and a velocity of 5 m/s. This analysis produced coefficients of drag that differ significantly from those used by McPherson (1987). However, as was noted by the author, there are several concerns with the data presented, the first being that the Reynolds number used would be significantly lower than that experienced in a shaft ($Re = 5e4$, whereas a typical shaft configuration has an $Re = 3e6$). In addition, the technique used assumed fully turbulent flow and the transition from laminar to turbulent flow was not noted. This problem is not unique to this analysis and has produced results that are less than 50% of the overall published figures for the coefficient of drag. This work did highlight the complexities of calculating the specific drag coefficient for various buntun configurations.

In 2007 a validation study was carried out by Wala et al. (2007). In this work a comparison was made between a scale model test and a CFD model of this test. The area modelled was the flow of ventilation air in a heading created by a continuous miner. The work consisted of the following:

- 1 Design and build a scale ventilation model of the area under consideration.
- 2 Measure the response of the model to the flow of air through it.
- 3 Develop a CFD model of the same area.
- 4 Compare the experimental results with those of the CFD model.

In this regard a 3D steady-state incompressible solution for the Navier-Stokes equation with species transport without chemical reaction was performed. The results showed significant correlation between the measured and the modelled airflow, with sufficient accuracy to allow the prediction of the airflow. This analysis, however, only considered an empty heading and did not include the equipment and other obstructions that would typically be found in such a heading. This is thought to be one of the first attempts to validate actual measurements with those of a CFD model.

In 2008 Jade and Sastry also carried out a comparison between the use of CFD modelling and measured results. In this instance, two-way junction splits were considered. Once again incompressible steady-state viscous flow was considered. This comparison again showed a good correlation between the predicted characteristics and the measured results. These results were also compared with results in the available literature for loss coefficient between these points. The literature results agreed with the modelled data for smooth-walled duct flow. However, although the correlation between the model and the measurements for rough walls was consistent, the

literature prediction of losses for rough walls was not accurate. This finding was expected.

In spite of the lack of shaft applications for CFD, the technique has been used extensively in the evaluation of problems similar to the shaft resistance concern. Berkoe and Lane (2000) noted that CFD is typically used for modelling continuous processes and systems. The software utilises a 'CAD-like' model-building interface, advanced numerical methods and state-of-the-art graphics visualisation. CFD eliminates the need for typical assumptions, such as equilibrium, plug flow, averaged quantities, heat transfer coefficients, etc., because the physical domain is replicated in the form of a computerised 'prototype'.

A typical CFD simulation begins with a CAD rendering of the geometry, adds physical and fluid properties, and then specifies natural system boundary conditions. By changing these parameters appropriately, countless 'what-if' questions can be answered quickly. One of the most important uses of CFD is to compare alternatives and to view the effects of upset conditions. It is therefore best used as a design tool and is particularly useful when it is important to know how the variables – temperature, pressure, concentration/composition, and velocity – change throughout the computational domain, in space and time.

2.4.2 Significance of Available Data

Although little information is available on the use of CFD in the evaluation of shaft systems, the evaluations that have been completed indicate that this tool is worth investigating for the evaluation of shaft resistances.

It is not proposed to evaluate the specific drag characteristics noted by Craig (2001). Rather it is proposed to use the technique to model significant portions of the shaft system which will produce a better understanding of the inter-related nature of the various effects.

2.5 SUMMARY AND CONCLUSIONS – CHAPTER 2

This section summarises the most important conclusions from this chapter.

2.5.1 Measurement

- The main findings were:
 - All shafts should be lined to reduce the roughness of the shaft walls as much as is practically possible.
 - Buntions and guides should be streamlined and should be placed as far apart as possible.

- It is important to ensure that the velocity profile and Reynolds number in any test section are as close to those of the shaft as possible.
- The above general guidelines were recommended in the majority of the papers reviewed. However, no definitive data are available on the actual manner in which the above systems should be designed.
- None of the papers noted above included any quantification of the results in accordance with the procedure presented by Bromilov (1960).
- Care must be taken when reviewing the results from this chapter because, although the manner in which the various measurements were taken is recorded, little information is available on the actual data measured and the details of the instrumentation used.
- One of the objectives of reviewing these papers was to try and find additional data to calibrate a computational model. In this instance the difficulties associated with the measurement of shaft resistances was highlighted, particularly with respect to ensuring that sufficient time is allowed in the shaft to complete these measurements.
- It was also noted that the horizontal test chamber showed little reduction in the shaft resistances when pipes and cables were introduced.
- The uniqueness of each shaft layout and the resultant effect on the turbulence of the shaft and, in turn, its effect on the measured coefficient of drag were highlighted.

2.5.2 Design

- The theory described in this section allows the complete mathematical design of a shaft system with respect to the resistance that the shaft will offer to air flowing through it, but some critical questions with respect to this analysis remain unanswered:
 - As the duty required of shafts increases and they are used to transport more services underground, the actual effect of the shaft fittings needs to be quantified.
 - The effect that conveyances have on the resistance of the shaft needs to be more explicitly quantified.
- The effect that the shaft steelwork has on the ventilation air has been quantified based on the drag resistance it offers to the airflow. In addition, it is noted that the further the buntons are away from each other the better.
- The maintenance of shaft systems must be optimised such that it takes as little time in the shaft as possible.

- Air velocities in equipped shafts may be as high as 12 m/s and air velocities of up to 22 m/s may be tolerated in unequipped shafts.

2.5.3 CFD

Although there is little data available on the use of CFD in the evaluation of shaft systems, the evaluations that have been completed indicate that this tool is worth investigating for the evaluation of shaft resistances.

It is not proposed to evaluate the specific drag characteristics that were noted by Craig (2001). Rather it is proposed to use the technique to model significant portions of the shaft system, which will produce a better understanding of the inter-related nature of the various effects.

CHAPTER 3 METHOD OF EXPERIMENTATION AND ANALYSIS

3.1 INTRODUCTION

This chapter presents the evaluation of the current theory with specific emphasis on the data that needed to be collected from working shafts to validate the theory for calculating pressure drops over shafts.

Thereafter, the manner in which the initial tests were conducted and the conclusions drawn from these tests are discussed. The specific outcome of this chapter is to validate the theory (as noted above), as well as to define a testing methodology for use on the remainder of the shafts to be tested.

The tests completed on various shafts are discussed and the relevance of the results is noted.

The final section consists of the CFD modelling of the selected shaft sections and the calibration of the model such that these sections can be accurately reflected. These models are then used to determine the various pressure loss components and the potential for modifying the current use of these components to reduce the overall pressure resistance that shafts offer to the ventilation air flowing through them.

3.2 THEORY FOR ANALYSIS OF SHAFT RESISTANCES

3.2.1 Static Resistance of Shafts

To calculate the expected pressure drop in a shaft, standard analysis techniques are used. The background and development of this theory was discussed in more detail in CHAPTER 2. Three different methods are used for the calculation of shaft friction resistances. All these methods are similar and are based on the same data produced by Stevenson (1956), whose work was later extrapolated and defined by Bromilov (1960) and McPherson (1987).

The methods referred to are:

- 1 Classic fluid dynamics theory using the Chezy-Darcy friction factors and the Darcy-Weisbach approach (White, 1986)
- 2 General mine ventilation approach using the Atkinson equation and friction calculations (Hemp, 1979, 1989)

3 The rational resistance theory as laid down by McPherson (1987)

Each of these methods is discussed in turn in the following sections.

3.2.1.1 Chezy-Darcy friction factor

The resistance that ducts offer to the flow of fluid through them is calculated using the Chezy-Darcy friction factor (f). This factor is used to calculate the pressure drop over a length of duct. It is valid for duct flows of any cross-section, as well as for laminar and turbulent flow. The manner in which this pressure loss is calculated is:

$$P_{L(Darcy)} = f \frac{L V^2 \rho}{2 ID} \quad \text{Equation 3-1}$$

- Where :
- f = Chezy-Darcy friction factor (dimensionless)
 - L = Length of duct (pipe) (m)
 - ID = Internal diameter (m)
 - V = Velocity of fluid in duct (pipe) (m/s)
 - ρ = Density of fluid (kg/m³)
 - $P_{L(Darcy)}$ = Pressure drop experienced over length of duct (calculated using the Darcy-Weisbach formula) (Pa)

This formula, however, requires the value for f in order to be used. The resistance that fluids encounter when flowing through pipes is dependent on whether the fluid flows through a smooth-walled pipe or a rough-walled pipe. The formula for a smooth-walled pipe was derived by Prandtl in 1953. This formula is dependent on whether the flow in the pipe is laminar or turbulent and it was thus required that the Reynolds number be calculated before the overall Chezy-Darcy friction factor number could be calculated. The formula was complemented by the equation for rough-walled pipes. These data were collated by Colebrook (in White, 1986), who developed an interpolation formula which incorporated both smooth-walled and rough-walled pipes. This formula is as follows:

$$\frac{1}{f^{1/2}} = 2.0 \times \log \left(\frac{\epsilon/D}{3.7} + \frac{2.51}{Re_d f^{1/2}} \right) \quad \text{Equation 3-2}$$

and

$$Re_d = \frac{V d}{\nu} = \frac{V D \rho}{\mu} \quad \text{Equation 3-3}$$

Where	:	f	=	Chezy-Darcy friction factor (dimensionless)
		Re_d	=	Reynolds number
		D	=	Diameter (m)
		ϵ	=	Surface asperities (m)
		μ	=	Coefficient of viscosity (kg/ms)
		ν	=	Kinematic viscosity (m ² /s)
		ρ	=	Density (kg/m ³)

This equation was plotted by Moody into what is now referred to as the Moody Chart for pipe friction. This chart is accurate to $\pm 15\%$ for design calculations. The equation above is cumbersome to use, requiring as it does the interpolation of f until the equation balances. An alternative explicit equation was completed by Haaland. This is accurate to 2% across the range shown in the Moody chart and is (White, 1986):

$$f \approx \left\{ \frac{1}{\left(-1.8 \log \left[\frac{6.9 \mu}{\rho V ID} + \left(\frac{\epsilon / ID}{3.7} \right)^{1.11} \right] \right)} \right\}^2$$

Equation 3-4

Where	:	f	=	Chezy-Darcy friction factor (dimensionless)
		μ	=	Coefficient of viscosity (kg/ms)
		ρ	=	Density (kg/m ³)
		V	=	Velocity (m/s) (Free Air Velocity in Shafts)
		ID	=	Internal diameter (of shaft) (m)
		ϵ	=	Surface asperities (m)

It should be noted here that some texts use a value of f that is four times that defined by others. Care must therefore be taken to ensure that the correct values are used.

3.2.1.2 Atkinson calculations

The Atkinson calculation (Chasteau, 1989) was formulated for fully developed turbulent flow in an airway and is therefore applicable to flows whose Reynolds numbers exceed 4 000 ($Re > 4\ 000$). This is

usually the case for airflow in ventilation ducts. The Atkinson equation is:

$$P_{L(Atkins)} = \Delta P = \frac{k \text{ Per } L V^2}{A} \frac{\rho}{\rho_{Std}} \quad \text{Equation 3-5}$$

Where	:	k	=	Atkinson friction factor (NS^2/m^4)
		L	=	Length of airway (m)
		Per	=	Perimeter of airway (m)
		A	=	Cross-sectional area of airway (m^2)
		V	=	Velocity of fluid in airway (m/s)
		ρ	=	Density of fluid (kg/m^3)
		ρ_{Std}	=	Standard density of fluid (kg/m^3) (usually $1.2 kg/m^3$)
		$P_{L(Atkinson)}$	=	Pressure drop experienced over length of duct (calculated using Atkinson equation)(Pa)

An additional parameter that can be defined from this equation is that of airway resistance (R). The equation for this is:

$$R = \frac{k \text{ Per } L}{A^3} \frac{\rho}{\rho_{Std}} \quad \text{Equation 3-6}$$

Where	:	k	=	Atkinson friction factor (NS^2/m^4)
		L	=	Length of airway (m)
		Per	=	Perimeter of airway (m)
		A	=	Cross-sectional area of airway (m^2)
		ρ	=	Density of fluid (kg/m^3)
		ρ_{Std}	=	Standard density of fluid (kg/m^3) (usually $1.2 kg/m^3$)
		R	=	Airway resistance due to wall roughness (Ns^2/m^8)

The values of k (the Atkinson friction factor) are taken from tables of measurements which have been compiled in the past. These values are readily available from any mine ventilation text.

This form of the calculation has the advantage of being widely used in mine ventilation circles. However, it has two shortcomings:

- 1 The values of k are measured at different fluid densities and therefore the data must

always be correct for the current circumstances before they can be used. This also implies that the data are not geometrical measures of airway resistance as they depend on this air density.

and

- 2 The exact circumstances surrounding the measurement of the data points is not known and inaccuracies can therefore develop if there are significant differences.

3.2.1.3 Rational resistance

The definition of the rational resistance as defined by McPherson (1971) is shown in the equation below:

$$f = 2 \frac{k}{\rho_{Std}} \quad \text{Equation 3-7}$$

and

$$\Gamma = \frac{R}{\rho} \quad \text{Equation 3-8}$$

Where	:	k	=	Atkinson friction factor (Ns ² /m ⁴)
		f	=	Chezy-Darcy friction factor
		ρ	=	Density of fluid (kg/m ³)
		ρ _{Std}	=	Standard density of fluid (kg/m ³) (usually 1.2 kg/m ³)
		R	=	Airway resistance due to wall roughness (Ns ² /m ⁸)
		Γ	=	Rational resistance (m ⁻⁴)

Γ is termed the 'rational resistance' and depends only on the airway geometry and roughness; it is independent of air density. The relationship between Γ and the Chezy-Darcy friction factor *f* is defined in the following equation:

$$\Gamma = \frac{f}{2} \times \frac{Per \times L}{A^3} \quad \text{Equation 3-9}$$

Where	:	f	=	Chezy-Darcy friction factor (dimensionless)
		L	=	Length of airway (m)
		Per	=	Perimeter of airway (m)
		A	=	Cross-sectional area of airway (m ²)

$$\Gamma = \text{Rational resistance (m}^{-4}\text{)}$$

The pressure loss is calculated from the following equation:

$$P_{L(\text{Rational})} = \Gamma \rho (V A)^2 = \Gamma \rho Q^2 \quad \text{Equation 3-10}$$

Where	:	Γ	=	Rational resistance (m ⁻⁴)
		L	=	Length of airway (m)
		V	=	Velocity of fluid in airway (m/s)
		A	=	Cross-sectional area of airway (m ²)
		ρ	=	Density of fluid (kg/m ³)

3.2.2 Shaft Friction Resistance

The current theory for the calculation of this resistance assumes that the resistance values each of the resistance sources listed below is independent of the others. This assumption is not strictly true but is required for the calculation to be completed.

The shaft friction resistance is calculated with respect to three criteria:

- i Friction resistance (standard fluid theory based on the Moody chart)
- ii Resistance offered by the shaft fittings (buntons, guides, pipes, etc.)
- iii Resistance offered by the movement of the conveyances in the shaft

Thus the overall Chezy-Darcy friction factor for the shafts is calculated by summing the individual Chezy-Darcy friction factors for each of the resistant components in the shaft

$$f_{\text{Total}} = f_{\text{Shaft}} + f_{\text{Buntons}} + f_{\text{Guides}} + f_{\text{Fittings}} + f_{\text{Cages}} \quad \text{Equation 3-11}$$

Where	:	f_{Total}	=	Combined Chezy-Darcy friction factor of complete shaft (dimensionless)
		f_{Shaft}	=	Chezy-Darcy friction factor for shaft wall (dimensionless)
		f_{Buntons}	=	Chezy-Darcy friction factor for shaft buntons (dimensionless)
		f_{Guides}	=	Chezy-Darcy friction factor for shaft guides (dimensionless)
		f_{Fittings}	=	Chezy-Darcy friction factor for shaft fittings (dimensionless)
		f_{Cages}	=	Chezy-Darcy friction factor for cages (dimensionless)

3.2.2.1 Friction resistance of shaft

The resistance that the shaft offers to ventilation airflow is calculated in accordance with the theory laid out in Section 3.2.1.1.

3.2.2.2 Resistance offered by shaft fittings

Longitudinal fittings

These fitting include pipes, guides, cables and other fittings which run parallel to the airflow through the shaft. According to both Bromilov and McPherson, model shaft tests have shown that these fittings can actually reduce the overall Chezy-Darcy friction factor of the shaft. Nevertheless, allowance is made for the longitudinal fittings by decreasing the effective shaft cross-sectional area by the cross-sectional area of these fittings.

The reduced 'effective' shaft diameter is then used for further calculation of the overall shaft losses.

Buntons

Buntons differ significantly from longitudinal fittings in that longitudinal fittings offer resistance to the airflow via boundary layer friction, whereas buntons form obstructions to the airflow perpendicular to that flow.

To calculate the overall pressure drop in the shaft it is also necessary to derive a Chezy-Darcy friction factor for the shaft fittings. To calculate the friction offered by the buntons, the aerodynamic drag of the buntons is considered. This is used to calculate the friction resistance of each of the buntons. This resistance is then multiplied by the number of buntons in the shaft and an overall buntion Chezy-Darcy friction factor for the shaft is calculated as follows:

$$f_{\text{Buntions}} = \frac{C_d A_b}{S \text{ Per}} \quad \text{Equation 3-12}$$

Where :

- C_d = Drag coefficient (dimensionless)
- A_b = Frontal area of buntions (facing airflow) (m^2)
- S = Spacing between buntions (m)
- Per = Perimeter of shaft (m)

and

$$\Gamma_{\text{Buntions}} = \frac{L}{S} C_d \frac{A_b}{2A_{\text{FS}}^3}$$

Equation 3-13

Where :

Γ_{Buntions}	=	Rational resistance of buntions (m^{-4})
L	=	Length of shaft (m)
C_d	=	Drag coefficient (dimensionless)
A_b	=	Frontal area of buntions (facing airflow) (m^2)
S	=	Spacing between buntions (m)
A_{FS}	=	Free cross-sectional area of shaft for flow (m^2)

However, the above assumes that the frictional resistance of each of the buntions is independent of that of the following buntion. This means that it is assumed that the turbulent eddies for each buntion set die out before the flow reaches the next buntion set. In reality, this is unlikely to happen. To mitigate against this Bromilov evaluated a total of 24 shafts of varying roughnesses and fitting regimes. This evaluation results in an interference factor (F) being introduced, which has the effect of reducing the overall resistance of the shaft and bringing it more in line with the modelled tests.

$$F = 0.0035 \frac{S}{W} + 0.44$$

Equation 3-14

Where :

F	=	Interference factor (dimensionless)
S	=	Buntion spacing (m)
w	=	Width of buntions (m)

To obtain the appropriate frictional resistance of the buntions for inclusion in the Darcy-Weisbach calculation, the following formula is used:

$$f_{\text{Bu}} = C_D \times \frac{A_b}{S \times \text{Per}} \left(0.0035 \times \frac{S}{W} + 0.44 \right)$$

Equation 3-15

Where :

C_D	=	Coefficient of drag for buntions
A_b	=	Frontal area of buntions (m^2)
S	=	Spacing between buntions (m)
Per	=	Perimeter of shaft (m)
W	=	Width of buntions (m)

and

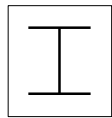
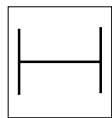
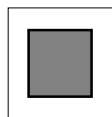
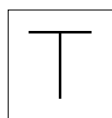
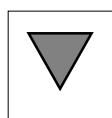
$$\Gamma_{Bu} = \frac{L}{S} \times C_D \times \frac{A_b}{2 \times A_{FS}^3} \left(0.0035 \times \frac{S}{W} + 0.44 \right) \quad \text{Equation 3-16}$$

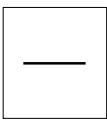
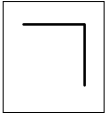
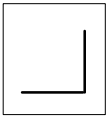
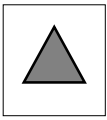
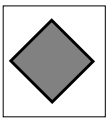

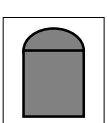
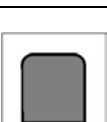
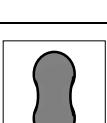
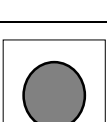
- Where :
- C_D = Coefficient of drag for buntions
 - Γ_{Bu} = Rational resistance of buntions (m^{-4})
 - A_b = Frontal area of buntions (m^2)
 - A_{FS} = Free cross-sectional area of shaft (m^2)
 - S = Spacing between buntions (m)
 - W = Width of buntions (m)

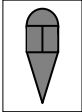
The results of these calculations then used to calculate the overall frictional resistance of the shaft in accordance with the three calculations discussed above.

In the interests of clarity, Table 3-1 contains the coefficients of drag for the various buntion shapes.

Table 3-1: Summary of drag coefficients of elongated bodies of infinite span (McPherson, 1987)

1		I - Girder	2.75	Skonchinsky (1952)
2		I – Girder	2.05	Hoerner (1951)
3		Rectangle	2.05	Hoerner (1951)
4		Tee	2.00	Hoerner (1951)
5		Triangle	2.00	Hoerner (1951)

6		Plate	1.98	Hoerner (1951)
7		Angle	1.98	Hoerner (1951)
8		Angle	1.82	Hoerner (1951)
9		Triangle	1.55	Hoerner (1951)
10		Square	1.55	Hoerner (1951)
11		Angle	1.45	Hoerner (1951)
12		Capped Rectangle	1.40	Estimated from results by Skonchinsky (1951) and Bareza and Hounerchts (1955)
13		Rounded Square	1.35	Approximate value – value depends on the ratio: radius of corner side of square
14		Dumbbell	1.30	Calculated from Martinson's results (1957)
15		Cylinder	1.20	Hoerner (1951)

16		Streamlined girder	1.03	Skonchinsky (1952)
----	---	--------------------	------	--------------------

3.2.2.3 Resistance offered by shaft cages

The resistance that the cage, skip or counterweight offers to the flow of air through the shaft is considered in two steps, namely:

- 1 The resistance as a result of the obstruction that the cage, skip or counterweight offers to the flow of air in the shaft
- 2 The transient effects which cause resistance to the airflow as a result of the motion of the conveyance in the shaft

Resistance due to obstruction

The standard equation for the 'shock' or pressure loss incurred by the flow of air when it is caused to change direction by an obstruction is as follows:

$$P_{SC} = X \rho \frac{V^2}{2} \tag{Equation 3-17}$$

- Where :
- P_{SC} = Pressure loss from stationary cage (Pa)
 - X = Shock loss factor
 - ρ = Density of airstream (kg/m^3)
 - V = Velocity of approaching airstream (m/s)

and

$$P_{SC} = \rho \Gamma_{conv} V^2 A_{FS}^2 \tag{Equation 3-18}$$

- Where :
- P_{SC} = Pressure loss from stationary cage (Pa)
 - Γ_{conv} = Rational resistance of conveyance (m^{-4})
 - ρ = Density of airstream (kg/m^3)
 - V = Velocity of approaching airstream (m/s)
 - A_{FS} = Area of free shaft section (m^2)

and

$$\Gamma_{\text{Conv}} = \frac{X}{2 A_{\text{FS}}^2} \quad \text{Equation 3-19}$$

Where :

- Γ_{Conv} = Rational resistance of conveyance (m^{-4})
- X = Shock loss factor
- A_{FS} = Free cross-sectional area of shaft (m^2)

The evaluation of X must now be completed. A comprehensive study of cage resistances was carried out by Stevenson (1956). McPherson (1987) performed the most recent analysis of these data. The results of this analysis are presented in Figure 3-1. These data show the variation of X with respect to the coefficient of fill (C_f) of the conveyance in the shaft.

$$C_f = \frac{A_{\text{Conv}}}{A_{\text{FS}}} \quad \text{Equation 3-20}$$

Where :

- C_f = Coefficient of fill
- A_{FS} = Free cross-sectional area of shaft (m^2)
- A_{Conv} = Frontal cross-sectional area of the conveyance (m^2)

The data in Figure 3-1 refer specifically to the length over width ratio of 1.5 and apply to a range of conveyances with height over width ratios of 1.5–6.0. These data can be extrapolated to suit all cages by multiplying the result by the correction factor which corresponds to the length over width ratio considered in any specific analysis.

In addition, the tests were completed on conveyances with open ends. In the case of cages or skips with closed ends, the X factor should be reduced by approximately 15% (Bromilov, 1960).

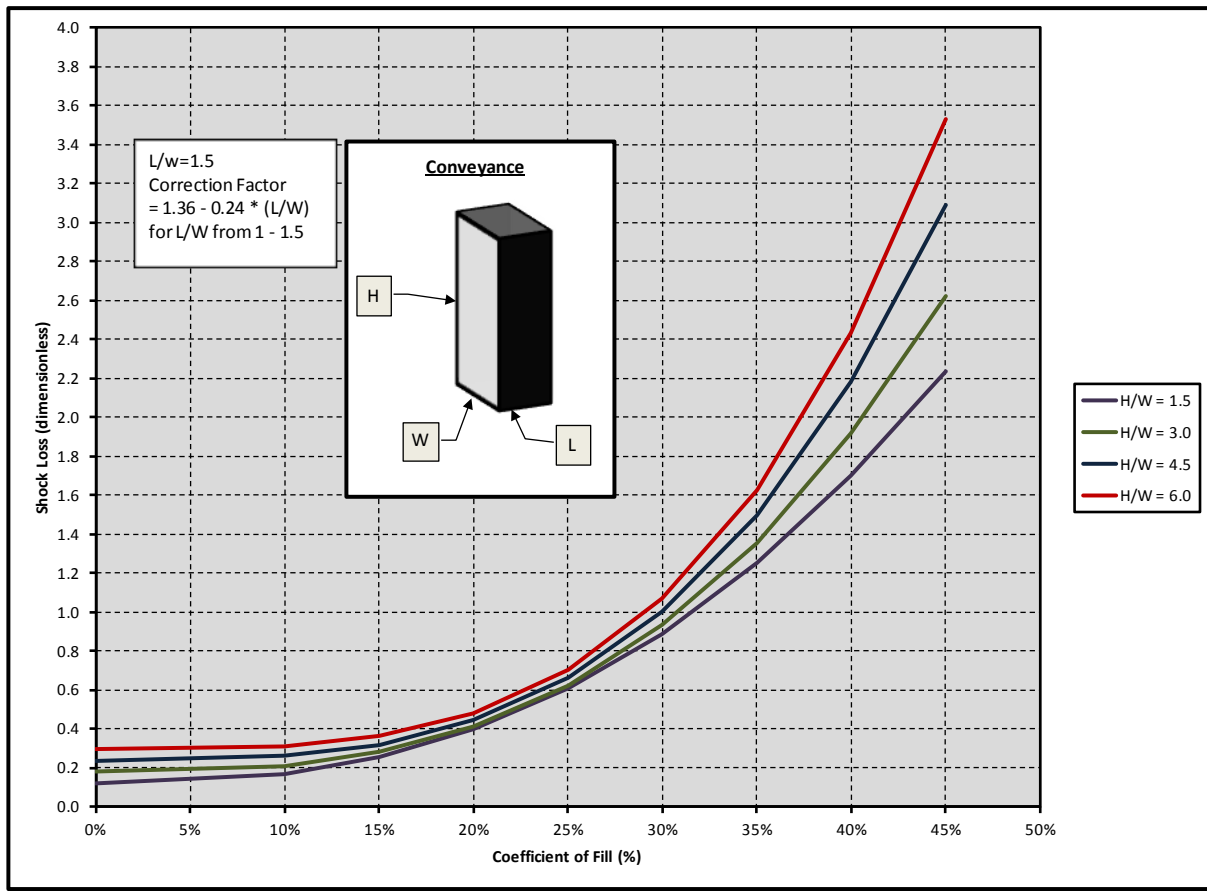


Figure 3-1: Conveyance shock loss estimation for conveyances

Resistance due to cage movement

The standard equation for pressure loss over an obstruction was defined in Equations 3–1 to 3-7. In order to calculate the maximum pressure loss for a cage that is moving, a slight modification is required to this equation. The equation is defined by the expression for an obstruction blocking airflow in a shaft and it is also assumed that the cage is standing still and that the velocity of the flow of air around the cage is equal to the velocity of the cage itself (V_{Conv}).

$$P_{MC} = X \rho \frac{V_{Conv}^2}{2} \tag{Equation 3-21}$$

- Where :
- P_{MC} = Pressure loss from moving cage (Pa)
 - X = Shock loss factor
 - ρ = Density of airstream (kg/m^3)
 - V_{Conv} = Velocity of conveyance (m/s)

There are two possible exist when calculating the pressure loss over a moving conveyance, namely:

- i The conveyance is moving in the same direction as the airflow. (The two expressions are added.)
- ii The conveyance is moving in the opposite direction to the airflow. (The two expressions are subtracted.)

$$P_{MC(Max)} = P_{SC} \left(1 + \frac{V_{Conv}^2}{V_{FS}^2} \right) \quad \text{Equation 3-22}$$

and

$$P_{MC(Min)} = P_{SC} \left(1 - \frac{V_{Conv}^2}{V_{FS}^2} \right) \quad \text{Equation 3-23}$$

- Where :
- $P_{MC(Max)}$ = Maximum pressure loss from moving cage (Pa)
 - $P_{MC(Min)}$ = Minimum pressure loss from moving cage (Pa)
 - V_{FS} = Free shaft velocity of approaching airstream (m/s)
 - V_{Conv} = Velocity of conveyance (m/s)
 - P_{SC} = Pressure loss from stationary cage (Pa)

The effective resistance of a moving conveyance can also be determined from the following:

$$P_{MC(Max)} = \Gamma_{MC(Max)} \rho V_{FS}^2 A_{FS}^2 \quad \text{Equation 3-24}$$

and

$$P_{MC(Min)} = \Gamma_{MC(Min)} \rho V_{FS}^2 A_{FS}^2 \quad \text{Equation 3-25}$$

- Where :
- $P_{MC(Max)}$ = Maximum pressure loss from moving cage (Pa)
 - $P_{MC(Min)}$ = Minimum pressure loss from moving cage (Pa)
 - V_{FS} = Free shaft velocity of approaching airstream (m/s)
 - $\Gamma_{MC(Max)}$ = Maximum rational resistance of moving conveyance (m^{-4})
 - $\Gamma_{MC(Min)}$ = Minimum rational resistance of moving conveyance (m^{-4})
 - ρ = Density of airstream (kg/m^3)
 - A_{FS} = Free cross-sectional area of shaft (m^2)

The rational resistance is defined as:

$$\Gamma_{MC(Max)} = \Gamma_{Conv} \left(1 + \frac{V_{Conv}^2}{V_{FS}^2} \right) \quad \text{Equation 3-26}$$

and

$$\Gamma_{MC(Min)} = \Gamma_{Conv} \left(1 - \frac{V_{Conv}^2}{V_{FS}^2} \right) \quad \text{Equation 3-27}$$

Where	:	V_{FS}	=	Free shaft velocity of approaching airstream (m/s)
		V_{Conv}	=	Velocity of conveyance (m/s)
		$\Gamma_{MC(Max)}$	=	Maximum rational resistance of moving conveyance (m ⁻⁴)
		$\Gamma_{MC(Min)}$	=	Minimum rational resistance of moving conveyance (m ⁻⁴)
		Γ_{Conv}	=	Rational resistance of conveyance (m ⁻⁴)

3.2.3 Accuracy Limits of the Theory

All the calculations described above are based on empirical values to which formulas are fitted in order to calculate the overall resistance of a shaft. Each of the particular areas discussed will now be evaluated in turn.

3.2.3.1 Accuracy of calculation for friction resistance of shaft

As was noted above, this calculation is based on the theory for flow of fluids through ducts. The Moody chart used for determination of the frictional resistance has an overall accuracy of $\pm 15\%$ for design calculations. In addition, the simplifying formula developed has an accuracy of $\pm 2\%$ across the range. This means an overall accuracy of 17.6%. This is directly proportional to the calculation and must be considered when the overall accuracy of the results is calculated.

However, the resistance offered by the shaft walls generally accounts for between 10% and 15% of the overall resistance of the shaft. This results in a potential inaccuracy of 0.2% for the shaft resistance calculation.

3.2.3.2 Accuracy of calculation for resistance offered by shaft fittings

The resistance offered by the shaft fittings is generally more than 80% of the overall shaft resistance. The accuracy of these calculations therefore makes the most significant contribution to the overall

accuracy. Paradoxically, the accuracy of these calculations is also the most difficult to quantify.

This evaluation consists initially of the values used for the drag coefficients of the buntons and the associated simplifying assumptions (discussed above). These values cannot be evaluated in isolation. Bromilov (1960) introduced an interference factor (F) to account for the effect the buntons will have on each other in relation to the flow of air through the shaft.

These results showed that for smooth-walled shafts, the drag coefficient and interference factor resulted in accuracies of $\pm 15\%$ against the measured values. This accuracy deteriorated abruptly when used for rough-walled shafts. This shows that the calculation must be used with care to ensure its validity for various shafts. No attempt was made to quantify the accuracy of the calculation with additional inclusions such as ladderways.

3.2.3.3 Accuracy of calculation for resistance offered by shaft cages

All the theory available for evaluation of the conveyances in a shaft is based on the work done by Stevenson (1956). In this work he used a horizontal duct of circular cross-section, 0.286 m (11¼ inches) in diameter and 27.432 m (90 ft) long. The tests were carried out over a range of Reynolds numbers. These data were analysed and re-used by McPherson (1987). They have not been verified and the accuracy of the calculations based on these measurements is therefore not known.

3.2.3.4 General comments on the accuracy of the theory

In CHAPTER 2 numerous papers were evaluated in order to try and obtain a clearer understanding of the actual accuracy of the current theory. The only paper that was found specifically to test the accuracy of these calculations was that by Deen (1991). In this paper he noted the accuracy of the theoretical calculation to be less than 5% on three of the shafts and 11.8% on the final shaft. Unfortunately, no information was supplied on how the tests were done or on the assumptions used for the basis of the calculation. Neither was a detailed comparison of the results given.

3.3 VALIDATION OF EXISTING THEORY AND INITIAL SHAFT TESTS

The necessary equations for calculating the theoretical pressure drop for the shaft have been provided in Section 3.2. As was noted in CHAPTER 2 of this document, few data are available to confirm the efficacy of these equations. In this regard Impala Platinum Mines was approached and the management kindly agreed to allow tests to be conducted on No. 14 shaft. The only proviso they attached to this was that the tests should not interrupt production in any manner or form.

3.3.1 Test Methodology

The details of the test methods available are discussed in Section 2.2.4 and will not be repeated here. In the tests conducted for this work, the density method of measurement was used. The reason for this is twofold:

- 1 The accuracy of the barometer has improved significantly and it can be used with ease.
- 2 As the tests were run on a continuous basis, no inclusions in the shaft were allowed.

This method consists of the simultaneous measurement of the following parameters (Hemp, 1989):

- 1 Barometric pressures (at point 1 and point 2)
- 2 Airflow
- 3 Wet-bulb temperature
- 4 Dry-bulb temperature

In addition, the two elevations should be known.

Once these parameters are known, the pressure loss can be calculated using the following equations:

$$P_{L(\text{meas})\text{oss}} = - (P_2 - P_1) - g \times \int w \, dZ \quad \text{Equation 3-28}$$

Where	:	$P_{L(\text{meas})}$	=	Measured pressure loss (Pa)
		P_1	=	Barometric pressure at point 1 (Pa)
		P_2	=	Barometric pressure at point 2 (Pa)
		g	=	Gravitational constant (m/s^2)
		$\int w \, dZ$	=	Theoretical pressure increase (Pa)

and

$$\int w \, dZ = 0.5 \times (\rho_1 + \rho_2) \times (Z_2 - Z_1) \quad \text{Equation 3-29}$$

Where	:	ρ_1	=	Calculated density at point 1 (kg/m^3)
		ρ_2	=	Calculated density at point 2 (kg/m^3)
		Z_1	=	Elevation at point 1 (m)
		Z_2	=	Elevation at point 2 (m)

3.4 TESTS USED TO VALIDATE THEORY

3.4.1 Test Methodology

For calculation of the pressure loss in a shaft as a result of its fittings, the ideal testing parameters would be as follows:

- 1 The shaft ventilation will remain constant.
- 2 The instruments used to measure the pressure, temperature and velocity must be placed in the shaft such that their placement will not interrupt the normal ventilation flow.
- 3 These instruments must be allowed to remain in place for a sufficient length of time to allow any movement in the measurements to subside.

During this test period the shaft must not be used for anything else. These requirements are, however, not possible to achieve as they would interrupt the production of the shaft.

It was therefore decided to complete the initial testing during the weekly shaft examinations. This had the advantage that the movement of the cages would be predictable and would also be at a slow speed; thus they would not affect the pressure readings significantly.

3.4.1.1 Main downcast shaft test procedure

Velocity

The main cage was chosen as the platform from which to take the necessary readings. One of the chief concerns was the measurement of the shaft ventilation velocity in an area where the measurement platform would not affect the readings. This concern was dealt with by using a Pitot tube arrangement. The Pitot itself was attached to a bracket which was in turn attached to the rope of the conveyance. This kept the tube at right angles to the ventilation air and also well above the cage. Thus the bulk of the cage did not affect the readings taken from it. The trailing tubes were lowered into the cage where the readings could be taken without hindrance.

Shaft inspections are normally done with all the conveyances moving down the shaft within shouting distance of each other. This would also have created a blockage and have affected the ventilation airflow. As a result, when the cage was stopped to take the measurement, the other conveyances were asked to move slightly further down the shaft.

Pressure

The pressure measurements were taken using a standard barometer. One of the concerns here was the spacing at which the measurements would be taken. In order to ensure these spacings were the

same, readings were taken every 20 bunton sets.

Temperatures

Wet and dry-bulb temperatures were taken using a standard whirling hygrometer. These were taken outside the cage to ensure that no insulating effect was apparent from within the cage.

Testing

In order to do the tests, it was requested that the cage be stopped at regular intervals while moving down the shaft. These intervals were counted and the cage was stopped to allow measurements to be taken every 20 bunton sets. At each point the following measurements were taken:

- 1 Wet-bulb temperature (T_{WB}) (°C)
- 2 Dry-bulb temperature (T_{DB}) (°C)
- 3 Velocity pressure (P_v) (Pa)
- 4 Static pressure (P_{Static})
- 5 Total pressure (P_{Tot})
- 6 Barometric pressure (P_{Bar})

Once the uninterrupted portion of the shaft had been tested, additional tests were done from just above each of the stations.

3.4.1.2 Test procedure in the rest of the mine shafts

The No. 14 shaft complex has a total of four shafts – two downcast and two upcast shafts. These are shown in Figure 1-9.

Each of these was tested in turn. The detailed results are presented in Appendix D. It was not possible to take measurements over the length of the upcast shaft or the length of the unequipped downcast shaft. In addition, although it was possible to measure the velocity and pressure in the upcast shaft from the fans, it was not possible to do this in the downcast shaft. However, the bulk air cooler and refrigeration systems were not in operation as it was winter, so it was possible to obtain general barometric and temperature readings from the shaft head. Figure 3-2 and Figure 3-3 show the brackets that were used to attach the Pitot tube to the conveyance rope, as well as the instrumentation used for this test. Figure 3-4 shows the remainder of the instrumentation used.



Figure 3-2: Pitot tube attachment bracket on rope above cage



Figure 3-3: Pitot tube attachment bracket (above cage)



Figure 3-4: Testing instrumentation – Pitot tube, barometer and whirling hygrometer

3.4.1.3 Accuracy and repeatability of test data

The following instruments were used for this evaluation:

- 1 ALNOR AXD – Pitot measurement
- 2 GPB 2300 – Barometric measurement
- 3 Whirling hygrometer

ALNOR AXD

Pressure	-	Range	:	-3 700–3 700 Pa
		Accuracy	:	±1% of reading
		Resolution	:	1 Pa
Velocity	-	Range	:	1.27–78.70 m/s
		Accuracy	:	±1.5% of reading

	Resolution	:	0.1 m/s
Operating temperature		:	5– 45°C

GPB 2300

Range	:	0–130 kPa
Accuracy	:	±0.25% of reading
Resolution	:	100 Pa
Operating temperature	:	-25–50°C

Whirling hygrometer

Range	:	0–50 °C
Accuracy	:	±2% of reading
Resolution	:	0.5 °C
Operating temperature	:	0–50°C

These accuracies are considered to be acceptable and should result in a cumulative accuracy of less than 5%.

3.4.1.4 Ideal test methodology

As was noted in the previous section, the indirect testing method is not ideal given the constraints of the accuracy requirements noted. In this regard, once the overall testing had been completed, the accuracy of these measurements was evaluated in line with the recommended procedures described above. The tests showed accuracies of 0.3%, thus indicating that the concerns raised were dealt with successfully in the methodology.

This is due primarily to the static nature of the tests (i.e. the conveyance was brought to a halt), as well as to the removal of dynamics in the shafts during the tests. The tests were therefore deemed to be acceptable.

3.4.2 Results of Tests

The detailed calculation of the test results can be found in Appendix D. However, a summary of the results is given in Table 3-2.

Table 3-2: Impala No. 14 shaft – details of tested shafts

No. 14 shaft	No. 14 V shaft	No. 14 A shaft	No. 14 B shaft	Units	Symbol	Description
7.4	4.9	5.6	5.8	m	diam.	Diameter of shaft
23.2	15.4	17.6	18.2	m	per	Perimeter of shaft
38.0	18.8	24.6	26.4	m ²	A _{FS}	Free cross-sectional area of shaft
868	620	1 060	1 152.6	m	L _{S (AS)}	Length of shaft (stops above the airway split)
10.1	17.2	21.1	15.6	m/s	V _{Shaft Average}	Average velocity of air in shaft (Free Air Velocity)
384	323	520	411	m ³ /s	Q	Volumetric flow rate in shaft
1.14	1.03	1.097	1.18	kg/m ³	ρ _{Average in Shaft}	Average density in shaft
437	334	570	484	kg/s	G	Volumetric flow rate in shaft
0.017	0.009	0.002	0.005	Ns ² /m ⁴	k	Measured Atkinson friction factor
0.014	0.006	0.003	0.006	Ns ² /m ⁴	k	Calculated Atkinson friction factor (Darcy-Weisbach)
0.021	0.003	0.004	0.003	Ns ² /m ⁴	k	Calculated Atkinson friction factor (rational resistance)
Measured Atkinson friction factor				This Atkinson friction factor was calculated based on the measured pressure losses.		
Calculated Atkinson friction factor (Darcy-Weisbach)				This Atkinson friction was calculated using McPherson's methodology using the Darcy-Weisbach option.		
Calculated Atkinson friction factor (rational resistance)				This Atkinson friction was calculated using McPherson's methodology using the Rational Resistance option.		
The shaft has standard concrete lining.						
Data from <i>Environmental Engineering in SA Mines</i> (Lloyd, 1989):						

Atkinson friction factor (Ns^2/m^4)			Description
0.0040	-	-	Concrete lined – No steelwork
0.0045	-	0.0250	Concrete lined – streamlined buntions
0.0075	-	0.0600	Concrete lined – RSJ buntions
0.0450	-	0.0900	Timbered rectangular shafts

As can be concluded from the data in Table 3-2, there is reasonable correlation between the data calculated and the data measured. This is in spite of the differences between the shafts. Three of these shafts were unequipped ventilation shafts (both upcast and downcast). The shaft of particular interest is No. 14 shaft as this is a fully equipped downcast shaft with a full suite of conveyances. The difference between the fan pressure and the flow rate can be found in tabular form in Table 1-2 and the mine configuration in Figure 1-8.

3.4.3 Conclusion and Recommendations

This shaft is equipped with streamlined buntions and is generously spaced with respect to the free area available for airflow. The Chezy-Darcy friction factors, both measured and calculated, were within the expected range. The rational resistance value calculated was, however, significantly higher than those of the measured value and the Chezy-Darcy friction factor value. This is attributed to the inaccuracies from the estimations in the calculation. These inaccuracies are detailed in Section 2.2.

These data show good correlation between the theory and the practice. It is thus appropriate to move on to the next phase of testing and that is to measure the pressure losses resulting from the dynamic nature of the moving conveyances.

3.4.4 Innovative Testing Methodology

To measure the pressure losses in a shaft, an innovative testing methodology is required which will allow remote testing of the shaft. This is primarily born out of the need to be able to measure various parameters in the shaft during normal operation. The following parameters are required:

- 1 Dry-bulb temperature (T_{DB}) ($^{\circ}C$)
- 2 Wet-bulb temperature (T_{WB}) ($^{\circ}C$) (or relative humidity, %)
- 3 Velocity of air in shaft (m/s)

- 4 Barometric pressure (P_{Bar})
- 5 Position and speed of all the conveyances in the shaft

All these measurements will be needed as functions in time so that meaningful calculations can be made with respect to actual pressure losses and the overall effect of the movement of the conveyances.

Ideally, the instrumentation should be placed in position and the various conveyances should then be allowed to move individually in the shaft so that the specific parameters for each of these can be measured and the pressure losses calculated. The data from the individual instruments would then be collated on a single computer to enable real-time comparisons to be made.

Unfortunately, this is not achievable as a result of the shaft time that would be required. Moreover, the necessary instrumentation and data-transfer mechanisms are expensive and difficult to install. Although most shafts already have data-transfer systems, these are used for production and, as stated earlier, the one proviso that Impala Platinum stipulated for these tests was that no interruption of production was to take place.

For this reason logging instrumentation was sought which would measure the required parameters at a set interval and log the results for later retrieval.

3.5 TESTS CONDUCTED ON SHAFTS

After discussion with the mine management, it was decided that the ideal time to put the instrumentation in place in the shaft would be during the weekly shaft inspections, for which purpose the testers would have to accompany the mine personnel on the inspection. This would have the benefit of allowing the testers to review the shaft arrangement and to take ventilation velocity measurements during the inspection.

It would not be possible to place the instrumentation in the shaft itself given the sensitivity of anything being placed in the shaft barrel and its potential effect on production. Thus the instruments would have to be placed immediately adjacent to the barrel on the stations. These instruments would then remain in place for at least a week before they could be recovered during subsequent shaft visits.

3.5.1 Equipment Used

3.5.1.1 Environmental instrumentation

The instrumentation required for the environmental tests had to have the following characteristics:

- 1 Must be able to measure the parameters at set intervals and log the data measured (a maximum interval of 10 seconds was chosen).
- 2 Must be insulated against the environment so that dust and moisture could not affect the readings.
- 3 Must have sufficient accuracy to allow the various measurements to be reliable.
- 4 Must be small and easy to transport and install.

These criteria were met by the EASYlog 80CL supplied by Greisinger. The instrument cannot measure the wet-bulb temperature, but it does measure the moisture content of the air. The EASYlog 80CL is battery operated and can withstand a harsh environment. The specifications of this instrument are listed in Table 3-3 and a photo picture of such a logger is shown in Figure 3-5.

Table 3-3: EASYlog 80CL specifications

Description	Measuring range		
Temperature	-25.0 °C	-	+60 °C
Humidity	0.0%	-	100.0%
Air pressure	30 kPa	-	110 kPa
	Resolution		
Resolution	0.1 °C	0.1% RH	0.01 kPa
	Accuracy (± 1 digit)		
Temperature	± 0.3 °C		
Humidity	± 2% RH (at range 0–90% RH)		
Air pressure	± 0.1 kPa (typical) – ±0.25 kPa (maximum)		
Nominal temperature	25 °C		
Operating temperature	-25.0 °C	-	+60 °C

Battery life			
Measuring cycle	4 seconds	3 minutes	15 minutes
Record period	11.5 days	521 days	7.1 years



Figure 3-5: EASYLog 80CL

3.5.1.2 Winder measurements

To ensure that the position of the various conveyances in the shaft is known, it is necessary that rotary encoders be connected to the winder. This did pose something of a problem as the only encoders available are digital encoders, which require logging from the PLC. The following combination was chosen.

Ruggedised rotary encoders from Leine and Linde, connected to a standard Honeywell PLC, operated using a standard touch screen interface, were chosen for this application. These encoders are attached to the shaft on the winder in question and therefore measure the overall revolutions of the winder. This arrangement requires a 220 V connection. This is considered a weakness as the early

tests showed that this connection was broken either by power trips on the shaft or personnel removing plug connections. To ensure that the status of these connections was known at all times, a GSM module was also attached to the PLC. Figure 3-6, Figure 3-7 and Figure 3-8 show the set-up.

These encoders have an operating range of -40 to 70 °C and are sufficiently accurate to measure up to 5 000 increments on a revolution. The PLC was programmed to store data every second and to record 50 points on each rotation. This is sufficient to allow the calculation of the position of each conveyance, as well as to calculate acceleration and deceleration.

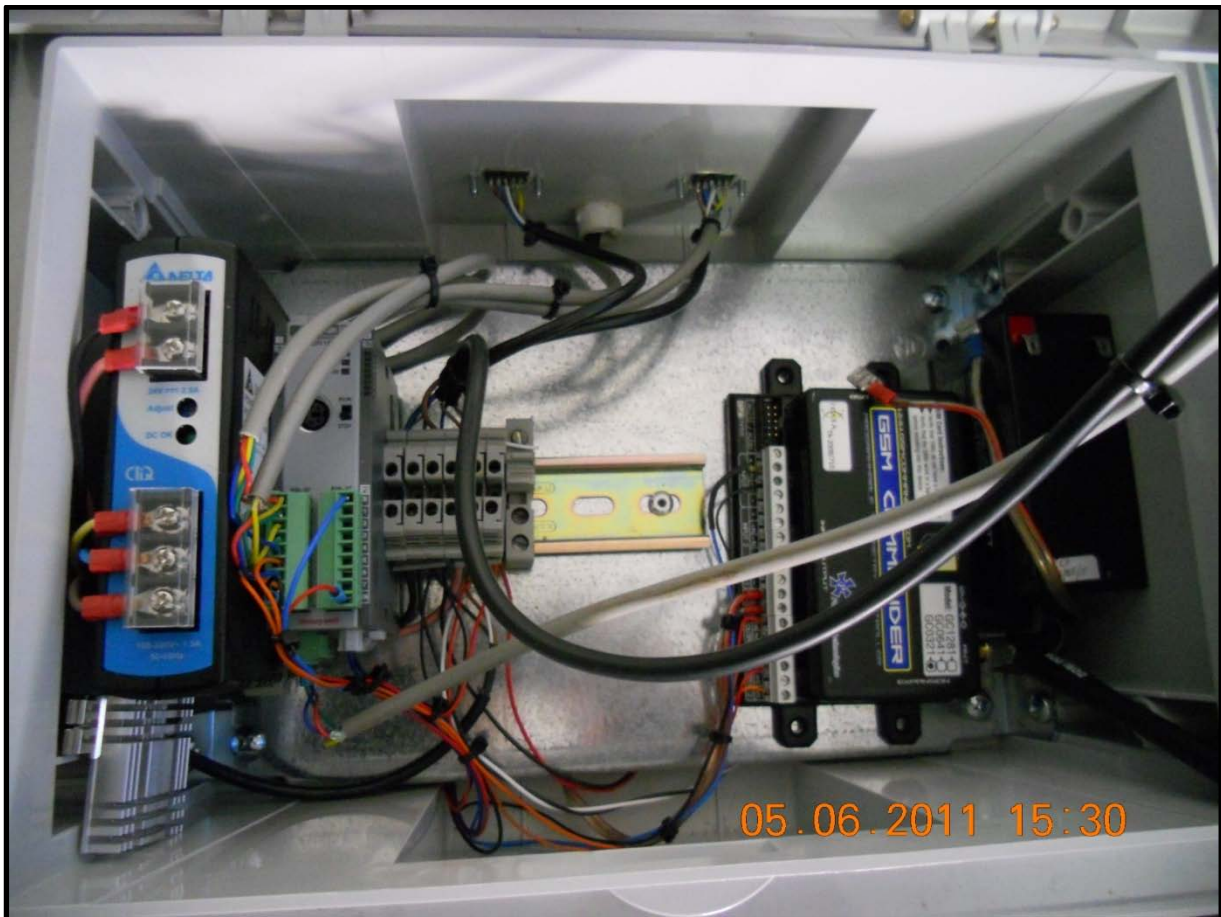


Figure 3-6: PLC, interface and GSM module for rotary encoder



Figure 3-7: Rotary encoder

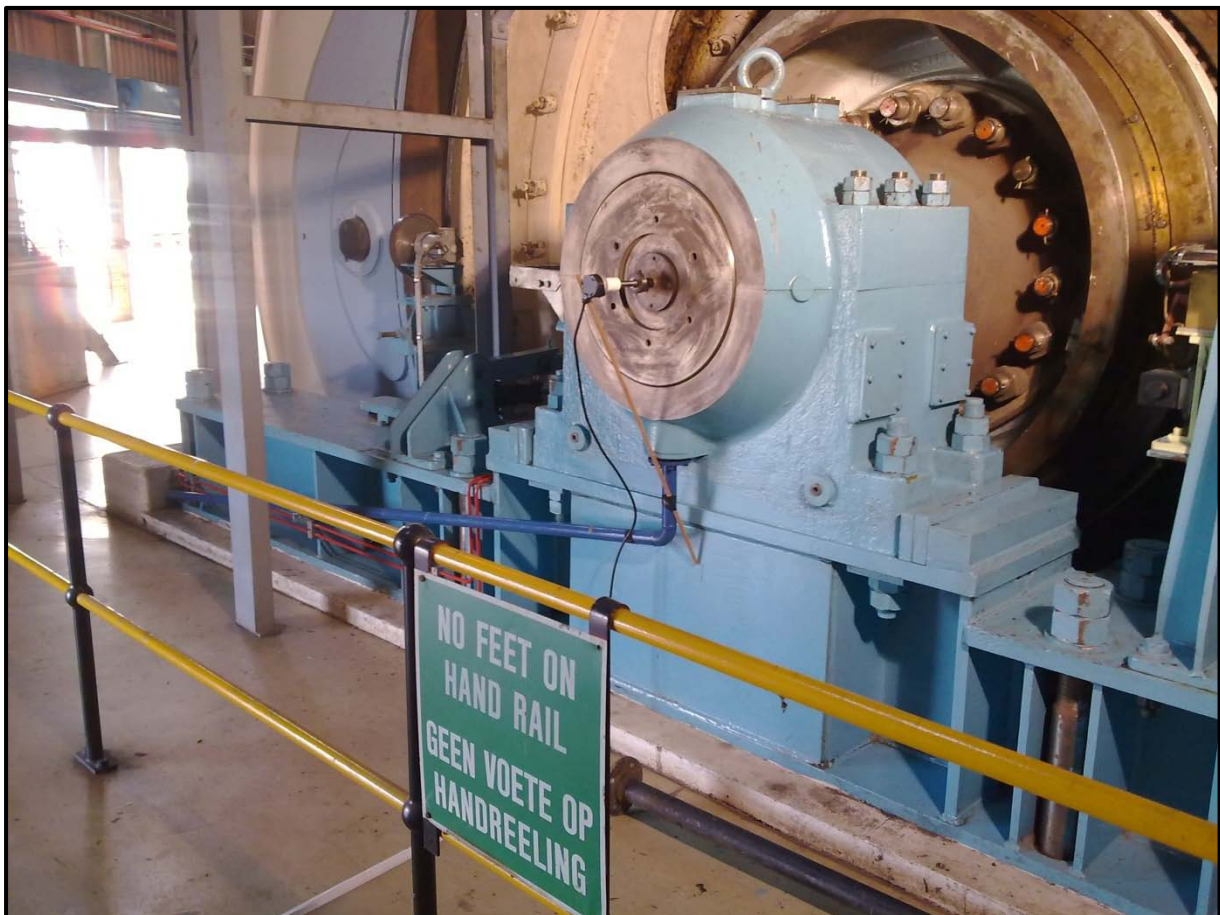


Figure 3-8: Rotary encoder connection on winder side shaft

3.5.1.3 Velocity measurements

The velocity measurements were taken during the shaft tests using a hand-held anemometer. These results were then compared with the information available from the ventilation department to ensure accuracy and consistency.

The instrument used was a Kestrel 4000 (see Figure 3-9), with the following specifications:

Range	:	0.4–60 m/s
Accuracy	:	±3% of reading
Resolution	:	0.1 m/s
Operating temperature	:	-29–70°C



Figure 3-9: Kestrel 4000 environmental logger

3.5.2 Data Collection and Collation

3.5.2.1 Data collection

The general procedure for the collection of data involved firstly the preparation of the instrumentation. This required confirmation of the battery life of the instrumentation, clearing of the logged data and synchronisation of all the instrumentation to a single computer. This was a specific

requirement because the various loggers were not connected and the single reference time point was therefore the only point that would allow the various measurements to be compared.

The environmental loggers were placed in positions that were determined in consultation with the mine ventilation officer. They were placed during the shaft inspection. During this inspection the shaft ventilation free air velocity was confirmed and the general condition and layout of the shaft was evaluated.

Once this had been completed, the loggers for the winders were put in place and the logging started.

All the instruments logged data for one week, at the end of which they were removed during the next scheduled shaft inspection.

3.5.2.2 Data collation

Once the data from the various loggers had been collected, they were all downloaded into a personal computer. To allow the data to be collected over a full week, the environmental loggers were set to record every 10 seconds and the winder loggers to record every second.

Environmental loggers

The data from these loggers required some manipulation before they could be used for a meaningful comparison. The following steps had to be taken:

- 1 Calculate the wet-bulb temperature.
- 2 Ensure timing compatibility.
- 3 Calculate the measured pressure drop.
- 4 Calculate the theoretical pressure drop.

The calculation of the wet-bulb temperature does pose a challenge. The usual calculation method requires an iterative evaluation. However, the large amount of data requiring collation meant that this could not be effectively achieved. An Excel Add-In package available from kW Engineering was therefore used. This calculates the wet-bulb temperature based on data published in the 1997 *ASHRAE Handbook of Fundamentals*.

The remainder of the parameters were calculated in the usual manner, as described above.

Winders

The data for the winders are collated against time. This allows the position of the conveyance in the shaft to be calculated and these data to be synchronised with those of the data logger. To do this the specific diameter of each of the winder drums under consideration must be known. This information is then used to calculate the speed and position of the conveyances against time. Once this is

completed, 10-second snapshots of the winder movements are taken to allow comparison against the environmental data.

A typical graph showing the results of the analysis is shown in Figure 3-10.

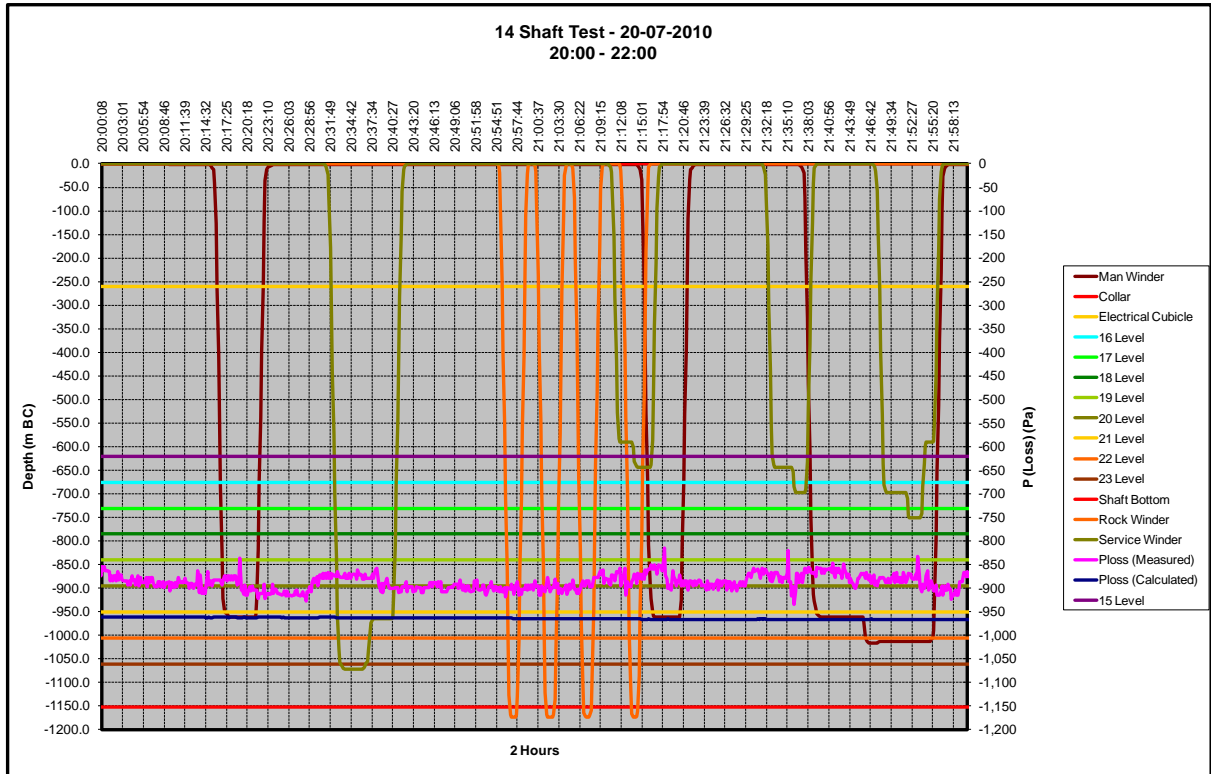


Figure 3-10: Typical graph of collated results (including environmental data and winder data)

3.5.3 Results and Conclusion

The results of the tests and the conclusions drawn from the analysis are discussed in CHAPTER 4.

3.5.4 Accuracy of Data Collation Instrumentation

The various instrumentation and loggers used for the evaluation of the various shaft systems have been discussed in the previous sections. In this section the accuracy of the measurements will be evaluated. In this evaluation, the input data to the various calculations is varied in accordance with the quoted instrument accuracy and the difference in the output is noted. The values from two points need to be considered. Thus in order to evaluate the accuracy of a measurement at two points, a total of 9 variations must be completed. These are:

- | | | |
|------|------------------------------------|-------------------------------------|
| i | Measured Value at Pt 1 | Measured Value at Pt 2 |
| ii | Measured Value at Pt 1 (+Variance) | Measured Value at Pt 2 |
| iii | Measured Value at Pt 1 (-Variance) | Measured Value at Pt 2 |
| iv | Measured Value at Pt 1 | Measured Value at Pt 2 (+ Variance) |
| v | Measured Value at Pt 1 | Measured Value at Pt 2 (- Variance) |
| vi | Measured Value at Pt 1 (+Variance) | Measured Value at Pt 2 (+ Variance) |
| vii | Measured Value at Pt 1 (+Variance) | Measured Value at Pt 2 (- Variance) |
| viii | Measured Value at Pt 1 (-Variance) | Measured Value at Pt 2 (+ Variance) |
| ix | Measured Value at Pt 1 (-Variance) | Measured Value at Pt 2 (- Variance) |

The details of the instrument used for the measurement of the temperatures and pressures in the shaft are noted in Table 3-3.

Table 3-4: Evaluation of Accuracy of Temperature Measurements on the Overall Results

Item	Temperature (Pt 1) (°C)	Temperature (Pt 2) (°C)	P _{Loss} (Difference from 1)
1	14.4	19.8	-890 Pa
2	14.7	19.8	0.6%
3	14.1	19.8	-0.6%
4	14.4	20.1	-0.6%
5	14.4	19.5	-0.6%
6	14.7	20.1	1.2%
7	14.7	19.5	-0.1%
8	14.1	20.1	0.1%
9	14.1	19.5	-1.2%

As can be seen from the above results, the accuracy of the measurement of temperature will have little effect on the overall results.

Table 3-5: Evaluation of Accuracy of Pressure Measurements on the Overall Results Typical)

Item	Pressure (Pt 1) (kPa)	Pressure (Pt 2) (kPa)	P _{Loss} (Difference from 1)
1	90.41	99.51	-890.55 Pa
2	90.51	99.51	-10.6%
3	90.31	99.51	13.4%
4	90.41	99.61	12.0%
5	90.41	99.41	-9.6%
6	90.51	99.61	-1.2%
7	90.51	99.41	-18.4%
8	90.31	99.61	-29.0%
9	90.31	99.41	-1.2%

As can be seen from the above results, the accuracy of these measurements can have the effect of increasing the calculated pressure losses by 12% or decreasing them by 29%. This relative accuracy must be borne in mind when evaluation the final results.

The details of the instrument used for the measurement of the velocity in the shaft are noted in section 3.5.1.3.

Table 3-6: Evaluation of Accuracy of the Velocity Measurements on the Overall Results Typical)

Item	Velocity (m/s)	P _{Loss} (Difference from 1)
1	9.4	-890.55 Pa
2	9.1	0.0%
3	9.7	0.0%

The free air velocity of the ventilation in the shaft was measured at various points in the shaft. This was found to be consistent along the length of the shaft. This consistency was valid as long as the no levels were passed which extracted ventilation air from the shaft.

As can be seen from the above results, the accuracy of these measurements can have the no effect on the calculated pressure losses.

3.6 COMPUTATIONAL FLUID DYNAMICS

The package used for the CFD analysis is the STAR-CCM+ from CD ADAPCO, supplied by Aerotherm in South Africa. This package allows the 3D modelling of the shaft section under consideration by solving the continuity and momentum equations inside discrete cells. The various shaft geometries were modelled in the software using the 3D-CAD module supplied. This module allows the complete model to be developed in readiness for the mesh generation.

3.6.1 Mesh Generation

The various shaft sections used in this analysis were modelled in the package using the 3D-CAD modelling features and the model was created on a 1-to-1 basis with no scaling required. This model was then meshed using a combination of the built-in polyhedral mesher for volumes and the surface remesher. The nature of the problem being examined also required that the effects of the solid interfaces and the air be modelled as accurately as possible. In this regard the Prism Layer option available as part of the meshing model was selected. This model applies additional elements at the solid interface to facilitate the accurate modelling of the turbulence around these points.

The length of the primary model section was chosen to be 20 m. However, to ensure that the flow regime within the shaft was fully developed before the pressure losses over the section were measured, the initial length of shaft to be simulated such that this flow regime could develop was 10 x the diameter of the shaft, in this instance 80 m. This required that the model be iterated four times (i.e. the output of the simulation becomes the input of the next simulation).

To ensure accurate results, a mesh refinement analysis was performed until a mesh size was found with small changes in the pressure losses. The results of this exercise are shown in Table 3-7.

Table 3-7: Mesh refinement evaluation

Base size	No. of cells in model	Reference pressure	P_{Drop} (over section)	% difference (against next value)	% of reference pressure
0.15 m	1 110 000	88 000 Pa	11.42	-5%	0.01%
0.20 m	470 000	88 000 Pa	11.74	3%	0.01%
0.25 m	350 000	88 000 Pa	11.19	15%	0.01%
0.30 m	210 000	88 000 Pa	12.87	NA	0.01%

As can be seen from Table 3-7, there is very little difference between the pressure drops measured for the mesh sizes of 0.15, 0.20 and 0.25 m.

As a result of this analysis, it was decided to use a base size of 0.25 m. This base size is sufficiently small to allow the shaft configurations to be accurately sized, but was also sufficiently large to allow the simulations to be run efficiently.

The next requirement was to determine the effect that using the prism layers would have. These layers provide additional cell data close to the skin of the cell and were thought to have an effect on the overall pressure losses over the shaft length. This setting causes the software to generate additional layers at each boundary surface, thus improving the accuracy of calculation for the surface interactions. There was, however, a negligible difference between the results from the simulations run with and without these prism layers. It was decided nonetheless to include a prism layer with a setting of 5 (i.e. five additional layers adjacent to the boundary surface) for the simulations. A schematic of the mesh arrangement is shown in Figure 3-11.

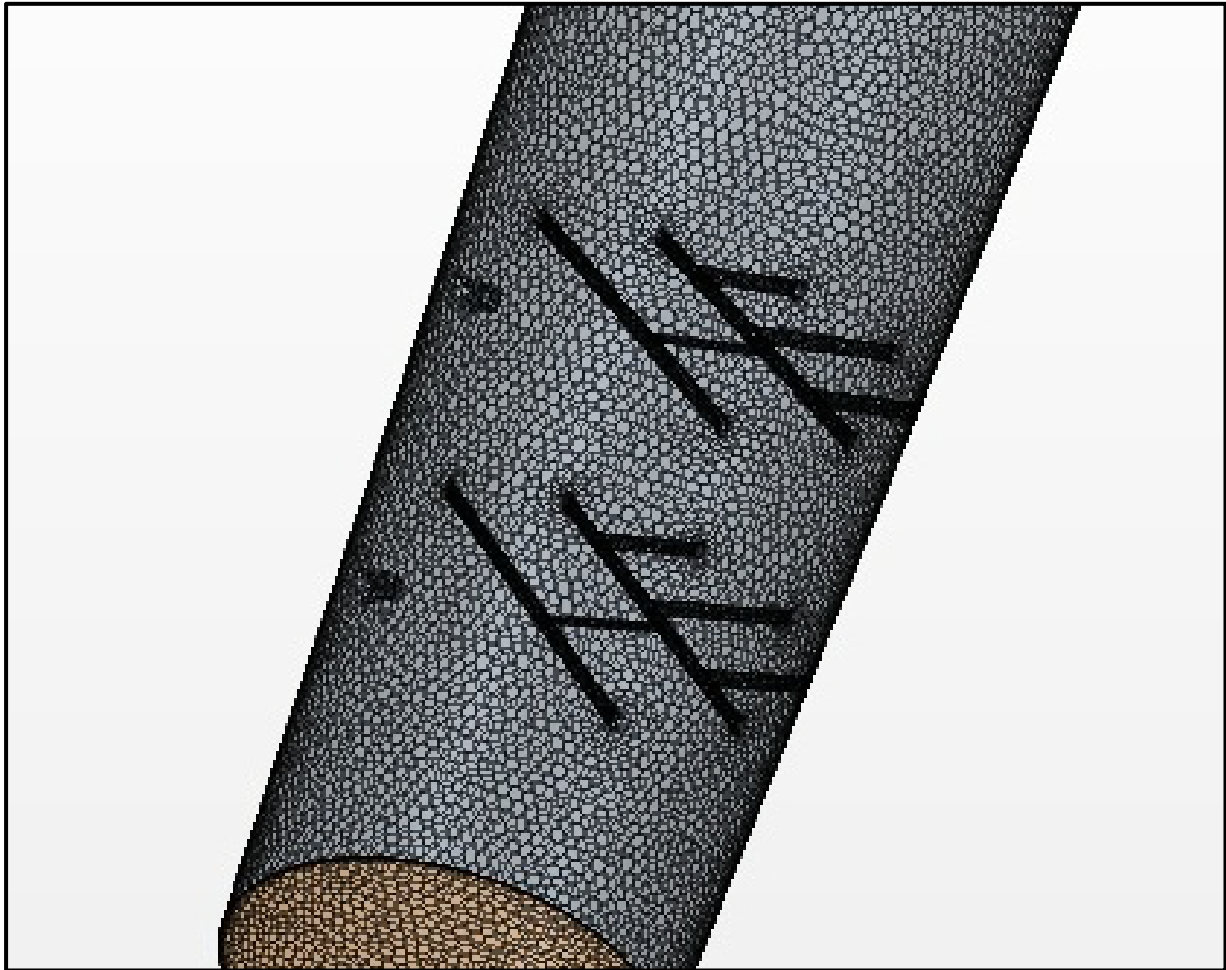


Figure 3-11: Schematic of meshed shaft arrangement

The above schematic shows a view of the mesh shaft section. Additional elements were also added to the model in accordance with the simulation requirements discussed in Section 3.6.5.

3.6.2 Fluid Model Selection

Once the geometry had been modelled and meshed, the appropriate fluid models were selected. In this instance, the thermodynamic and body forces were assumed to be small and the fluid used for the analysis was an ideal gas. The system was modelled in three dimensions and the K-Omega turbulence model was also used. These were resolved using the SIMPLE algorithm to solve the continuity and momentum equations in every cell.

The convergence requirement was set to 1×10^{-4} for continuity and momentum. This was achieved in most cases, although in some cases a convergence of 1×10^{-1} was accepted. In all instances the simulation was run until the data showed repeatability. This required that the respective curves were constant before the analysis was stopped and the results recorded.

3.6.3 Boundary Conditions

The following boundary conditions were used:

- 1 *Inlet*: The inlet was defined as a constant-velocity inlet for the first section simulated. Subsequent to this, the velocity profile used for the input was taken from the output of the previous simulation.
- 2 *Outlet*: The outlet was defined as being a constant pressure. This was consistent throughout all the simulations.
- 3 *Wall conditions*: The wall were defined as a rough wall with an asperity of 10 mm. This resulted in a Y^+ along the wall of approximately 90, which is acceptable.

It is worth noting that using the mass flow of the fluid as the input would have been ideal. However this was not possible, suffice to say the variation of the mass flow over the test section never exceeded 2.5% of the total mass flow. This is sufficiently small to not be a concern.

3.6.4 Simulation Runs

Each of the simulations was run on a personal computer running Windows XP. The computer had a hard drive with a 500 GB capacity and 4 GB of RAM. All the simulations were run using STAR-CCM+ version 6.02.007. Each simulation took between six and eight hours to complete, including all the required iterations.

3.6.5 Simulations Completed for this Analysis

To ensure a thorough understanding of the interaction between the various items contained in a shaft, it was decided to build the CFD model systematically and to include the various pieces of equipment progressively. This would allow the effect of the individual items to be evaluated. In this regard the following series of tests were completed.

3.6.5.1 T01 – Shaft barrel pressure losses

This consisted of measuring the pressure loss over a segment of the shaft barrel. Care was taken to ensure that the flow was fully developed before the results were collated.

3.6.5.2 T02 – Shaft barrel and one bunton across the shaft

This consisted of placing one bunton across the middle of the shaft in the middle of the test section. This test was used to determine the resistance that this bunton would offer to airflow through the shaft. A fully developed flow was therefore introduced at the entrance and the effect of the shaft segment evaluated.

3.6.5.3 T03 – Shaft barrel and two buntions across the shaft

This consisted of placing two buntions across the middle of the shaft at the same spacing that the buntions would normally have. This test was used to determine the resistance that the buntions would offer airflow through the shaft, including an evaluation of the interference factor that is used in the general analysis. A fully developed flow was therefore introduced at the entrance and the effect of the shaft segment evaluated.

3.6.5.4 T04 – Shaft barrel and full buntions set

This consisted of placing a full buntions set across the middle of the shaft at the same spacing that the buntions would normally have. This test was used to determine the resistance that the buntions set would offer airflow through the shaft, including an evaluation of the interference factor that is used in the general analysis. A fully developed flow was therefore introduced at the entrance and the effect of the shaft segment evaluated.

3.6.5.5 T05 – Shaft barrel and pipes at pipe diameter

This consisted of using the full shaft barrel and placing the pipes in the barrel, consistent with the normal placement and size of the pipes in the shaft under consideration. This test was used to determine the actual resistance and flow characteristics of the ventilation air around the pipes.

3.6.5.6 T06 – Shaft barrel and pipes at flange diameter

This consisted of using the full shaft barrel and placing the pipes in the barrel, consistent with the normal placement of the pipes in the shaft under consideration. The pipes were, however, modelled to have a diameter equal to that of the flanges for that pipe. This test was used to determine the actual resistance and airflow characteristics of the ventilation air around the pipes when they are modelled, as is recommended by the current theory.

3.6.5.7 T07 – Shaft barrel and pipe including flanges

This consisted of using the full shaft barrel and placing the pipes in the barrel, consistent with the normal placement of the pipes in the shaft under consideration. The pipes were modelled at the standard pipe diameter and the flanges were included at a spacing consistent with the spacing of the buntions. This test was used to determine the actual resistance and flow characteristics of the ventilation air around the pipe including the discontinuity that the flanges introduce.

3.6.5.8 T08 – Shaft barrel and buntions and pipes at pipe diameter

This consisted of using the full shaft barrel, including the buntions particular to each shaft, and placing the pipes in the shaft. These pipes were positioned consistent with the normal placement of

the pipes in the shaft under consideration.

3.6.5.9 T09 – Shaft barrel and buntions and pipes at flange diameter

This consisted of using the full shaft barrel, including the buntions particular to each shaft, and placing the pipes in the shaft, but with the pipes modelled at the same diameter as the flanges. These pipes were positioned consistent with the normal placement of pipes in the shaft under consideration.

3.6.5.10 T10 – Shaft barrel and buntions and pipe including flanges

This consisted of using the full shaft barrel, including the buntions particular to each shaft, and placing the pipes in the shaft. The pipes were modelled at the standard pipe diameter and the flanges were included at a spacing consistent with the spacing of the buntions. These pipes were positioned consistent with the normal placement of pipes in the shaft under consideration.

3.6.5.11 T11 – Shaft barrel and buntions and pipe including flanges and skip 1

The full shaft barrel was modelled, including all the buntions and pipes. The skip in this instance was modelled in position in the shaft.

3.6.5.12 T12 – Shaft barrel and buntions and pipe including flanges and skip 2

The full shaft barrel was modelled, including all the buntions and pipes. The skip in this instance was modelled in position in the shaft.

3.6.5.13 T13 – Shaft barrel and buntions and pipe including flanges and man cage 1

The full shaft barrel was modelled, including all buntions and pipes. The man cage in this instance was modelled in position in the shaft.

3.6.5.14 T14 – Shaft barrel and buntions and pipe including flanges and man cage 2

The full shaft barrel was modelled, including all the buntions and pipes. The man cage in this instance was modelled in position in the shaft.

3.6.5.15 T15 – Shaft barrel and buntions and pipe including flanges and service cage

The full shaft barrel was modelled, including all the buntions and pipes. The service cage in this instance was modelled in position in the shaft.

3.7 ECONOMICS

The emphasis of the work reported on in this thesis was on comparing the overall lifecycle cost of different equipping options and the associated capital costs to elicit a total cost for the life of mine (LOM).

The basis for this comparison was 20 years at a lower-than-anticipated electrical tariff increase of 10% per annum.

3.7.1 Shaft Modifications

This was not evaluated in detail for the reasons discussed in Section 1.5.1. The costs associated with the different diameters are shown in Figure 1-11.

3.7.2 Shaft Equipping

This refers to the potential modifications to the steelwork and fittings in the shaft. Such modifications can be classified into three sections:

- 1 *Shaft steelwork:* These are the buntons and the guides that are used to guide the shaft cages and skips while they are traversing the shaft. The cost of the shaft steelwork will be based on a R/m basis. The potential increase or decrease in this value was evaluated against recent data obtained for the equipping of shafts.
- 2 *Installation time:* Discussions with shaft-sinking professionals showed that the installation times for the various buntion configurations are sufficiently similar to ensure that these costs will be the same whatever the shape.
- 3 *Shaft service:* The requirement of the shaft services (i.e. piping, cables, etc.) is defined by the mining operations and is beyond the purview of this work. However, the placement of these items in the shaft in order to optimise the pressure losses in the shaft is within the scope of this work. The installation time for these should be the same no matter where they are installed around the shaft circumference. This will, however, be reviewed and any potential differences between the capital costs will be evaluated in a similar manner to that described in points 1 and 2 above.

3.7.3 Shaft Conveyances

This evaluation will pertain primarily to the slight modifications that can be made to the conveyances which will potentially give the largest savings.

3.7.4 Operating Costs

These costs are generally the most difficult to evaluate. However, most shaft maintenance activities are completed during the legally required shaft inspections. These inspections are carried out weekly, and it is during this time that the general cleaning and basic maintenance work is carried out.

Generally, any additional work required on the shaft results from external factors or activities, e.g. corrosion, pipe misalignment due to impact from a falling object, steelwork alignment due to long use, etc. It is therefore appropriate to derive the operating costs of the shafts from the electrical requirement to transfer the ventilation air through the shaft. Thus a pressure and flow requirement for the shaft will be calculated and the electrical costs required to deliver this pressure and flow will be calculated.

It is not possible to compare the specific costs associated with each shaft as this is dependent on variables specific to that shaft, e.g. the transmission zone. The transmission zones are the zones into which Eskom has divided the country to allow for a cost associated with the supplying of a specific geographical location. The calculation will therefore be made from the MEGAFLEX (non-local authority rate) as supplied in the Eskom 2011 Tariff book (Eskom, 2011). These costs and the assumptions used for the calculation are listed below:

- 1 Transmission zone – Assumed to be ≥ 600 km and ≤ 900 km
- 2 Voltage – ≥ 500 V ≤ 66 kV
- 3 Charges will be calculated excluding VAT
- 4 Assumed to be a key customer
- 5 Equipment will be assumed to be running 24 hours a day, 7 days a week, for comparative reasons.

3.8 SUMMARY OF METHOD OF EXPERIMENTATION AND ANALYSIS

The objectives of the work presented in this chapter were the following:

- 1 Present the current theory used for the evaluation of pressure drops in shafts.
- 2 Define a methodology for the testing of working shafts to validate this theory.
- 3 Define the CFD analysis techniques to be used for the evaluation of the shafts.
- 4 Define the method by which the economic evaluation of the shaft systems will be carried out.

The current theory for the evaluation of shaft resistances is based on a mix between the standard fluid dynamics Chezy-Darcy friction factor theory for duct flow, an extrapolation of drag coefficients for various buntion shapes and an extrapolation of data for the resistance that shaft conveyances offer when moving in a shaft. The resistances offered to the ventilation flow by the buntions, guides, shaft fittings and rough surface of the shaft wall are all calculated separately. These resistances are reduced to a value of the standard Chezy-Darcy friction factor (f). This factor is then applied to the standard fluid dynamics equation for the calculation of friction losses in ducts.

The pressure loss resulting from the movement of a conveyance in the shaft is calculated separately from the empirical data. This pressure loss is then added to or subtracted from the shaft pressure losses calculated from fluid dynamic theory depending on the direction in which the conveyance is travelling.

To validate the current theory, it was necessary to complete tests on working shafts. These were conducted on Impala Platinum shafts. A methodology for the additional dynamic tests on the shafts was presented in this chapter. This included the use of loggers to ensure that the ventilation response to the use of conveyances is understood. Measurement devices were installed in the shaft at appropriate intervals. These results were collated with those from the rotary encoders that were placed on the winder in order to determine the position of the conveyances in the shaft. The combination of these results gave the standard resistance of the shaft when the conveyances were stationary as well as when they were moving. The results of this analysis are discussed in CHAPTER 4.

Once the analysis had been completed and the general verification of these shafts against the current theory had been done, the next phase of the work was to model the shaft. This was done to try and gain an understanding of the various items in the shaft and the resistance they offer to the ventilation flow. For this purpose computational fluid dynamic (CFD) analysis was used. This analysis was completed using the STAR-CCM+ package. Various CFD models were evaluated, with specific emphasis on building the models by introducing the various items in the shaft into subsequent models. The purpose was to determine the effect that each of these items had on the overall resistance that the buntions and fittings offered to the ventilation flow.

The goal of the analysis presented in this thesis is to find ways in which to reduce the resistance the shaft offers to ventilation flow through it. In this regard, it is important to evaluate the potential solutions in order to determine the savings that could be achieved. To do this, the effect of various modifications was evaluated against the reduced operating and capital costs for those modifications. These costs were calculated from the Eskom 2011 Tariff book.

CHAPTER 4 RESULTS AND EVALUATION OF SHAFT TESTS

4.1 RESULTS OF SHAFT TESTS

4.1.1 Tests on No. 14 shaft

4.1.1.1 Shaft details and installation of equipment

The tests for No. 14 shaft of Impala Platinum were conducted from 15 to 22 July 2010. The required instrumentation was installed in the following positions in the shaft:

- 1 Surface (environmental logger was installed in the winder house immediately adjacent to the shaft)
- 2 20 level – Environmental logger (895 m BC)
- 3 21 level – Environmental logger (950 m BC)
- 4 22 level – Environmental logger (1 005 m BC)
- 5 23 level – Environmental logger (1 060 m BC)
- 6 Rock winder (6.3 m diam.) – Rotary encoder – PLC1 (log channels 3 and 4) (double drum winder) (measured conveyance speed – 15.2 m/s)
- 7 Man winder (6.9 m diam.) – Rotary encoder – PLC2 (log channels 1 and 2) (double drum winder) (measured conveyance speed – 14.1 m/s)
- 8 Service winder (4.3 m diam.) – Rotary encoder – PLC2 (log channels 3 and 4) (single drum winder) (measured conveyance speed – 13.2 m/s)
- 9 Free Air Velocity of ventilation air in shaft – measured as 9.4 m/s

It is not necessary to have the data collected over such an extended period but, as discussed above, shaft access was only available during the weekly shaft inspections.

This is a 7.4 m diameter shaft which has been equipped with the airflow buntons. The conditions of the shaft were found to be generally good with little or no interference in the shaft as a result of additional fittings and extraneous installations. This shaft was also concrete-lined.

The ventilation air is introduced into the shaft via a sub-bank air duct. It was not possible to place the environmental data loggers directly in the shaft. These were therefore placed immediately adjacent to the shaft on the levels indicated above.

The dimensions of the various cages, skips and fittings in the shaft can be found on a detailed shaft cross-section in Appendix D.

It should be noted at this point that it was not possible to place a rotary encoder on each drum of the double drum winders. This was because no external shaft was available on the motor side of the winder. However, the standard policy at Impala limits clutching of a winder (i.e. the moving of one drum and its associated conveyance) to the shift-change period only. These times are easily discernible from the data and have not been used in this analysis. A schematic of the shaft cross-section is provided in Figure 4-1.

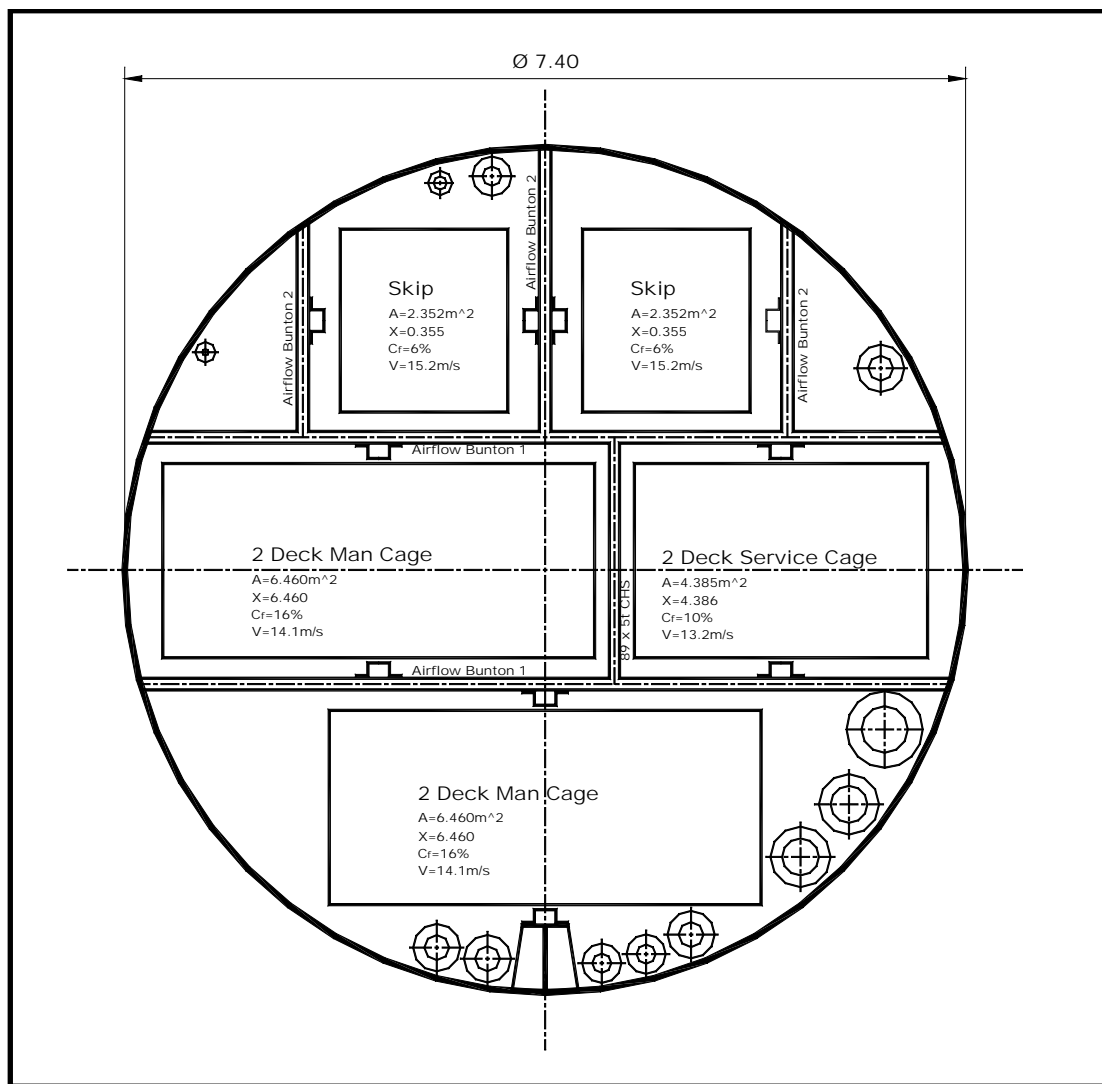


Figure 4-1: Cross-section of No. 14 shaft

4.1.1.2 Environmental loggers

All the environmental loggers were time-stamped from a common computer before they were installed. These data were then sorted to display the results from each of the days on which testing took place.

The test results from the first day were discarded as a result of inconsistencies in the readings from the surface data logger. This logger had been moved by the mine personnel. It was repositioned appropriately and the remainder of the results were found to be consistent and could be used for the rest of the test.

It should be noted that there were times in the shaft when the pressure readings varied significantly. These times are consistent with the times that the ventilation fans were not operating at full flow. These periods were also avoided in the evaluations given below.

4.1.1.3 Rotary encoders

The PLCs associated with these encoders were time-corrected to the same computer used for the environmental loggers. The results of these encoders were corrected to show the conveyances in appropriate positions in the shaft. This was done primarily by using the drum diameter and matching the conveyance position on each of the levels to the movement of the drum.

The PLCs measured the position of the conveyance every second, whereas the environmental loggers measured every 10 seconds. The winder data were therefore also corrected to start and stop at equivalent times to the environment loggers.

The PLCs attached to these encoders were placed in the drivers' cabins where appropriate. These were not tampered with for the duration of the experiment.

4.1.1.4 Summary of data from tests on No. 14 shaft

The friction losses in the shaft were measured and calculated in accordance with the theory discussed in previous chapter of this thesis. The analysis was completed using the data between surface and 20 level as these data showed the least amount of scatter. A summary of these results is given in Table 4-1 to Table 4-4.

Table 4-1: No. 14 shaft test results – Data

Item	Value	Symbol	Units	Description
1	0.076	f_{BTotal}	-	Total bunton Chezy-Darcy friction factor(
2	0.022	f_{Shaft}	-	Shaft asperities Chezy-Darcy friction factor
3	0.098	$f_{Total Shaft}$	-	Total shaft Chezy-Darcy friction factor
4	1.099	$X_{Skip 1 Corr}$	-	Skip shock loss correction factor
5	0.434	$X_{Cage 1 Corr}$		Man cage shock loss correction factor
6	0.466	$X_{Service Cage Corr}$		Service cage shock loss correction factor

Table 4-2: No. 14 shaft test results – Service cage

	P_{loss} (measured) (surface to 20 level)	P_{loss} (calculated) (surface to 20 level)	Units	Description
1	891.1	645.0	Pa	Below 20 level in shaft
2	1.77	1.28	Pa/m	Below 20 level in shaft
3	899.5	644.7	Pa	Above 20 level in shaft
4	1.78	1.28	Pa/m	Above 20 level in shaft

Note: The measured pressure measurements were taken at a time when the conveyances were not moving. The calculated pressure loss has, therefore, been completed assuming no conveyances are moving in the shaft.

Table 4-3: No. 14 shaft test results – Rock skip

	P_{loss} (measured) (surface to 20 level)	P_{loss} (calculated) (surface to 20 level)	Units	Description
1	897.5	630.1	Pa	No conveyance moving
2	1.78	1.25	Pa/m	No conveyance moving
3	893.5	630.1	Pa	Rock skip moving
4	1.77	1.25	Pa/m	Rock skip moving

Note: The measured pressure measurements were taken at a time when the conveyances were not moving. The calculated pressure loss has, therefore, been completed assuming no conveyances are moving in the shaft.

Table 4-4: No. 14 shaft test results – Man cage

	P_{loss} (measured) (surface to 20 level)	P_{loss} (calculated) (surface to 20 level)	Units	Description
1	930.0	636.8	Pa	No conveyance moving
2	1.85	1.26	Pa/m	No conveyance moving
3	947.9	635.4	Pa	Man cage moving
4	1.88	1.26	Pa/m	Man cage moving

Note: The measured pressure measurements were taken at a time when the conveyances were not moving. The calculated pressure loss has, therefore, been completed assuming no conveyances are moving in the shaft.

4.1.2 Tests on No. 11 shaft

4.1.2.1 Shaft details and installation of equipment

The tests for No. 11 shaft of Impala Platinum were conducted from 13 January 2011 to 21 July 2011.

The required instrumentation was installed in the following positions in the shaft:

- 1 Surface (environmental logger was installed in the winder house immediately adjacent to the shaft)
- 2 14 level – Environmental logger (619m BC)
- 3 15 level – Environmental logger (674m BC)
- 4 18 level – Environmental logger (839m BC)
- 5 19 level – Environmental logger (894m BC)
- 6 20 level – Environmental logger (949m BC)
- 7 Rock winder (5.5 m diam.) – Rotary encoder – PLC1 (log channels 1 and 2) (double drum winder) (measured conveyance speed – 14.3 m/s)
- 8 Man winder (4.5 m diam.) – Rotary encoder – PLC2 (log channels 1 and 2) (Blair winder) (measured conveyance speed – 15.9 m/s)
- 9 Service winder – This shaft has no service winder
- 10 Free Air Velocity of ventilation air in shaft – measured as 10.0 m/s

It is not necessary to have the data collected over such an extended period but, as discussed above, shaft access was only available during the weekly shaft inspections.

This is a 6.2 m diameter shaft which has been equipped with the airflow buntons. The condition of the shaft was found to be generally good with little or no interference in the shaft as a result of additional fittings. This shaft was also concrete-lined.

The ventilation air is introduced into the shaft via a sub-bank air duct. It was not possible to place the environmental data loggers directly in the shaft. These were therefore placed immediately adjacent to the shaft on the levels indicated above. The dimensions of the various cages, skips and fittings in the shaft can be found on a detailed shaft cross-section in Appendix E.

It should be noted at this point that it was not possible to place a rotary encoder on each drum of the double drum winders. This was because no external shaft was available on the motor side of the winder. However, the standard policy on Impala limits clutching of a winder (i.e. the moving of one drum and its associated conveyance) to the shift-change period only. These times are easily

discernible from the data and have not been used in this analysis. A schematic of the shaft cross-section is provided in Figure 4-2.

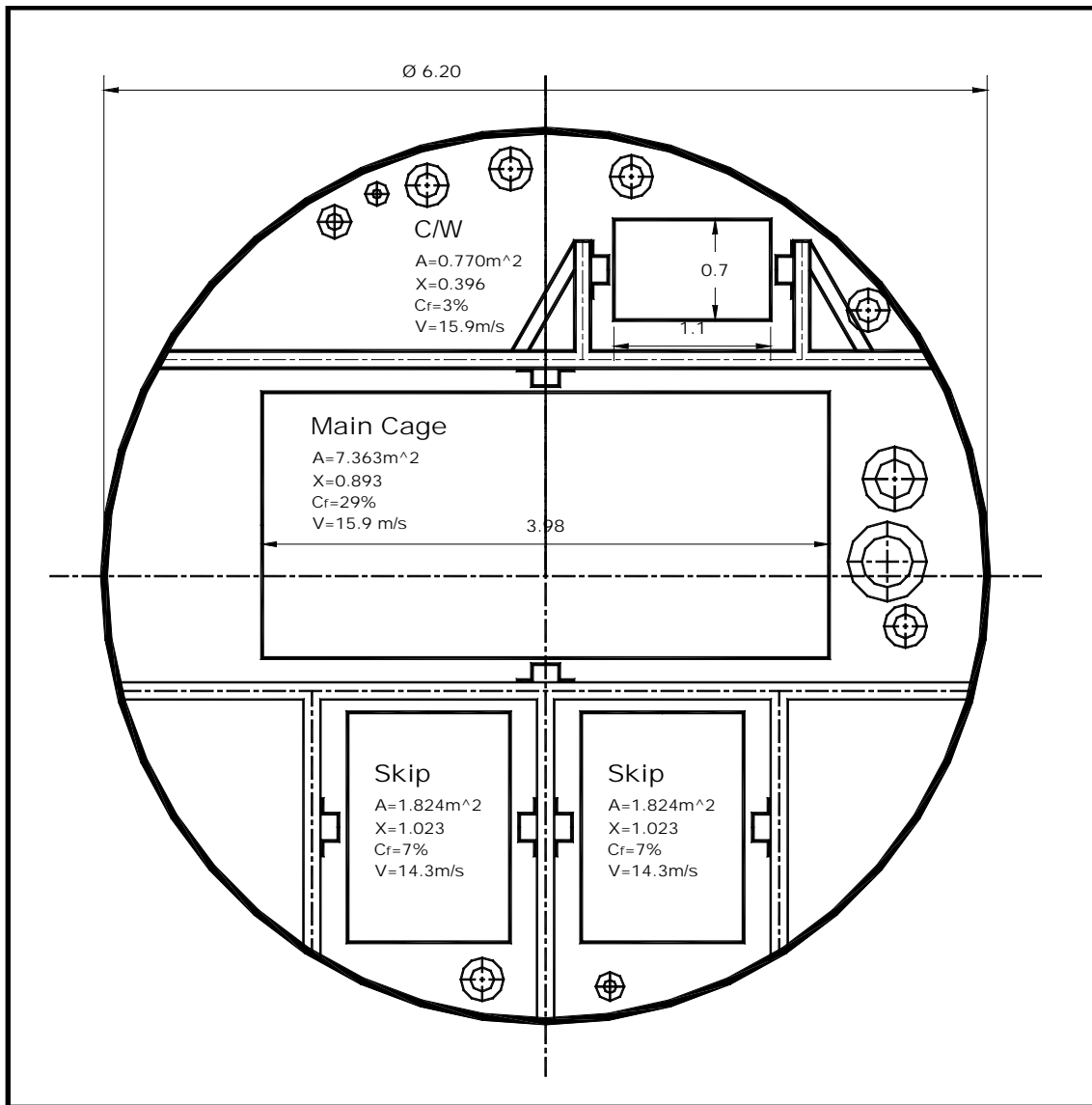


Figure 4-2: Cross-section of No. 11 shaft

4.1.2.2 Environmental loggers

All the environmental loggers were time-stamped from a common computer before they were installed. These data were then sorted to display the results from each of the days on which testing took place.

It should be noted that there were times in the shaft when the pressure readings varied significantly. These times are consistent with the times that the ventilation fans were not operating at full flow. These periods were also avoided in the evaluations given below.

4.1.2.3 Rotary encoder

The PLCs associated with these encoders were time-corrected to the same computer used for the environmental loggers. The results of these encoders were corrected to show the conveyances in appropriate positions in the shaft. This was done primarily by using the drum diameter and matching the conveyance position on each of the levels to the movement of the drum.

The initial two days of test results associated with the man winder encoder were discarded. This was a result of the attachment to the winder coming adrift. The attachment was reconnected and the rest of the tests showed good results which were used.

The PLCs measured the position of the conveyance every second, whereas the environmental loggers measured every 10 seconds. The winder data were therefore also corrected to start and stop at equivalent times to the environment loggers.

The PLCs attached to these encoders were placed in the drivers' cabins where appropriate. These were not tampered with for the duration of the experiment.

4.1.2.4 Summary of data from tests on No. 11 shaft

The friction losses in the shaft were measured and calculated in accordance with the theory discussed in the previous chapter of this thesis. The analysis was completed using the data between surface and 14 level as these data showed the least amount of scatter. A summary of these results is given in Table 4-5 and Table 4-6.

Table 4-5: No. 11 shaft test results – Data

Item	Value	Symbol	Units	Description
1	0.079	f_{BTotal}	-	Total bunton Chezy-Darcy friction factor
2	0.023	f_{Shaft}	-	Shaft asperities Chezy-Darcy friction factor
3	0.105	$f_{Total Shaft}$	-	Total shaft Chezy-Darcy friction factor
4	1.023	$X_{Skip 1 Corr}$	-	Skip shock loss correction factor
5	0.881	$X_{Cage 1 Corr}$	-	Man cage shock loss correction factor

Table 4-6: No. 11 shaft test results

	P_{loss} (measured) (surface to 14 level)	P_{loss} (calculated) (surface to 14 level)	Units	Description
1	721.3	585.7	Pa	No conveyances moving
2	1.16	0.95	Pa/m	No conveyances moving
3	756.3	584.3	Pa	Rock winder in operation
4	1.22	0.94	Pa/m	Rock winder in operation
5	796.3	587.7	Pa	Man winder in operation
6	1.29	0.95	Pa/m	Man winder in operation

Note: The measured pressure measurements were taken at a time when the conveyances were not moving. The calculated pressure loss has, therefore, been completed assuming no conveyances are moving in the shaft.

4.1.3 Tests on No. 1 shaft

4.1.3.1 Shaft details and installation of equipment

The tests for No. 1 shaft of Impala Platinum were conducted from 12 to 16 March 2011. The required instrumentation was installed in the following positions in the shaft:

- 1 Surface (environmental logger was installed in the winder house immediately adjacent to the shaft)
- 2 7 level – Environmental logger (503m BC)
- 3 8 level – Environmental logger (549m BC)
- 4 9 level – Environmental logger (595m BC)
- 5 10 level – Environmental logger (641m BC)
- 6 Rock winder (4.9 m diam.) – Rotary encoder – PLC2 (log channels 1 and 2) (double drum winder) (measured conveyance speed – 14.5 m/s)
- 7 Man winder (4.35 m diam.) – Rotary encoder – PLC2 (log channels 3 and 4) (double drum winder) (measured conveyance speed – 12.2 m/s)

8 Service winder (3.5 m diam.) – Rotary encoder – PLC2 (log channels 3 and 4) (single drum winder) (measured conveyance speed – 10.0 m/s)

9 Free Air Velocity of ventilation air in shaft – measured as 7.7 m/s

It is not necessary to have the data collected over such an extended period but, as discussed above, shaft access was only available during the weekly shaft inspections.

This is a 7.7 m diameter shaft which has been equipped with the angled buntons. The condition of the shaft was found to be generally good with little or no interference in the shaft as a result of additional fittings. This shaft was also concrete-lined.

The ventilation air is introduced into the shaft via a sub-bank air duct. It was not possible to place the environmental data loggers directly in the shaft. These were therefore placed immediately adjacent to the shaft on the levels indicated above.

The dimensions of the various cages, skips and fittings in the shaft can be found on a detailed shaft cross-section in Appendix F.

It should be noted that it was not possible to place a rotary encoder on each drum of the double drum winders. This was because no external shaft was available on the motor side of the winder. However, the standard policy on Impala limits clutching of a winder (i.e. the moving of one drum and its associated conveyance) to the shift-change period only. These times are easily discernible from the data and have not been used in this analysis. A schematic of the shaft cross-section is provided in Figure 4-3.

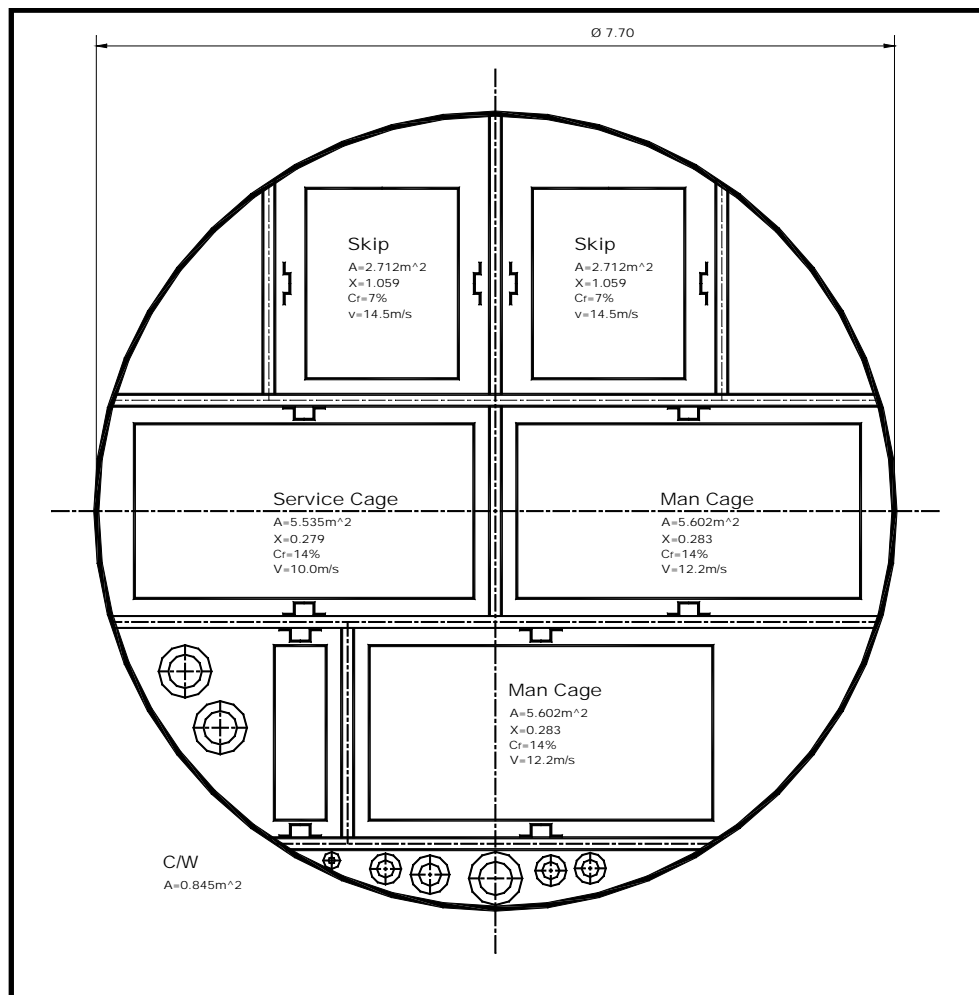


Figure 4-3: Cross-section of No. 1 shaft

4.1.3.2 Environmental loggers

All the environmental loggers were time-stamped from a common computer before they were installed. These data was then sorted to display the results from each of the days on which testing took place.

It should be noted that there were times in the shaft when the pressure readings varied significantly. These times are consistent with the times that the ventilation fans were not operating at full flow. These periods were also avoided in the evaluations given below.

4.1.3.3 Rotary encoder

The PLCs associated with these encoders were time-corrected to the same computer used for the environmental loggers. The results of these encoders were corrected to show the conveyances in appropriate positions in the shaft. This was done primarily by using the drum diameter and matching the conveyance position on each of the levels to the movement of the drum.

When the instrumentation was put in place, the service winder had been tripped. The winder only showed movement on 13 March 2011. All the data collation therefore started at this point. In addition, there was a power interruption to the PLC attached to the man and rock winder on 14 March 2011 at approximately 11:00. This left a small but sufficient window in which to evaluate the necessary data from 00:00 on 13 March to 11:00 on 14 March 2011.

The PLCs measured that position of the conveyance every second, whereas the environmental loggers measured every 10 seconds. The winder data were therefore also corrected to start and stop at equivalent times to the environment loggers.

The PLCs attached to these encoders were placed in the drivers' cabins where appropriate. These were not tampered with for the duration of the experiment.

4.1.3.4 Summary of data from tests on No. 1 shaft

The friction losses in the shaft were measured and calculated in accordance with the theory discussed in the previous chapter of this thesis. The analysis was completed using the data between surface and 14 level as these data showed the least amount of scatter. A summary of these results is given in Table 4-7 and Table 4-8.

Table 4-7: No. 1 shaft test results – Data

Item	Value	Symbol	Units	Description
1	0.102	f_{BTotal}	-	Total bunton Chezy-Darcy friction factor
2	0.021	f_{Shaft}	-	Shaft asperities Chezy-Darcy friction factor
3	0.123	$f_{Total Shaft}$	-	Total shaft Chezy-Darcy friction factor
4	1.059	$X_{Skip 1 Corr}$	-	Skip shock loss correction factor
5	0.281	$X_{Cage 1 Corr}$	-	Man cage shock loss correction factor
6	0.278	$X_{Service Cage Corr}$	-	Service cage shock loss correction factor

Table 4-8: No. 1 shaft test results

	P_{loss} (measured) (surface to 14 level)	P_{loss} (calculated) (surface to 14 level)	Units	Description
1	248.2	275.1	Pa	No conveyances moving
2	0.49	0.55	Pa/m	No conveyances moving
3	216.8	279.2	Pa	Service winder in operation
4	0.43	0.55	Pa/m	Service winder in operation
5	231.4	274.1	Pa	Rock winder in operation
6	0.46	0.54	Pa/m	Rock winder in operation
7	242.0	274.7	Pa	Man winder in operation
8	0.48	0.54	Pa/m	Man winder in operation

Note: The measured pressure measurements were taken at a time when the conveyances were not moving. The calculated pressure loss has, therefore, been completed assuming no conveyances are moving in the shaft.

4.1.4 Tests on No. 11C shaft

4.1.4.1 Shaft details and installation of equipment

The tests for No. 11C shaft of Impala Platinum were conducted from 9 April 2011 to the 12 April 2011. The requisite instrumentation was installed in the following positions in the shaft:

- 1 Surface (environmental logger was installed in the winder house immediately adjacent to the shaft).
- 2 24 level – Environmental logger (1 160 m BC)
- 3 25 level – Environmental logger (1 215 m BC)
- 4 26 level – Environmental logger (1 257 m BC)
- 5 27 level – Environmental logger (1 308 m BC)
- 6 28 level – Environmental logger (1 382 m BC)
- 7 Man winder (4.9 m diam.) – Rotary encoder – PLC1 (log channels 1 and 2) (double drum winder) (measured conveyance speed – 12.2 m/s)
- 8 Free Air Velocity of ventilation air in shaft – measured at 9.0 m/s

It is not necessary to have the data collected over such an extended period but, as discussed above, shaft access was only available during the weekly shaft inspections.

This is a 5.6 m diameter shaft which has been equipped with the airflow buntons. The condition of the shaft was found to be generally good with little or no interference in the shaft as a result of additional fittings. It should be noted that below 24 level the ventilation is split. This is reflected by the inconsistency of the readings below this level. Therefore the readings used in this evaluation will be those above this level. This shaft was also concrete-lined.

The ventilation air is introduced into the shaft via a sub-bank air duct. It was not possible to place the environmental data loggers directly in the shaft. They were therefore placed immediately adjacent to the shaft on the levels indicated above.

The dimensions of the various cages, skips and fittings in the shaft can be found on a detailed shaft cross-section in Appendix G.

It should be noted that it was not possible to place a rotary encoder on each drum of the double drum winders. This was because no external shaft was available on the motor side of the winder. This shaft, however, uses only a cage and counterweight and therefore the clutching concerns were not a problem. This shaft does not have a loading station as yet as it is still in the development phase. All the rock is hoisted from the shaft in rail hoppers. A schematic of the shaft cross-section is provided in Figure 4-4.

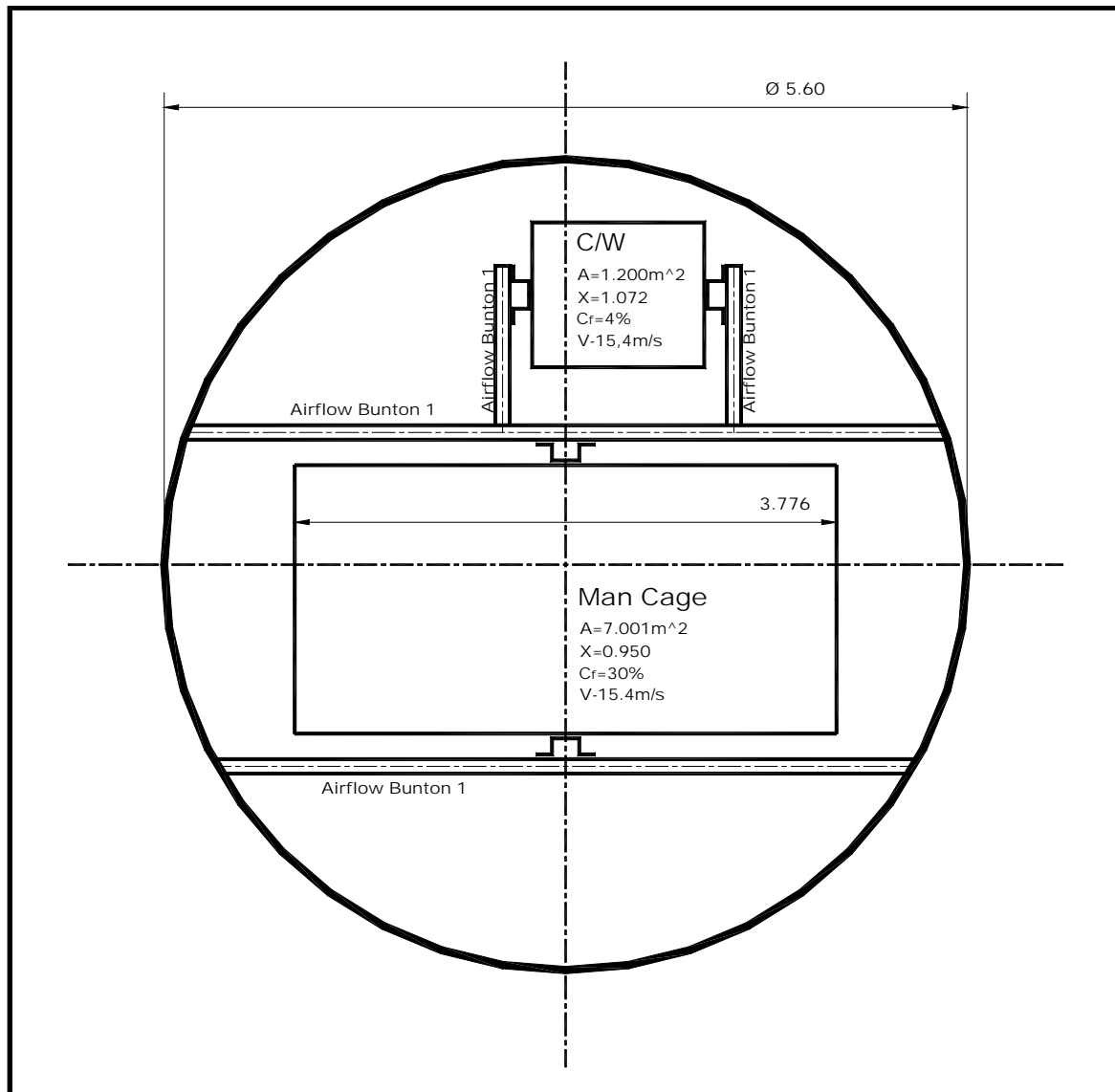


Figure 4-4: Cross-section of No. 11C shaft

4.1.4.2 Environmental loggers

All the environmental loggers were time-stamped from a common computer before they were installed. These data were then sorted to display the results from each of the days on which testing was done.

It should be noted that there were times in the shaft when the pressure readings varied significantly. These times are consistent with the times that the ventilation fans were not operating at full flow. These periods were also avoided in the evaluations given below.

4.1.4.3 Rotary encoder

The PLCs associated with these encoders were time-corrected to the same computer used for the

environmental loggers. The results from these encoders were corrected to show the conveyances in appropriate positions in the shaft. This was done primarily by using the drum diameter and matching the conveyance position on each of the levels to the movement of the drum.

The PLCs measured that position of the conveyance every second, whereas the environmental loggers measured every 10 seconds. The winder data were therefore also corrected to start and stop at equivalent times to the environment loggers.

The PLCs attached to these encoders were placed in the drivers' cabins where appropriate. These were not tampered with for the duration of the experiment.

4.1.4.4 Summary of data from tests on No. 11c shaft

The friction losses in the shaft were measured and calculated in accordance with the theory discussed in the previous chapter of this thesis. The analysis was completed using the data between surface and 14 level as these data showed the least amount of scatter. A summary of these results is given in Table 4-9 and Table 4-10.

Table 4-9: No. 11C shaft test results – Data

Item	Value	Symbol	Units	Description
1	0.047	f_{BTotal}	-	Total bunton Chezy-Darcy friction factor
2	0.023	f_{Shaft}	-	Shaft asperities Chezy-Darcy friction factor
3	0.070	$f_{Total Shaft}$	-	Total shaft Chezy-Darcy friction factor
5	0.941	$X_{Cage 1 Corr}$	-	Cage shock loss correction factor

Table 4-10: No. 11C shaft test results

	P_{loss} (measured) (surface to 14 level)	P_{loss} (calculated) (surface to 14 level)	Units	Description
1	752.4	678.4	Pa	No conveyances moving
2	0.65	0.58	Pa/m	No conveyances moving
3	856.1	682.9	Pa	Man winder in operation
4	0.74	0.59	Pa/m	Man winder in operation

Note: The measured pressure measurements were taken at a time when the conveyances were not moving. The calculated pressure loss has, therefore, been completed assuming no conveyances are moving in the shaft.

4.1.5 Tests on No. 12N shaft

4.1.5.1 Shaft details and installation of equipment

The tests for No. 12N shaft of Impala Platinum were conducted from 17 to 21 June 2011. The required instrumentation was installed in the following positions in the shaft:

- 1 Surface (environmental logger was installed in the winder house immediately adjacent to the shaft)
- 2 Loading station – Environmental logger (880 m BC) (In this test two data loggers were placed on this level. This redundancy proved fortunate as one of these failed during the test period.)
- 3 Rock winder (4.9 m diam.) – Rotary encoder – PLC2 (log channels 3 and 4) (double drum winder) (measured conveyance speed – 16.2 m/s)
- 4 Free Air Velocity of ventilation air in shaft – measured at 11.0 m/s

It is not necessary to have the data collected over such an extended period but, as discussed above, shaft access was only available during the weekly shaft inspections.

This is a 8.5m diameter shaft which has been equipped with rope guides sufficient for two skips. This shaft also has a brattice wall installed, which results in an irregularly shaped shaft necessitating the

use of the hydraulic diameter in the resolution of the theoretical calculation.

The condition of the shaft was found to be generally good with little or no interference in the shaft as a result of additional fittings. This shaft was also concrete-lined.

The ventilation air is introduced into the shaft via a sub-bank air duct. It was not possible to place the environmental data loggers directly in the shaft. These were therefore placed immediately adjacent to the shaft on the levels indicated above.

The dimensions of the various cages, skips and fittings in the shaft can be found on a detailed shaft cross-section in Appendix H.

It should be noted that it was not possible to place a rotary encoder on each drum of the double drum winders. This is because no external shaft was available on the motor side of the winder. This shaft, however, only sent skips to one level and therefore the clutching concern for determining the placement of the conveyances in the shaft is not valid. A schematic of the shaft cross-section is provided in Figure 4-5.

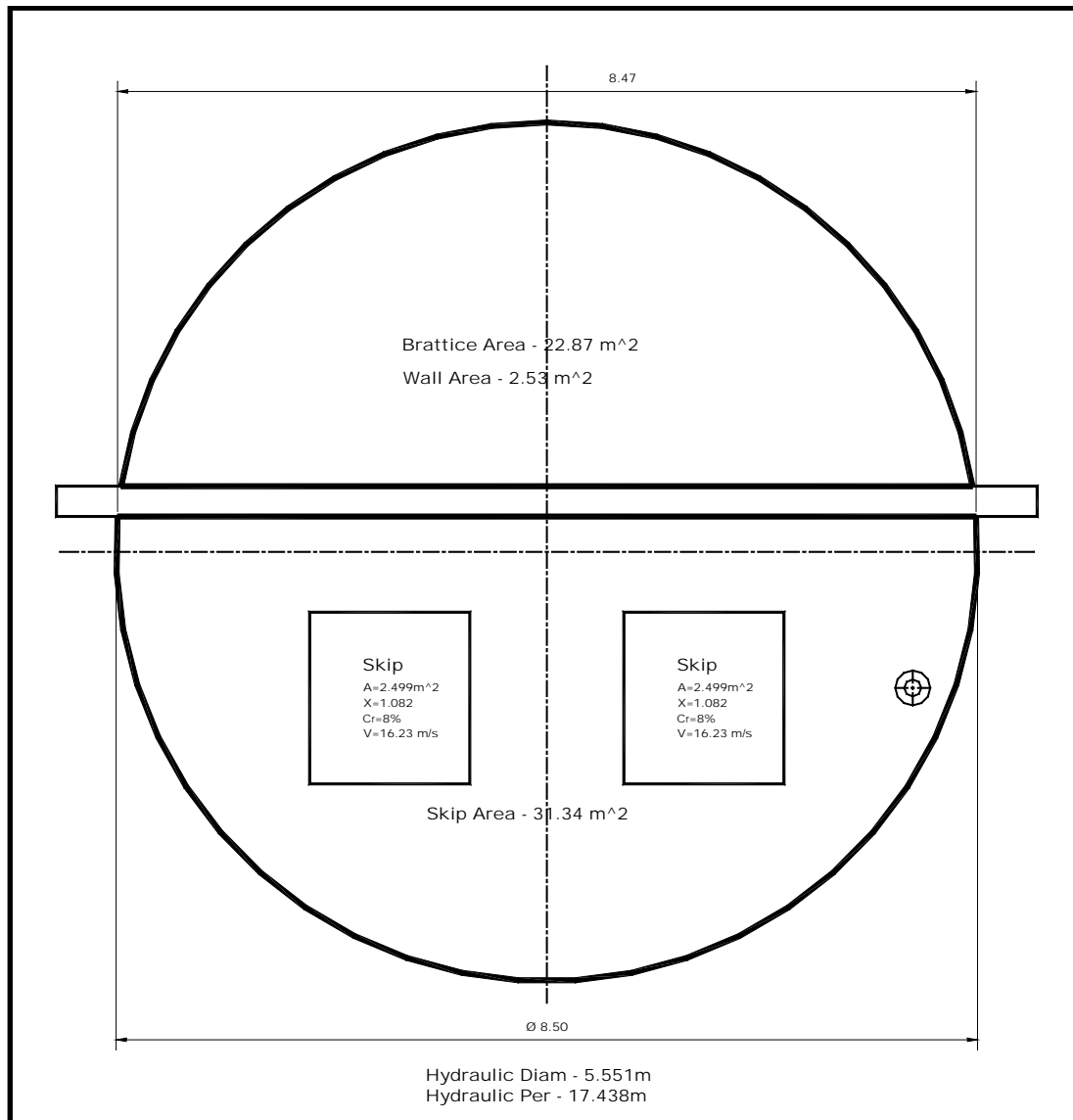


Figure 4-5: Cross-section of No. 12N shaft

4.1.5.2 Environmental loggers

All the environmental loggers were time-stamped from a common computer before they were installed. These data were then sorted to display the results from each of the days on which testing took place.

It should be noted that there were times in the shaft when the pressure readings varied significantly. These times are consistent with the times that the ventilation fans were not operating at full flow. These periods were also avoided in the evaluations given below.

4.1.5.3 Rotary encoder

The PLCs associated with these encoders were time-corrected to the same computer used for the environmental loggers. The results from these encoders were corrected to show the conveyances in appropriate positions in the shaft. This was done primarily by using the drum diameter and matching the conveyance position on each of the levels to the movement of the drum.

The PLCs measured the position of the conveyance every second, whereas the environmental loggers measured every 10 seconds. The winder data were therefore also corrected to start and stop at equivalent times to the environment loggers.

The PLCs attached to these encoders were placed in the drivers' cabins where appropriate. These were not tampered with for the duration of the experiment.

4.1.5.4 Summary of data from tests on No. 12N shaft

The friction losses in the shaft were measured and calculated in accordance with the theory discussed in the previous chapter of this thesis. The analysis was completed using the data between surface and 14 level as these data showed the least amount of scatter. A summary of these results is given in Table 4-11 and Table 4-12.

Table 4-11: No. 12N shaft test results – Data

Item	Value	Symbol	Units	Description
1	0.000	f_{BTotal}	-	Total buntun Chezy-Darcy friction factor
2	0.028	f_{Shaft}	-	Shaft asperities Chezy-Darcy friction factor
3	0.028	$f_{Total Shaft}$	-	Total shaft Chezy-Darcy friction factor
5	1.082	$X_{Cage 1 Corr}$	-	Cage shock loss correction factor

Table 4-12: No. 12N shaft test results

	P_{loss} (measured) (surface to 14 level)	P_{loss} (calculated) (surface to 14 level)	Units	Description
1	917.6	311.2	Pa	No conveyances moving
2	1.04	0.35	Pa/m	No conveyances moving
3	866.0	297.8	Pa	No conveyances moving
4	0.98	0.34	Pa/m	No conveyances moving

Note: The measured pressure measurements were taken at a time when the conveyances were not moving. The calculated pressure loss has, therefore, been completed assuming no conveyances are moving in the shaft.

4.2 SUMMARY OF AND CONCLUSIONS FROM THE SHAFT TEST RESULTS

4.2.1 Accuracy of the Results

The shaft tests discussed here were all conducted on shafts at Impala Platinum. In total five different shafts were tested for time periods varying from 4 to 8 days. The objective of the tests was to obtain sufficient measurements to allow the calculation of the pressure drops in an operating shaft. For this purpose environmental data loggers were placed immediately adjacent to a shaft at various points along the shaft length. In some instances it was not possible to place instrumentation on all the shaft levels. When this occurred discussions were held with the shaft ventilation officer to determine the ideal positions for this instrumentation. These positions were generally at the highest level in the shaft and at the stations where most of the ventilation air left the shaft. The data obtained from these instruments allowed the calculation of the pressure drop over the shaft using the barometric calculation.

In addition, rotary encoders were placed on each of the winders used for the conveyances in the shaft. This allowed the evaluation of the shaft pressure drops in conjunction with the movement of the conveyances within the shaft.

The placement of the various pieces of instrumentation for these tests does give rise to some experimental errors which must be considered when evaluating the test results. These are primarily

the entrance losses for the ventilation air, as well as losses resulting from the indirect manner in which the pressures in the shaft were measured.

The pressure on surface was measured and used to evaluate the total pressure loss in the shaft. This did not take into consideration the pressure losses that would occur as a result of the transfer flow of air down the ventilation duct and into the shaft as well as on to the station. Generally, these losses are around 100 Pa, depending on the drift configuration.

In addition, there are other factors that cannot be effectively quantified as a result of the placement of the underground pressure sensors. These sensors were placed immediately adjacent to the shaft at various stations, as appropriate for the shaft under consideration. Therefore both *vena contracta* effects and the effects of the station steelwork should be considered.

Finally, the accuracies intrinsic to the instrumentation used as well as the calculation methodology must be considered. These were noted in section 3.5.4 above. These accuracies are repeated here for convenience:

- 1 Potential differences across the range as a result of the instrumentation (+12% to -29%)
- 2 Potential differences inherent in the calculation of the pressure losses resulting from the shaft wall (+15% to -15%)
- 3 At this stage the potential inaccuracies for the calculation of the flow of the ventilation across and buntons and pipes is not known.

4.2.2 Summary of the Various Shaft Tests

4.2.2.1 Summary of results from the No. 14 shaft tests

There is a significant difference between the measured data and the calculated data (between 38 and 49%) for the data points considered. This difference is between 246 and 312 Pa. The reasons for these differences are discussed in Section 4.2.

There was very little change in the measured pressure as a result of the service cage moving by itself in the shaft. This is attributed directly to the small coefficient of fill that the service cage has on the shaft $C_f = 13\%$. This is in spite of the fact that the theory showed that an increase in pressure loss of 58 Pa should be apparent when the cage was moving upwards in the shaft.

One of the more surprising findings is the increase in pressure loss of approximately 50 Pa as a result of the skip when it is moving consistently between surface and the shaft bottom. The available theory does offer a prediction of the shaft losses as a result of the movement of conveyances through the shaft, but states that, in the case of paired conveyances (i.e. conveyances of similar

dimensions moving in opposite directions), the overall effect of the pressure from the conveyance moving will be cancelled out. This finding is therefore not consistent with the theory. However, if one evaluates this pressure rise as an obstruction in the shaft, the predicted increase for one skip blocking the airflow is 54 Pa, which is similar to the pressure increase noted above.

There is little difference between the pressure loss calculated for the shaft between the time when the man cage is moving and the pressure loss when it is not moving. This is consistent with the theory as the cages move in pairs.

This shaft is well laid out and the overall coefficients of fill of each of the individual conveyances is well within the recommended maximum of 30% (Figure 4-1).

4.2.2.2 Summary of results from the No. 11 shaft tests

There is a significant difference between the measured data and the calculated data (between 23 and 35% for the data points considered). This difference is between 135 and 208 Pa. The reasons for these differences are discussed in Section 4.2.

There is no evidence of pressure spikes when the skip and cages are moving and when they are not. This is consistent with the theory as the conveyances move in pairs.

A perusal of the measured data against time did, however, show some pressure spikes of approximately 150 Pa indirectly associated with the movement of the man cage. In some instances this spike lagged the movement of the cage by 2 to 3 minutes. This was especially noticeable when this cage was moving alone in the shaft. This pressure surge could be construed to result from the cage movement but was always short in duration when it did occur (total pressure swing of less than 30 seconds). Given the large C_f of the cage of 29%, this is to be expected and it is close to the value of 164 Pa predicted by the theory.

There was no general increase in the overall pressure loss measured in the shaft when the skip was in constant operation as was noted in the 14 shaft tests. This was in spite of the fact that the C_f of the skips in both shafts was identical (7%).

4.2.2.3 Summary of results from the No. 1 shaft tests

There is not a significant difference between the measured data and the calculated data (between 9 and 22% for the data points considered). This difference is between 26 and 62 Pa. The reasons for these differences are discussed in Section 4.2.

There is no evidence of pressure spikes when the skip and cages are moving and when they are not. This is consistent with the theory as the conveyances move in pairs.

In addition, there is no evidence of the anticipated pressure spikes when the service cage is moving

and when it is not. The theory predicted a pressure rise of 24 Pa in this instance.

This small difference can be attributed to the small C_f that the cages and skips have in comparison with the shaft. These skips had $C_f = 7\%$ as in the other shafts, while the man cage and service cage had $C_f = 14\%$. Both of these coefficients are significantly smaller than the recommended maximum of 30%.

4.2.2.4 Summary of results from No. 11C shaft

There is not a significant difference between the measured data and the calculated data (between 10 and 25% for the data points considered). This difference is between 74 and 173 Pa. The reasons for these differences are discussed in Section 4.2.

There is evidence of the anticipated pressure spikes from when the cage is moving and when it is not. This pressure spike of 100 Pa did, however, lag the movement of the cage by 1 to 2 minutes and was always short in duration (total pressure swing of less than 30 seconds). The cage has a $C_f = 30\%$. The measured pressure rise of 100 Pa and the theory predicted a pressure rise of 167 Pa.

4.2.2.5 Summary of results from No. 12N shaft

There is a significant difference between the measured data and the calculated data (between 190 and 194% for the data points considered). This difference is between 568 and 606 Pa. The reasons for these differences are discussed in Section 4.2.

There is evidence of the anticipated pressure spike when the skips are moving. This pressure spike of 100 Pa did lag the movement of the skips by 1–1.5 minutes and was always short in duration (total pressure swing of less than 30 seconds). The skips move in pairs and this pressure spike is therefore not consistent with the theory.

However, if one evaluates this pressure rise as an obstruction in the shaft, the predicted increase for one skip blocking the airflow is 74 Pa, which is close to the pressure increase noted above.

4.2.3 Summary and Conclusions from the Shaft Test Results

4.2.3.1 Accuracy of the data

The results of the tests completed on all the shafts are listed in Table 4-13. As can be seen from this table, the results show varying agreement with the values calculated from the current theory. The specific circumstances surrounding the measurements were discussed in section 4.2.1.

The most significant difference is noted for the results of the tests for No. 12N shaft. These showed very little agreement with the theory. This difference is attributed primarily to the fact that it was

necessary to place the pressure-measuring instrument in the steelwork associated with the shaft bottom. It is assumed that the additional losses resulting from this steelwork resulted in the significant pressure difference in these readings. Unfortunately, this also means that the results of this test are of little use in the context of this work.

Table 4-13: Summary of shaft test results

Item	P_{Loss} (measured)	P_{Loss} (calculated)	% Diff.	Difference		Chezy-Darcy friction factors		$f_{B Total} /$ $f_{Total Shaft}$
No. 14 shaft								
1	909.9	637.0	43%	272.9	Pa	$f_{B Total}$	0.076	78%
2	1.81	1.26	43%	0.54	Pa/m	$f_{Total Shaft}$	0.098	
No. 11 shaft								
3	757.9	585.9	29%	172.0	Pa	$f_{B Total}$	0.079	78%
4	1.22	0.95	29%	0.28	Pa/m	$f_{Total Shaft}$	0.102	
No. 1 shaft								
5	234.6	275.8	15%	-41.2	Pa	$f_{B Total}$	0.102	83%
6	0.47	0.55	15%	-0.08	Pa/m	$f_{Total Shaft}$	0.123	
No. 11C shaft								
7	804.3	680.6	18%	123.6	Pa	$f_{B Total}$	0.047	67%
8	0.69	0.59	18%	0.11	Pa/m	$f_{Total Shaft}$	0.070	
No. 12N shaft								
9	891.8	304.5	193%	587.3	Pa	$f_{B Total}$	0.000	0%
10	1.01	0.35	193%	0.67	Pa/m	$f_{Total Shaft}$	0.028	

The four remaining shafts show accuracies varying from an average of 42% in the case of No. 14

shaft to 15% in the case of No. 1 shaft. To try and understand the reasons for these differences, the shaft configurations need to be considered.

The two shafts that show the least agreement are No. 14 shaft and No. 11 shaft. These two shafts both use the airflow buntons, each of which contributed 78% of the calculated Chezy-Darcy friction factors for these shafts. These shafts are of similar configuration to No. 1 shaft, which showed agreement between the measured results and the calculated results of 15%. The shaft asperities in the calculation were all equal at 10 mm and the ventilation flow rates for the shafts did not vary significantly (7.7 m/s for No. 1 shaft, 10 m/s for No. 11 shaft and 9.4 m/s for No. 14 shaft). In addition the ventilation air was introduced to these shaft sub bank via well designed evase's. This leaves two variables that could account for the differences, namely the drag coefficient used for the evaluation of the buntons resistance to the ventilation flow and the number and placement of pipes in the shafts.

The values used for the drag coefficient for the evaluation were taken from the tables supplied by McPherson (1987). In this instance, the shape closest to the airflow buntun was that of a dumbbell. This drag coefficient was calculated from the data presented by Martinson (1957), whose paper was reviewed in Section 2.2.2. The same table was used to obtain the drag coefficient used for the triangular buntun used in No. 1 shaft. This coefficient was obtained from measured data.

This drag coefficient does highlight the potential pitfalls in calculations of this nature. The buntun Chezy-Darcy friction factors supply a large portion of the resistance within the shaft and thus the effect of assumptions in the quantification of these data can be significant.

The additional resistance that a shaft offers to ventilation air flowing through it as a result of the pipes in the shaft is difficult to quantify. The theory indicates that this should be accommodated by reducing the free area of the shaft by the area of the pipe and adjusting the rubbing surface of the shaft in the calculation accordingly. This approach results in a Chezy-Darcy friction factor for the pipes of less than 1% of the overall Chezy-Darcy friction factor. This is not sufficient to account for the differences noted above. However, the contribution of the piping to the overall Chezy-Darcy friction factor was more fully investigated during the CFD evaluation.

4.2.4 Conveyances Moving in the Shaft

The results of these data do not allow a meaningful conclusion to be drawn. The data from No. 14 shaft did not show significant differences in the measured pressure losses as a result of the cage movement. However, a small increase in the overall pressure was noted, consistent with the blockage that one of the skips would apply to the shaft if it remained stationary. This only occurred once the skip was being used to its full capacity and was moving up and down the shaft consistently.

This small increase was attributed to the length of time that the skip spent in the shaft. It was not noted in any of the other tests.

In the tests associated with No. 11 and No. 11C shaft, delayed pressure spikes were apparent when the cages moved up and down the shaft. These spikes were consistent with the predicted theory. In both of these instances, the cages occupied respectively 29% and 30% of the total shaft area available.

Interestingly, the measurement at No. 12N shaft exhibited similar results in spite of the skips in this shaft occupying no more than 8% of the total shaft area. However, the skips occupy the central portion of the shaft in which the ventilation air would be flowing the most freely, i.e. without the effects of the irregular shaft shape.

In all instances, the pressure spikes lagged the passing of the cage by 1–3 minutes. This pressure spike did, however, dissipate before the cages passed the same point again. This was also in spite of the fact that the pressure changes caused by cages moving up and down the shaft in pairs should cancel each other out. This was attributed to the damping effect of a shaft filled with air.

The results of this analysis show that the effects of a cage moving in the shaft can be largely ignored. This conclusion is, however, valid only for shafts of similar cross-section to those considered here.

4.2.5 Conclusions from the Results and Evaluation of Shaft Tests

The following specific conclusions can be drawn from the results of the tests and the comparison of these results with the current theory:

- 1 The differences between the results from the various tests and the theory for shafts of similar configuration demonstrate the importance of ensuring that the appropriate factors for the drag of the buntons are considered. The test results that showed the least agreement with the theory all used drag coefficients derived from tests on previous shafts. The shaft that showed the most agreement between the measurement and the theoretical evaluation used a drag coefficient taken from measurements on a scale model. The buntons are calculated to contribute approximately 78% of the total friction resistance in the shaft, and any discrepancy in the coefficient of drag can, therefore, make a significant contribution to the overall calculated friction resistance.
- 2 The contribution that pipes and fittings make to the overall friction resistance is calculated by considering the overall decrease in the shaft area that the inclusion of these pipes and fittings result in. This does not take into account the placement of these pipes and fittings with respect to the airflow, or the inclusion of flanges which would contribute further to the interruption of the airflow.

- 3 The movement of the conveyances within the shaft does not seem to have a large effect on the pressure drops over the shaft. This is attributed to the shaft being well laid out and the cages and skips all being below the recommended C_f of 30%. When it was apparent that the passing of the conveyances had created a pressure spike, this was small, of short duration and lagged the passing of the conveyance by between 1 and 3 minutes. This was attributed to the large compressibility of the air in a typical shaft and the damping effect this would have on any pressure spike in the shaft.
- 4 When evaluating these results, the potential inaccuracies of the instrumentation must be borne in mind as these could also account for the noted discrepancies.

CHAPTER 5 RESULTS AND EVALUATION OF CFD ANALYSIS

5.1 RESULTS OF CFD ANALYSIS

It should be noted in the presentation of these results that the overall pressure differences are given for the shafts being considered. These pressure differences are calculated for the particular shaft length and are, therefore, difficult to compare with each other. Thus a value of pressure loss per m of shaft is also included to allow for this comparison.

5.1.1 CFD Simulation No. 1 (Shaft Barrel)

The shaft asperity for this simulation was modelled as being 10 mm. This value was based on observations in the shaft and was used for the evaluation of all the CFD models except the 12N shaft. A value of 20 mm was used for the 12N shaft. The results of the simulations for all the shafts under consideration are shown in Table 5-1.

Table 5-1: CFD simulation No. T01 – Shaft barrel pressure losses

	14 Shaft	11 Shaft	1 Shaft	11c Shaft	12N Shaft
Total calculated pressure loss over shaft length (Pa)	123.4	117.9	44.1	212.9	266.0
Calculated pressure loss (per m) (Pa/m)	0.14	0.19	0.09	0.18	0.30
Calculated shaft Chezy-Darcy friction factor (f)	0.021	0.022	0.021	0.023	0.028
Total calculated pressure loss over shaft length (CFD) (Pa)	65.8	56.8	23.0	103.6	89.5
Measured pressure loss (per m) (CFD) (Pa/m)	0.08	0.09	0.05	0.09	0.10
Resultant Chezy-Darcy friction factor from CFD data (f)	0.011	0.011	0.011	0.011	0.010
Reynolds number (Re)	3 923 672	3 290 971	3 245 682	2 977 968	3 770 693
% Difference	47%	52%	48%	51%	55%

This comparison shows that there are significant differences between the CFD results and the calculated results. This is in part attributed to the large relative roughness of the shaft as well as the high Reynolds number. In addition, the formula used for the calculation of the Chezy-Darcy friction factor does not take into account that there is an accuracy of plus or minus 15% on the values for the Moody chart (White, 1986). This cumulative inaccuracy should be taken into consideration.

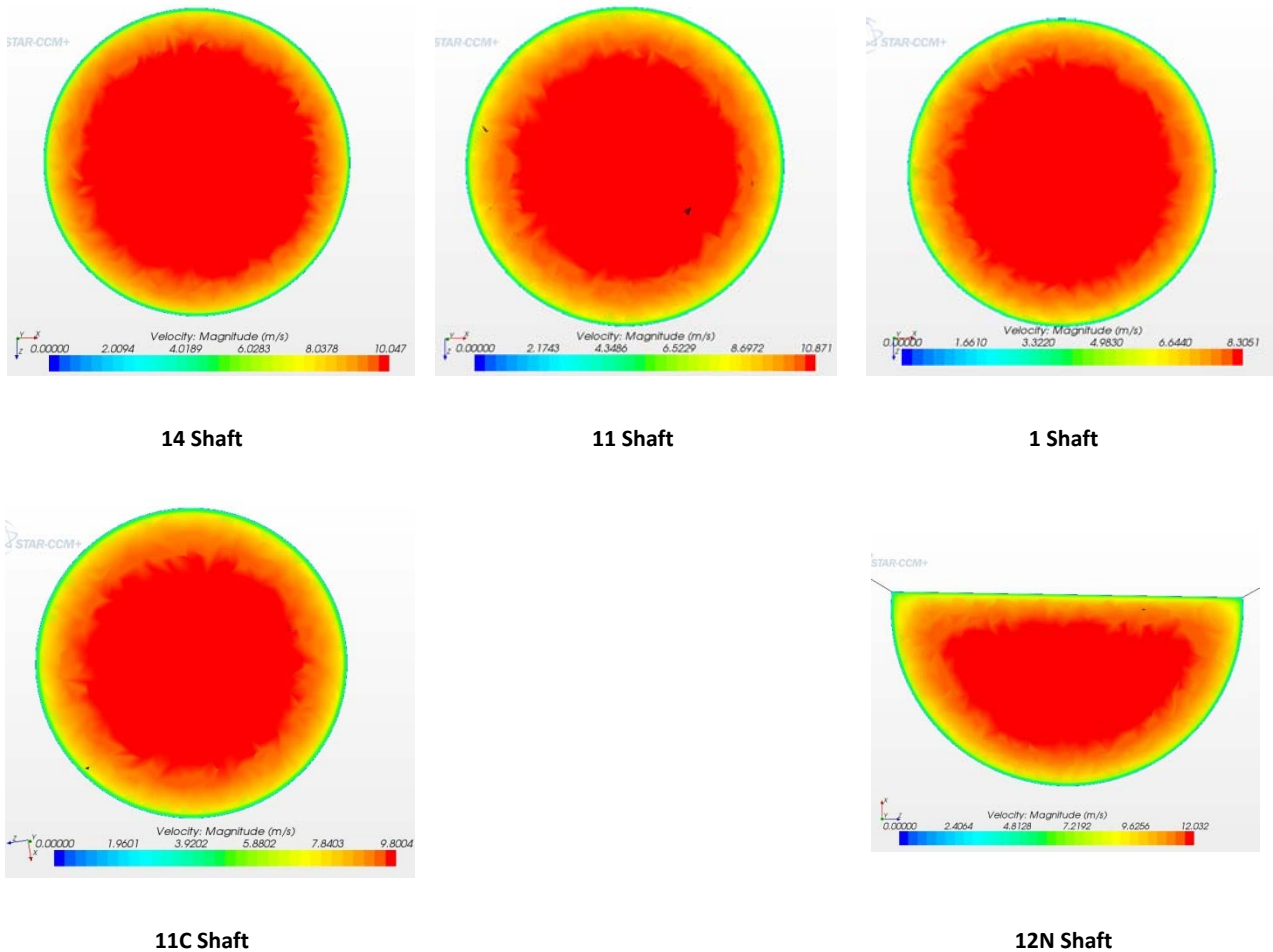


Figure 5-1: Velocity profiles for simulation T01 – Shaft barrel pressure losses

The shaft cross-sections showing the velocity profiles for the various shafts are shown in Figure 5-1. There is nothing untoward in these profiles, but they should be borne in mind as a basis of comparison when viewing subsequent cross-sections.

5.1.2 CFD Simulations Nos T02, T03 and T04

(T02 – Shaft barrel and 1 bunton across the shaft; T03 – Shaft barrel and 2 buntions across the shaft; T04 – Shaft barrel and full bunton set)

It is appropriate that these simulations be discussed together as they all seek to provide a better understanding of the behaviour of ventilation flow around the buntions in the shaft. The results of these simulations are given in Table 5-2.

Table 5-2: CFD simulations Nos T02, T03 and T04

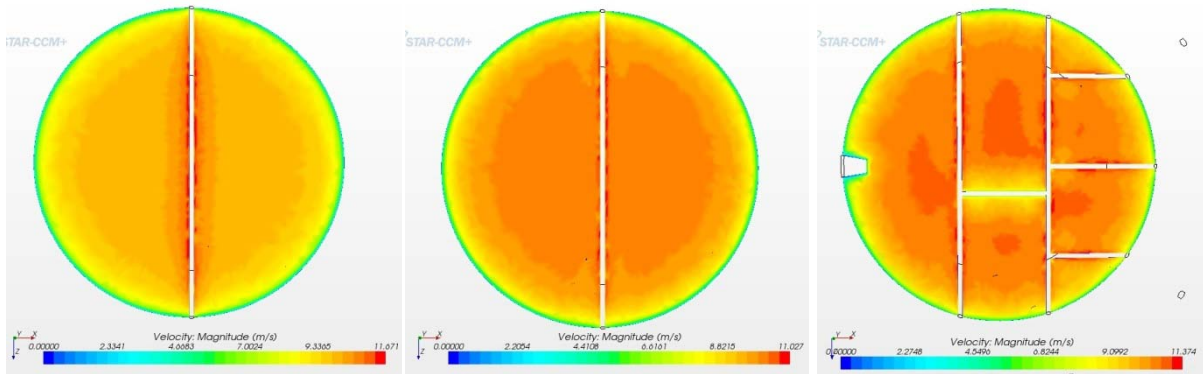
(T02 – Shaft barrel and 1 bunton across the shaft; T03 – Shaft barrel and 2 buntions across the shaft; T04 – Shaft barrel and full bunton set)

	14 Shaft	11 Shaft	1 Shaft	11C Shaft	12N Shaft
Simulation No. T02 – Shaft barrel and 1 bunton across the shaft					
Total calculated pressure loss over shaft length (Pa)	174.6	165.1	65.6	296.6	-
Calculated pressure loss (per m) (Pa/m)	0.20	0.27	0.13	0.26	-
Drag coefficient (assumed) (C_D)	1.30	1.30	1.55	1.30	-
Total calculated pressure loss over shaft length (CFD) (Pa)	93.4	97.9	37.4	177.6	-
Measured pressure loss (per m) (CFD) (Pa/m)	0.11	0.16	0.07	0.15	-
Drag coefficient (CFD) (C_D)	0.90	1.47	1.33	1.49	-
% Difference	47%	41%	43%	40%	-

	14 Shaft	11 Shaft	1 Shaft	11C Shaft	12N Shaft
Simulation No. T03 – Shaft barrel and 2 buntions across the shaft					
Total calculated pressure loss over shaft length (Pa)	246.8	386.8	175.9	479.6	-
Calculated pressure loss (per m) (Pa/m)	0.28	0.62	0.35	0.42	-
Drag coefficient (assumed) (C_D)	1.30	1.30	1.55	1.30	-
Total calculated pressure loss over shaft length (CFD) (Pa)	135.4	136.0	51.0	245.1	-
Measured pressure loss (per m) (CFD) (Pa/m)	0.16	0.22	0.10	0.21	-
Drag coefficient (CFD) (C_D)	0.74	0.49	0.33	0.70	-
% Difference	45%	65%	71%	49%	-
Simulation No. T04 – Shaft barrel and full bunton set					
Total calculated pressure loss over shaft length (Pa)	564.9	540.8	259.6	671.5	-
Calculated pressure loss (per m) (Pa/m)	0.65	0.87	0.52	0.58	-
Drag coefficient (assumed) (C_D)	1.39	1.37	1.55	1.30	-
Total calculated pressure loss over shaft length (CFD) (Pa)	382.3	337.0	139.3	425.3	-
Measured pressure loss (per m) (CFD) (Pa/m)	0.44	0.54	0.28	0.37	-
Drag coefficient (CFD) (C_D)	1.01	0.92	0.84	0.93	-
% Difference	32%	38%	46%	37%	-

The following should be noted when reviewing the data in Table 5–2.

- i The drag coefficients from the CFD results were calculated after the pressure losses from the shaft barrel calculated in simulation T01 had been subtracted. The remaining pressure loss was assumed to be directly attributable to the buntuns.
- ii All the data were corrected for the density differences that were obtained from the test results in the shaft.

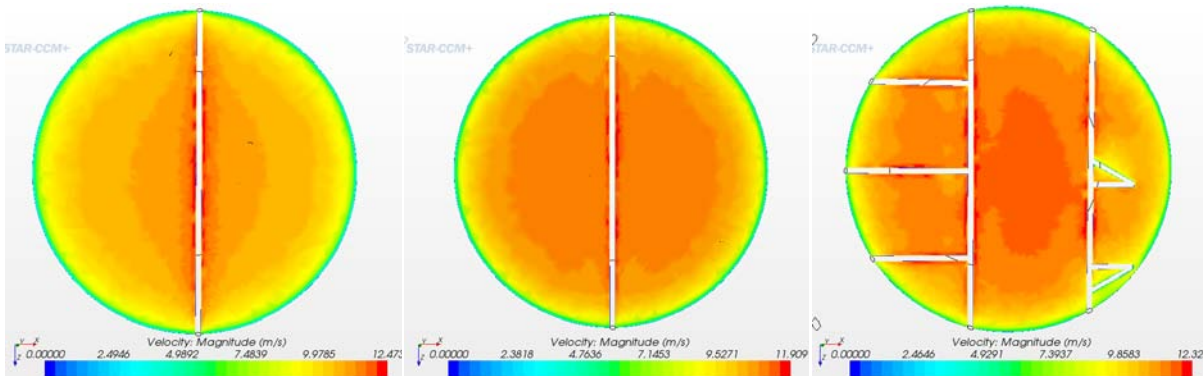


1 Buntun

2 Buntuns in Series

Complete Buntun Set

14 Shaft



1 Buntun

2 Buntuns in Series

Complete Buntun Set

11 Shaft

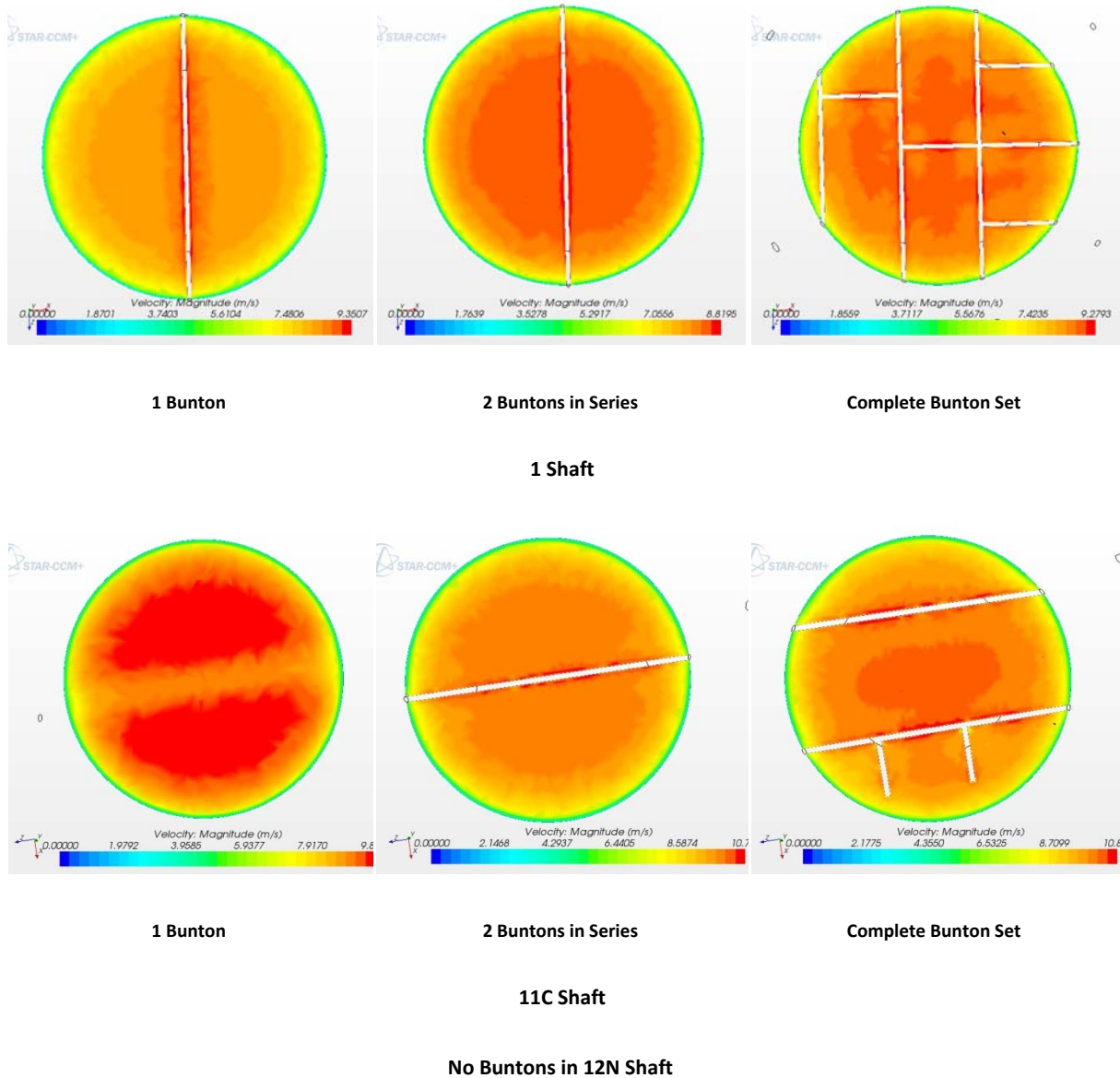


Figure 5-2: Velocity profiles for simulations T02, T03 and T04

(T02 – Shaft barrel and 1 bunton across the shaft; T03 – Shaft barrel and 2 buntons across the shaft; T04 – Shaft barrel and full bunton set)

The shaft cross-sections showing the velocity profiles for the various shafts are shown in Figure 5-2. What is interesting to note from these profiles is the comparative increase in the velocities as the additional buntons are added. This is most apparent when the increase in the velocity for the central portion of the shaft for simulation T04 is noted. It should be noted the areas of maximum velocity are also the areas where conveyances will travel.

5.1.3 CFD Simulation Nos T05, T06 and T07

(T05 – Shaft barrel and pipes at pipe diameter; T06 – Shaft barrel and pipes at flange diameter; T07 – Shaft barrel and pipes including flanges)

It is appropriate that these simulations be discussed together as they all seek to provide a better understanding of the behaviour of ventilation flow around the pipes in the shaft. The results of these simulations are given in Table 5-3.

Table 5-3: CFD simulations Nos 5, 6 and 7

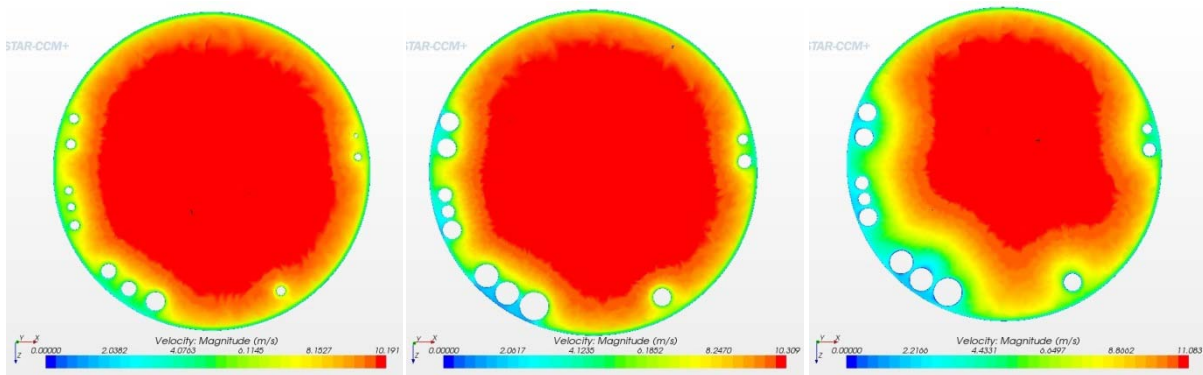
(T05 – Shaft barrel and pipes at pipe diameter; T06 – Shaft barrel and pipes at flange diameter; T07 – Shaft barrel and pipes including flanges)

	14 Shaft	11 Shaft	1 Shaft	11C Shaft	12N Shaft
Simulation No. T05 – Shaft barrel and pipes at pipe diameter					
Total calculated pressure loss over shaft length (Pa)	125.4	173.5	44.7	-	265.7
Calculated pressure loss (per m) (Pa/m)	0.14	0.28	0.09	-	0.30
Calculated pressure loss over shaft length due to piping (Pa)	0.4	54.0	0.1	-	0.0
Total calculated pressure loss over shaft length (CFD) (Pa)	62.0	61.5	23.2	-	89.0
Measured pressure loss (per m) (CFD) (Pa/m)	0.07	0.10	0.05	-	0.10
Pressure loss over shaft length due to piping (CFD) (Pa)	-3.8	4.8	0.3	-	-0.5
% Difference	51%	65%	48%	-	67%

	14 Shaft	11 Shaft	1 Shaft	11C Shaft	12N Shaft
Simulation No. T06 – Shaft barrel and pipes at flange diameter					
Total calculated pressure loss over shaft length (Pa)	130.0	181.0	45.9	-	266.0
Calculated pressure loss (per m) (Pa/m)	0.15	0.29	0.09	-	0.30
Calculated pressure loss over shaft length due to piping (Pa)	1.4	58.1	0.4	-	0.0
Total calculated pressure loss over shaft length (CFD) (Pa)	63.9	64.8	23.2	-	93.9
Measured pressure loss (per m) (CFD) (Pa/m)	0.07	0.10	0.05	-	0.11
Pressure loss over shaft length due to piping (CFD) (Pa)	-1.9	8.1	0.3	-	4.4
% Difference	51%	64%	49%	-	67%
Simulation No. T07 – Shaft barrel and pipes including flanges					
Total calculated pressure loss over shaft length (Pa)	123.0	181.0	45.9	-	266.0
Calculated pressure loss (per m) (Pa/m)	0.15	0.29	0.09	-	0.30
Calculated pressure loss over shaft length due to piping (Pa)	1.4	58.1	0.4	-	0.0
Total calculated pressure loss over shaft length (CFD) (Pa)	95.8	79.9	28.3	-	107.7
Measured pressure loss (per m)	0.11	0.13	0.06	-	0.12

	14 Shaft	11 Shaft	1 Shaft	11C Shaft	12N Shaft
(CFD) (Pa/m)					
Pressure loss over shaft length due to piping (CFD) (Pa)	30.0	23.2	5.3	-	18.2
% Difference	26%	56%	38%	-	67%

A number of interesting differences from the current theory for the calculation of the pressure drops resulting from the pipes in a shaft are apparent in the above data. There are, once again, significant differences between the pressure drops calculated from the theory and those from the CFD calculations.

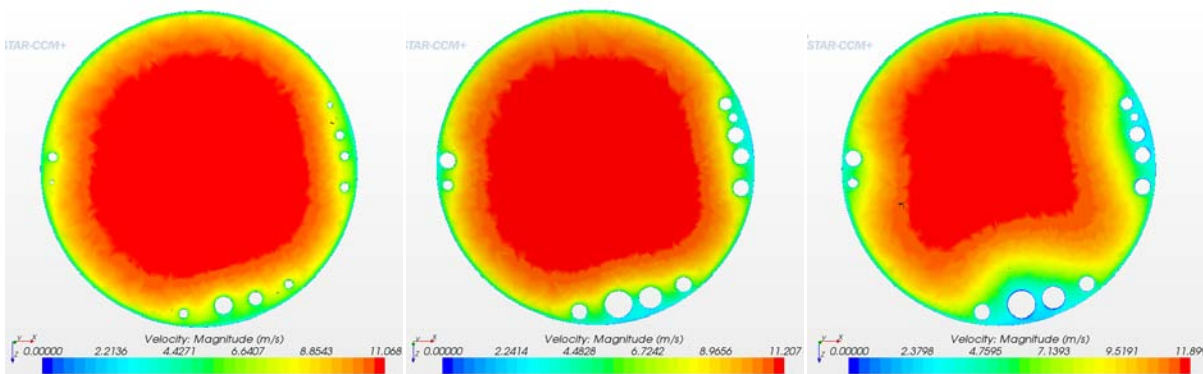


Pipes at Pipe Diameter

Pipes at Flange Diameter

Pipes including Flanges

14 Shaft

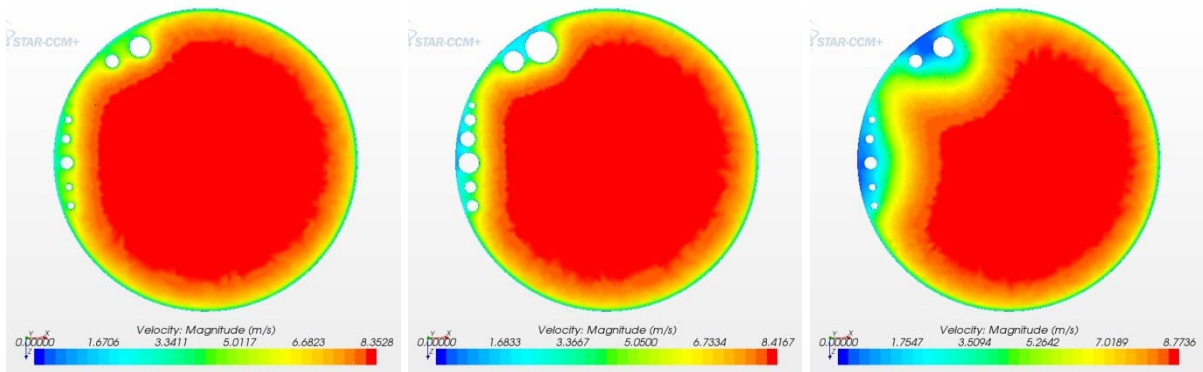


Pipes at Pipe Diameter

Pipes at Flange Diameter

Pipes including Flanges

11 Shaft



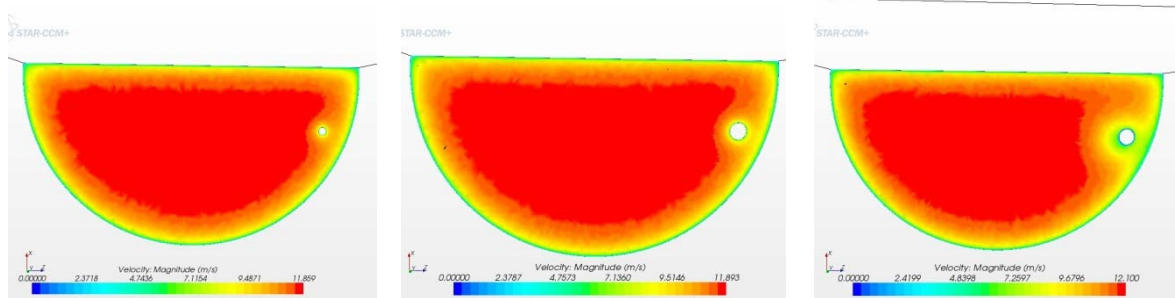
Pipes at Pipe Diameter

Pipes at Flange Diameter

Pipes including Flanges

1 Shaft

No Pipes in Section of 11C Shaft



Pipes at Pipe Diameter

Pipes at Flange Diameter

Pipes including Flanges

12N Shaft

Figure 5-3: Velocity profiles for simulations 5, 6 and 7

(T05 – Shaft barrel and pipes at pipe diameter; T06 – Shaft barrel and pipes at flange diameter; T07 – Shaft barrel and pipes including flanges)

The shaft cross-sections showing the velocity profiles for the various shafts are shown in Figure 5-3. It can be seen that the inclusion of the pipes (T05), even at flange diameter (T06), has significantly less effect on the flow of the ventilation air through the shaft than the inclusion of the pipes with the flanges (T07). This effect is not accounted for in the current theory.

5.1.4 CFD Simulations Nos T08, T09 and T10

(T08 – Shaft barrel and buntions and pipes at pipe diameter; T09 – Shaft barrel and buntions and pipes at flange diameter; T10 – Shaft barrel and buntions and pipes including flanges)

It is appropriate that these simulations be discussed together as they all seek to provide a better understanding of the behaviour of ventilation flow around the pipes in the shaft in conjunction with the buntions. The results of these simulations are given in Table 5-4.

Table 5-4: CFD simulations Nos 8, 9 and 10

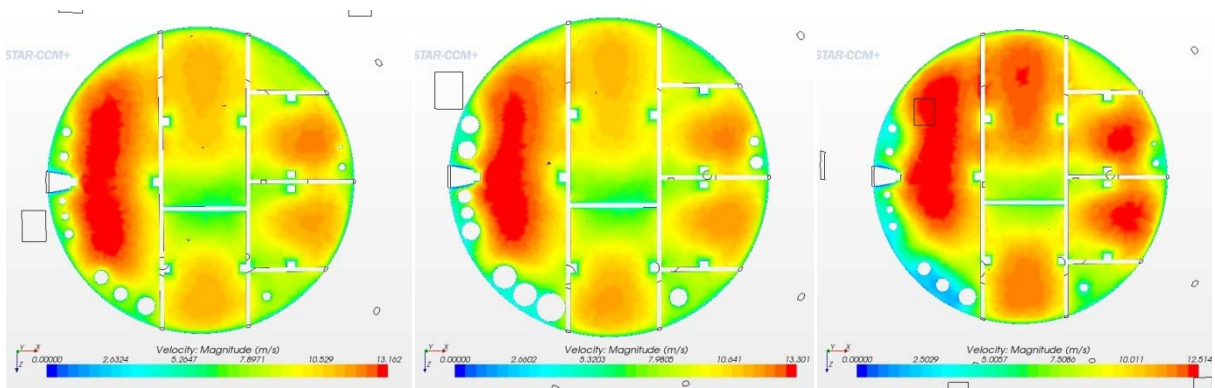
(T08 – Shaft barrel and buntions and pipes at pipe diameter; T09 – Shaft barrel and buntions and pipes at flange diameter; T10 - Shaft barrel and buntions and pipes including flanges)

	14 Shaft	11 Shaft	1 Shaft	11C Shaft	12N Shaft
Simulation No. T08 – Shaft barrel, and buntions and pipes at pipe diameter					
Total calculated pressure loss over shaft length (Pa)	579.5	552.0	265.0	-	-
Calculated pressure loss (per m) (Pa/m)	0.67	0.89	0.53	-	-
Total calculated pressure loss over shaft length (CFD) (Pa)	538.1	479.1	210.0	-	-
Measured pressure loss (per m) (CFD) (Pa/m)	0.62	0.77	0.42	-	-
Unaccounted pressure losses (Pa)	159.7	137.2	70.4	-	-
% Difference	7%	13%	21%	-	-

	14 Shaft	11 Shaft	1 Shaft	11C Shaft	12N Shaft
Simulation No. T09 – Shaft barrel and buntions and pipes at flange diameter					
Total calculated pressure loss over shaft length (Pa)	612.5	583.9	276.1	-	-
Calculated pressure loss (per m) (Pa/m)	0.71	0.94	0.55	-	-
Total calculated pressure loss over shaft length (CFD) (Pa)	552.0	499.3	209.7	-	-
Measured pressure loss (per m) (CFD) (Pa/m)	0.64	0.81	0.42	-	-
Unaccounted pressure losses (Pa)	171.6	154.3	70.2	-	-
% Difference	10%	14%	24%	-	-
Simulation No. 10 – Shaft barrel and buntions and pipes including flanges					
Total calculated pressure loss over shaft length (Pa)	612.5	584.0	276.1	-	-
Calculated pressure loss (per m) (Pa/m)	0.71	0.94	0.55	-	-
Total calculated pressure loss over shaft length (CFD) (Pa)	615.3	537.0	209.2	-	-
Measured pressure loss (per m) (CFD) (Pa/m)	0.71	0.87	0.42	-	-
Unaccounted pressure losses (Pa)	203.0	176.9	64.6	-	-
% Difference	0%	8%	24%	-	-

The overall correlation between the calculated data and those taken from the CFD simulations in these tests was much closer than in any of the previous tests. The differences between the theory and the simulation results were between 3 and 23%. This decrease in the differences was not anticipated.

It is interesting to note that the increase in pressure from the CFD simulations was a direct result of the piping in the shaft being modelled in conjunction with the buntons. This combination resulted in additional pressure losses which were not predicted by the theory.

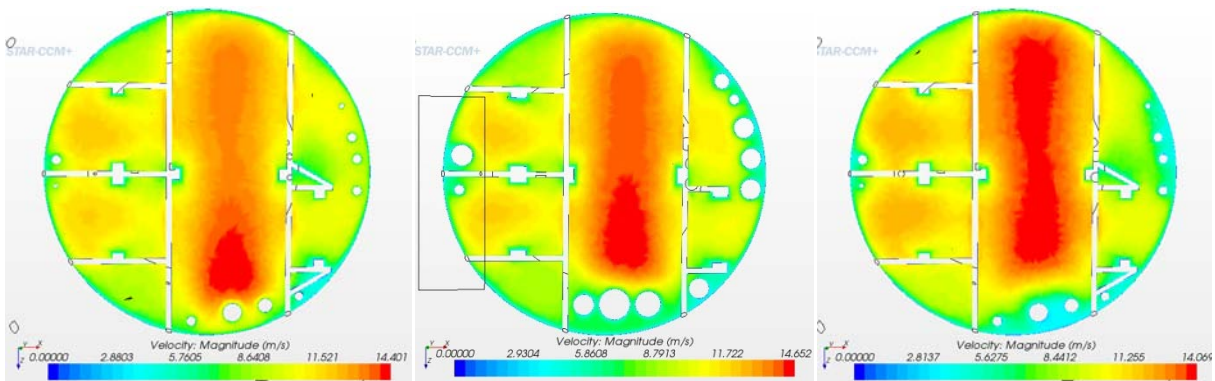


Full Buntun Set, Pipes at Pipe Diameter

Full Buntun Set, Pipes at Flange Diameter

Full Buntun Set, Pipes including Flanges

14 Shaft

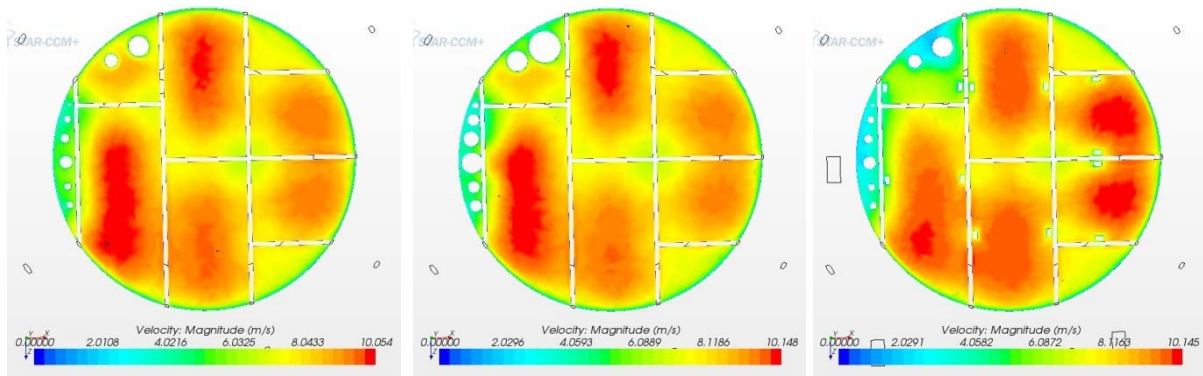


Full Buntun Set, Pipes at Pipe Diameter

Full Buntun Set, Pipes at Flange Diameter

Full Buntun Set, Pipes including Flanges

11 Shaft

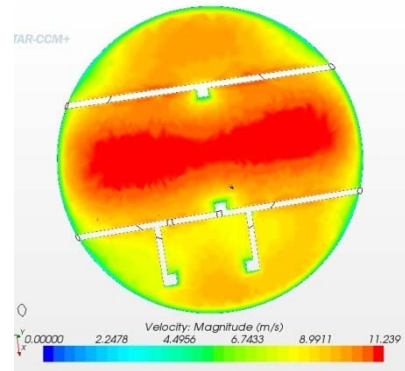


Full Bunton Set, Pipes at Pipe Diameter

Full Bunton Set, Pipes at Flange Diameter

Full Bunton Set, Pipes including Flanges

1 Shaft



Full Bunton Set, No Pipes

No Pipes in Section of 11C Shaft

No Buntons in 12N Shaft

Figure 5-4: Velocity profiles for simulations 8, 9 and 10

(T08 – Shaft barrel and buntons and pipes at pipe diameter; T09 – Shaft barrel and buntons and pipes at flange diameter; T10 – Shaft barrel and buntons and pipes including flanges)

In the velocity plots of the cross-sections of the various shafts shown in Figure 5-4, a number of interesting facts are apparent.

In the 14 shaft test, the small connection between the two main buntons is a square section. The area of reduced velocity around this section is significantly larger than that for the more aerodynamic sections. The free-velocity section of the shafts also decreases more for the piping with flanges than for the piping without them. This is consistent with the observations from simulations T05, T06 and T07.

5.1.5 CFD Simulations Nos T11, T12, T13, T14 and T15

(T11 – Shaft barrel and buntions and pipes including flanges and skip 1; T12 – Shaft barrel and buntions and pipes including flanges and skip 2; T13 – Shaft barrel and buntions and pipes including flanges and man cage 1; T14 – Shaft barrel and buntions and pipes including flanges and man cage 2; T15 – Shaft barrel and buntions and pipes including flanges and service cage)

It is appropriate that these simulations be discussed together as they all seek to provide a better understanding of the behaviour of ventilation flow around the conveyances when they are assumed to have been stopped in the shaft. The results of these simulations are given in Table 5-5.

Table 5-5: CFD simulations Nos 11, 12, 13, 14 and 15 T15

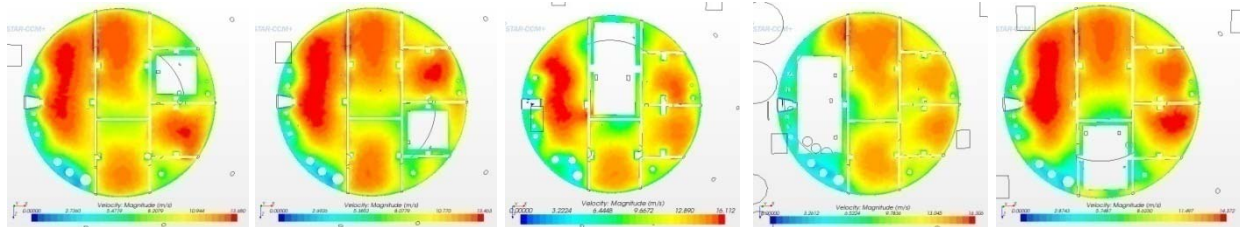
(T11 – Shaft barrel and buntions and pipes including flanges and skip 1; T12 – Shaft barrel and buntions and pipes including flanges and skip 2; T13 – Shaft barrel and buntions and pipes including flanges and man cage 1; T14 – Shaft barrel and buntions and pipes including flanges and man cage 2; T15 – Shaft barrel and buntions and pipes including flanges and service cage)

	14 Shaft	11 Shaft	1 Shaft	11C Shaft	12N Shaft
Simulation No. T11 – Shaft barrel and buntions and pipes including flanges and skip 1					
Pressure loss calculated from theory	706.1	638.2	310.0	-	332.0
Calculated pressure loss (per m) (Pa/m)	0.81	1.03	0.61	-	0.38
Pressure loss calculated from CFD (Pa)	618.7	541.0	211.1	-	112.8
Measured pressure loss (per m) (CFD) (Pa/m)	1.02	1.50	0.81	-	0.68
Unaccounted pressure losses (Pa)	206.5	180.8	66.5	-	-84.5
% Difference	12%	15%	32%	-	72%

	14 Shaft	11 Shaft	1 Shaft	11C Shaft	12N Shaft
Simulation No. T12 – Shaft barrel and buntions and pipes including flanges and skip 2					
Total calculated pressure loss over shaft length (Pa)	706.1	638.2	310.0	-	377.0
Calculated pressure loss (per m) (Pa/m)	0.81	1.03	0.61	-	0.43
Total calculated pressure loss over shaft length (CFD) (Pa)	618.6	541.1	211.6	-	112.8
Measured pressure loss (per m) (CFD) (Pa/m)	1.00	1.53	0.80	-	0.57
Unaccounted pressure losses (Pa)	206.3	180.9	66.9	-	-84.4
% Difference	12%	15%	32%	-	75%
Simulation No. T13 – Shaft barrel and buntions and pipes including flanges and man cage 1					
Total calculated pressure loss over shaft length (Pa)	649.5	630.6	285.1	713.8	-
Calculated pressure loss (per m) (Pa/m)	0.75	1.02	0.57	0.62	-
Total calculated pressure loss over Shaft Length (CFD) (Pa)	631.2	568.0	215.0	444.8	-
Measured pressure loss (per m) (CFD) (Pa/m)	2.06	4.79	1.30	3.62	-
Unaccounted pressure losses (Pa)	218.9	207.8	70.4	19.5	-
% Difference	3%	10%	25%	38%	-

	14 Shaft	11 Shaft	1 Shaft	11C Shaft	12N Shaft
Simulation No. T14 – Shaft barrel and buntions and pipes including flanges and man cage 2					
Total calculated pressure loss over shaft length (Pa)	649.5	-	285.1	-	-
Calculated pressure loss (per m) (Pa/m)	0.75	-	0.57	-	-
Total calculated pressure loss over shaft length (CFD) (Pa)	634.6	-	215.9	-	-
Measured pressure loss (per m) (CFD) (Pa/m)	2.35	-	1.43	-	-
Unaccounted pressure losses (Pa)	222.3	-	71.2	-	-
% Difference	2%	-	24%	-	-
Simulation No. T15 – Shaft barrel and buntions and pipes including flanges and service cage					
Total calculated pressure loss over shaft length (Pa)	652.2	-	285.0	719.8	-
Calculated pressure loss (per m) (Pa/m)	0.75	-	0.57	0.63	-
Total calculated pressure loss over shaft length (CFD) (Pa)	627.8	-	214.7	426.8	-
Measured pressure loss (per m) (CFD) (Pa/m)	1.44	-	1.26	0.68	-
Unaccounted pressure losses (Pa)	247.5	-	70.1	1.6	-
% Difference	4%	-	25%	41%	-

The pressure losses noted in these tests once again show a significant decrease in the difference between the pressures calculated from the theory and those calculated from the CFD results. This reduction in the overall difference is again attributed to the ‘unaccounted’ pressure losses which the CFD results show. The actual increase in the pressure losses in the overall shaft is not significant when the conveyance is in the shaft.



Skip 1

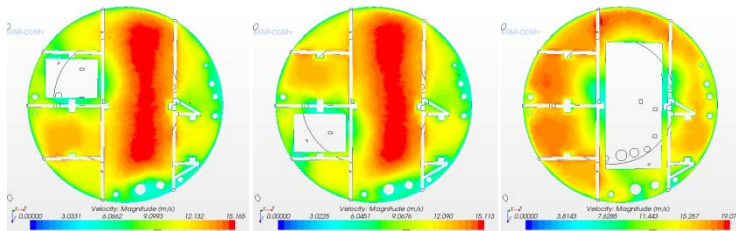
Skip 2

Man Cage 1

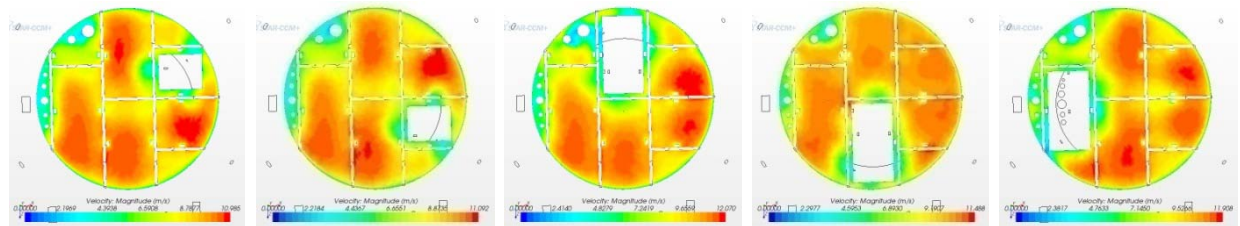
Man Cage 2

Service Cage

14 Shaft



11 Shaft



Skip 1

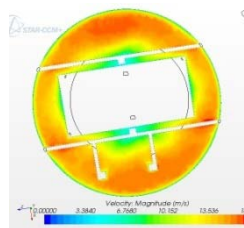
Skip 2

Man Cage 1

Man Cage 2

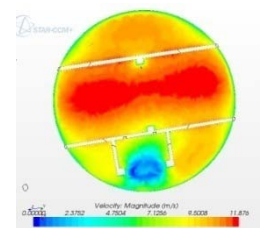
Service Cage

1 Shaft

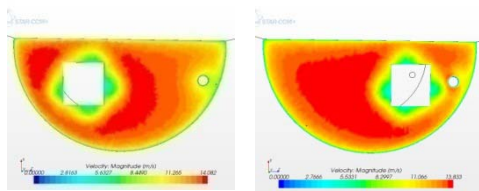


Man Cage 1

11C Shaft



Counterweight



12N Shaft

Figure 5-5: Velocity profiles for simulations 11, 12, 13, 14 and 15

(T11 – Shaft barrel and buntions and pipes including flanges and skip 1; T12 – Shaft barrel and buntions and pipes including flanges and skip 2; T13 – Shaft barrel and buntions and pipes including flanges and man cage 1; T14 – Shaft barrel and buntions and pipes including flanges and man cage 2; T15 – Shaft barrel and buntions and pipes including flanges and service cage)

In the velocity plots of the cross-sections of the various shafts shown in Figure 5-5, a number of interesting facts are apparent.

The velocity profile for each of the plots changes significantly when the different conveyances are placed in the shaft. This is expected. It also highlights the fact that, as the conveyance moves through the shaft, the velocity profile in the shaft changes significantly. The additional pressure losses as the ventilation air is forced in different directions as the conveyance moves through the shaft have not been calculated here. This constant change in direction could account for the additional losses that are apparent from the measured tests and those losses calculated for the CFD analysis and the theoretical analysis.

5.2 Summary and Conclusions from the CFD Simulation Results

Overall, the results of the individual sections of the CFD simulations showed little agreement with those of the theoretical calculations for the initial simulations. There are potentially a number of reasons for this which will be discussed in more detail here. The most importance factor which must be borne in mind are the inaccuracies inherent in the calculations. These are quoted to have an accuracy $\pm 15\%$ for the calculation of the pressure losses resulting from the shaft wall. (See section 3.2.1.1).

The initial simulations (T01 to T10) were completed in such a way as to allow the evaluation of the individual contributors to the overall shaft pressure drops, as well as to evaluate the effect of these being combined.

It is interesting to note that the initial simulations (T01 to T07) showed very little correlation between the theoretical calculations and those derived from the CFD analysis. The same variables

were used in the overall evaluation of both of the techniques.

The evaluation of the contribution that the buntons make to the overall friction losses also showed little correlation with the calculated data. It can be seen, however, that the correlation between the theory and the CFD results improves as the complexity of the buntion arrangement increases. It is also significant that the C_D calculated from the CFD data is closest to the assumed value with the single buntion in the shaft. This accuracy decreases in simulation T03 and again increases with simulation T04. This is attributed primarily to the interference factor which is included for the calculation of the theoretical pressure loss. The C_D 's for the CFD results calculated without this factor are significantly lower than those assumed for the theoretical evaluation. This does show the importance of including the effect from adjacent buntions when calculating the overall drag coefficient. However, as the differences in the drag coefficient between the assumed values and those calculated from the CFD do not match the percentage differences noted from the pressure drops over the section considered, it does raise a concern as to the accuracy of the factors used for the theoretical evaluation.

In addition, once the pressure losses from the shaft barrel have been removed, there is only a marginally better correlation between the theoretical and the CFD calculations (approximately 2% better) in these initial tests.

The correlation between the theoretical results and the CFD results also showed differences. In simulation T05, the anticipated pressure drops from the theory were very low, with the exception of the 11 shaft. This difference was attributed primarily attributed to the two large pipes in the 11 shaft cross-section. The CFD results, however, showed an even smaller pressure loss. In the case of the results for the 1 and 12N shafts, this result was negative, thus showing that there was a reduction in the pressure drop over these shafts. This negative value was obtained once the pressure losses from the shaft barrel simulation had been subtracted from the simulation T05 pressures. This negative value persisted in the simulation T06 results. Both of these shafts have fewer pipes than the 14 shaft or the 11 shaft. This result is consistent with the observations made by Bromilov (1960). In this paper he noted that there seems to be a small decrease in the pressure losses when pipes are included in the shaft cross-section. However, the above results seem to indicate that this effect is disappears after a certain additional number of pipes have been added in the shaft.

Simulation T07 (i.e. when the pipes are assumed to be flanged) showed significant increases in the pressure losses for all the shafts for the CFD analysis. However, even with the flanges included in the simulation, there is still a significant difference between the calculated pressures losses and those from the CFD simulations.

Simulations T08, T09 and T10 showed significantly better correlations between the theoretical

pressure losses and those of the CFD analysis. The theoretical analysis relies on the arithmetic addition of the Chezy-Darcy friction factors being contributed by the various items discussed above. However, the CFD analysis showed different results. To try and discern the reason for this, the pressure losses calculated for the previous tests for the piping and buntons were subtracted from the overall pressure value. This showed an additional unaccounted for pressure loss of approximately 30% of the overall pressure loss. The only reason that could be found for this pressure loss is the interaction between the various components in the shaft. This is not consistent with the theory and indicates that the friction losses for the various components cannot be added to obtain the final Chezy-Darcy friction factor. Figure 5-6 shows the velocity profiles over the shaft cross-sections for the various configurations. These cross-sections provide indicative information as to the reason for the additional pressure losses. The nominal ventilation velocity for this shaft is 10 m/s.

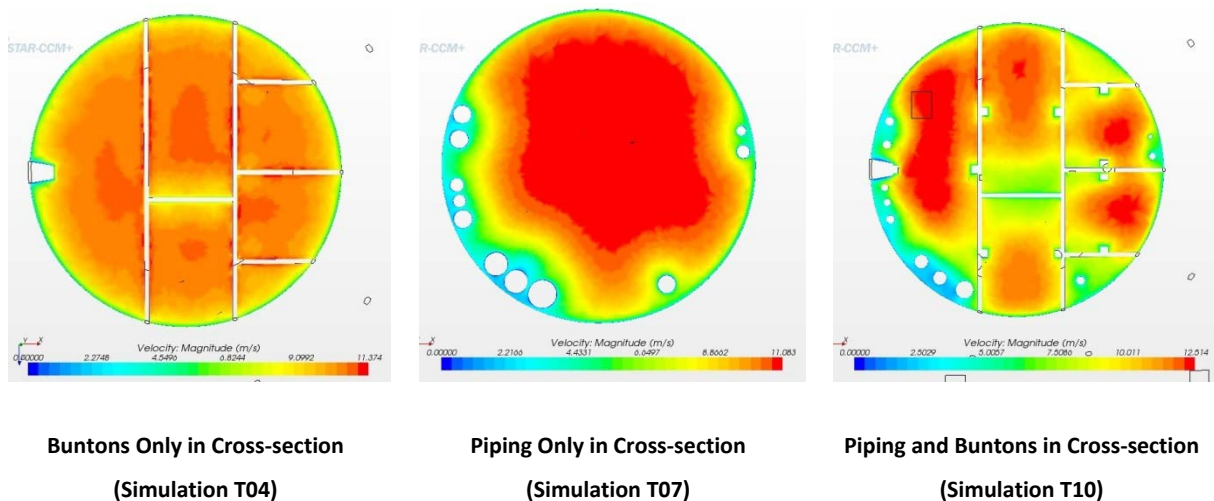


Figure 5-6: Velocity profiles for simulations T04, T07 and T10

(T04 – Shaft barrel and full buntton set; T07 – Shaft barrel and pipes including flanges; T10 – Shaft barrel and bunttons and pipes including flanges)

The final evaluation relates to the placement of the skips and cages. In this instance there is good correlation between the conveyances and the theoretical data. It must, however, be noted that this correlation includes the unaccounted pressure losses. These still make up approximately 30% of the total pressure loss. The overall pressure loss as a result of the cages from the conveyance is not large, assuming each of the conveyances is alone in the shaft. This is attributed to the fact that none of the conveyances in the shaft is considered to be especially large in comparison with the shaft size. The maximum coefficient of fill was 30%.

5.2.1 Conclusions from the CFD Simulation Results

The following specific conclusions can be drawn from the CFD simulations:

- 1 The CFD simulation results for the various shafts containing only the buntions or the pipes show little correlation with the theory. These results are however on the extremity of the accuracies shown for the calculations.
- 2 The inclusion of pipes in the shaft resulted in a small decrease in the overall pressure drop in the shaft. This decrease was only apparent in the shafts that had comparatively fewer pipes. The expected decrease in the pressure drop seems to apply only when the total number of pipes is below a certain limit.
- 3 The small pressure drops as a result of pipes being included in the shaft are not apparent when the pipes are assumed to be flanged. In this instance there is an increase in the overall pressure drop.
- 4 The calculation of the pressure drop for the buntions is highly dependent on the interference of each buntion set with the others, as well as on the selected coefficient of drag. This interference factor has been included in the calculation.
- 5 The overall correlation between the pressure drops predicted by the theory and those taken from the simulations showed significantly better correlation once the complexity of the buntions and the fittings within the shaft increased. This emphasised the interrelated nature of the buntions and fittings in the shaft cross-section. It also highlighted the deficiencies in the current theoretical analysis techniques.
- 6 The theoretical calculations of the pressure losses resulting from the conveyances in the shaft showed good correlation when compared with those predicted by the simulation results.

CHAPTER 6 COLLATION OF ALL RESULTS

6.1 GENERAL

This section considers all the results from the work presented in the previous chapters. It is only possible to compare the results from simulations T10, T11, T12, T13, T14 and T15. The other simulations all considered only portions of the shaft which it was not possible to test independently.

The results from simulation T10 will be considered first.

Table 6-1: CFD simulation No. T10 – Shaft barrel and buntions and pipes including flanges

	14 Shaft	11 Shaft	1 Shaft	11C Shaft	12N Shaft
Simulation No. T10					
Pressure loss calculated from theory (Pa)	612.5	584.0	276.1	671.5	266.0
Pressure loss calculated from CFD (Pa)	615.3	537.0	209.2	425.3	88.5
Pressure loss from measurements (Pa)	891.1	721.3	248.1	752.4	917.6

The results in Table 6-1 are considered separately as simulation No. T10 is the only test that assumed that there is nothing in the shaft except the fittings. As can be seen from this analysis, there is a substantial difference between the measured data and those of both the theoretical calculations and the CFD analysis, the specifics of this have been discussed in section 4.2.1. The concern regarding the estimation of the coefficient of drag has already been discussed. Suffice it to say that there is consistency between the CFD data and the theory, albeit for different reasons.

Table 6-2: CFD simulations Nos T11, T12, T13, T14 and T15

	14 Shaft	11 Shaft	1 Shaft	11C Shaft	12N Shaft
Simulation No. T11 – Shaft barrel and buntions and pipes including flanges and skip 1					
Pressure loss calculated from theory (Pa)	706.1	638.2	310.0	-	331.7
Pressure loss calculated from CFD (Pa)	618.7	541.0	211.1	-	94.0
Pressure loss from measurements (Pa)	897.5	756.3	231.4	-	866.0
Simulation No. T12 – Shaft barrel and buntions and pipes including flanges and skip 2					
Pressure loss calculated from theory (Pa)	706.1	638.2	309.9	-	377.0
Pressure loss calculated from CFD (Pa)	618.6	541.1	211.1	-	93.9
Pressure loss from measurements (Pa)	897.5	756.3	231.4	-	866.0
Simulation No. T13 – Shaft barrel and buntions and pipes including flanges and man cage 1					
Pressure loss calculated from theory (Pa)	649.5	630.6	285.1	713.8	-
Pressure loss calculated from CFD (Pa)	647.7	568.0	215.0	444.8	-
Pressure loss from measurements (Pa)	930.0	796.3	242.0	856.1	-

	14 Shaft	11 Shaft	1 Shaft	11C Shaft	12N Shaft
Simulation No. T14 – Shaft barrel and buntions and pipes including flanges and man cage 2					
Pressure loss calculated from theory (Pa)	649.5	-	285.1	-	-
Pressure loss calculated from CFD (Pa)	634.6	-	214.9	-	-
Simulation No. 15 – Shaft barrel and buntions and pipes including flanges and service cage					
Pressure loss calculated from theory (Pa)	652.2	-	285.0	719.7	-
Pressure loss calculated from CFD (Pa)	627.8	-	214.7	426.8	-
Pressure loss from measurements (Pa)	891.1	-	216.8	752.4	-

As can be seen from Table 6-2 and as has been noted before, there is good correlation between the theoretical calculation and the CFD analysis. However, there is consistently poor correlation between the measured results and both the theoretical and CFD results.

It is interesting to note that this does not apply to the 1 shaft tests. This is the only shaft that did not use the airflow buntions. This would seem to add strength to the concern raised above about the accuracy of the drag coefficient data used for the theoretical calculations.

The discrepancies noted in 12N shaft have been discussed previously in this thesis and will not be re-evaluated here.

The differences noted between the other shafts and the data above do, however, highlight the potential differences that arise when evaluating complex systems from the theoretical perspective. It is not possible to include the effects of various items such as imperfections between the lining rings, the inclusion of slinging points in the shaft, large cable pocket installations, intermediate pump stations and other shaft openings. The differences noted above are attributed to these as well as the other inaccuracies noted above.

This also highlights the importance of ensuring that there is sufficient capacity in any designed system to accommodate future requirements, which it is not possible to anticipate in the design phase. In this instance the data indicates that the allowance should be of the order of a 30% increase should be made.

One of the variables that was not measured against time for the duration of the test was the velocity of the ventilation air within the shaft. This can make a significant contribution to the overall pressure losses calculated and should be measured in future tests.

6.2 SUMMARY AND CONCLUSIONS

The following specific points can be made from the collation of all the results:

- 1 There is not a reasonable correlation between the results from the theoretical calculations and the results of the CFD simulations in the initial tests. There is however good correlation between the theoretical calculations and the results of the CFD simulations in the tests evaluating the complete shaft. The specific conclusions which can be drawn from this are discussed in Section 8.2.
- 2 There is not a good correlation between the measured data and the theoretical or CFD results. These differences are in part attributed to imperfect installations such as the kerb ring during installation, as well as to the mid-shaft cable pockets, cable installation attachments and other miscellaneous items that can be found in the shafts. These differences do highlight the importance of understanding the limitation of any theoretical analysis when comparing it with a physical installation.
- 3 It is important to note that, once the theoretical analysis has been completed, an additional factor should be added to ensure that the non-homogenous imperfections of any installation can be effectively accommodated. This factor is shown to be of the order of 30%.

CHAPTER 7 ECONOMIC EVALUATION OF SHAFT OPTIONS

7.1 SUMMARY OF OPTIONS

To ensure that the recommendations made in this work are valid, a number of additional options were evaluated using the CFD technique described above. The following specific scenarios were evaluated on a typical shaft system:

- 1 Bunton arrangements
 - Shaft bunton arrangement with airflow buntons
 - Shaft bunton arrangement with streamlined buntons
 - Shaft bunton arrangement with square buntons
 - Shaft bunton arrangement with I-beam buntons
- 2 Piping placement (This option will be completed with airflow buntons.)
 - Piping placed in same place along edge of shaft
 - Piping placed near centre of shaft
 - Piping distributed around shaft
 - Option with the least resistance, including flanges
- 3 Cage fill factors (This option will be completed with airflow buntons.)
 - Cage $C_f = 10\%$
 - Cage $C_f = 20\%$
 - Cage $C_f = 30\%$
 - Cage $C_f = 40\%$
 - Cage $C_f = 50\%$
 - Cage $C_f = 30\%$ (cage with fairings at top of cage)
 - Cage $C_f = 30\%$ (cage with fairings at bottom of cage)
 - Cage $C_f = 30\%$ (cage with fairings at top and bottom of cage)

The above options were evaluated and the pressure losses over the shaft length were calculated. The dimensions used for the shaft are as follows:

- Shaft diameter: 9 m
- Shaft depth: 2 000 m
- Ventilation velocity: 10 m/s

The basic fan power required to deliver the flow rate and the calculated pressure, as well as the overall costs for the power to deliver this were calculated. This cost for the power requirement was used to evaluate the current and potential costs of the options under consideration.

The cross-section of the shaft is shown in Figure 7-1.

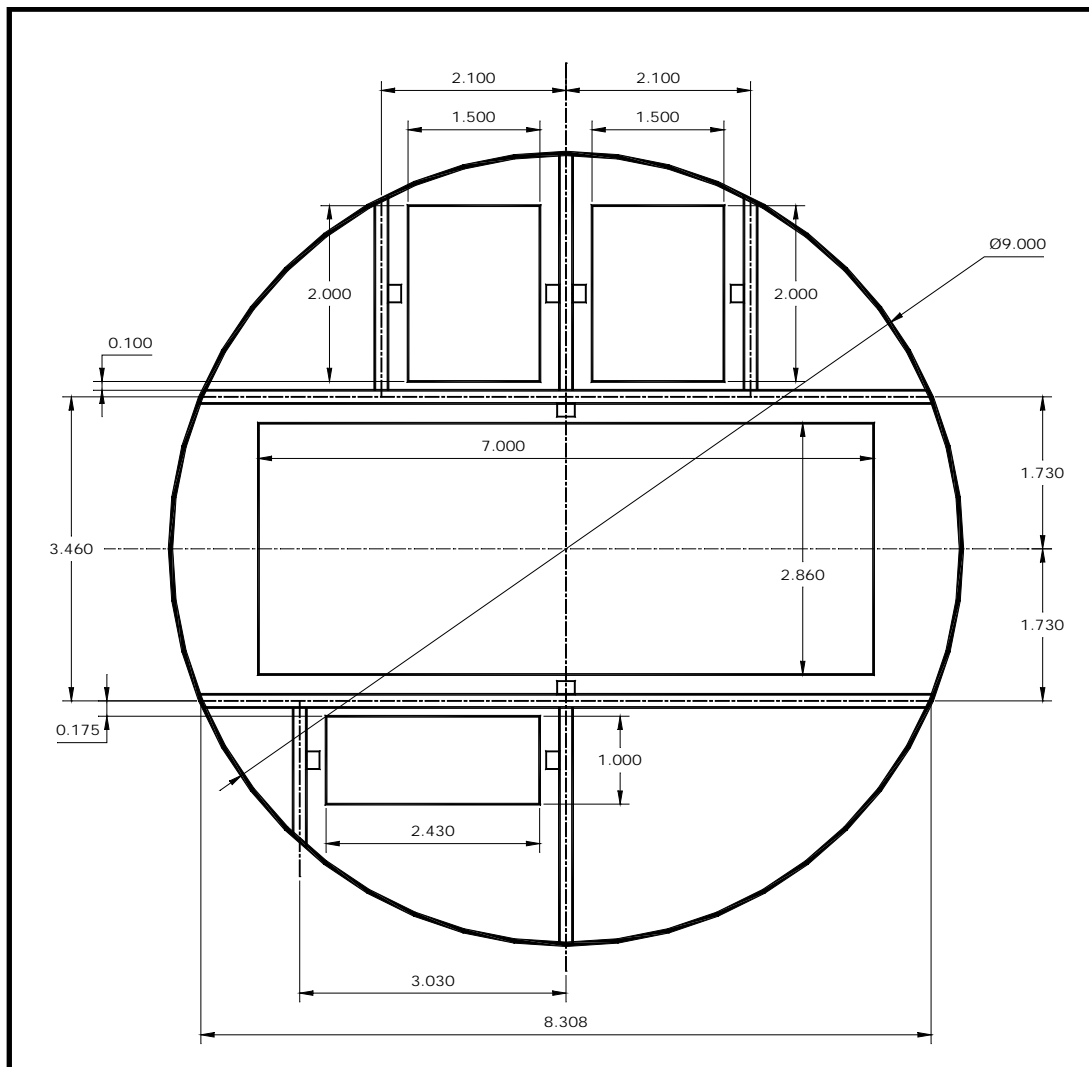


Figure 7-1: Typical cross-section

A summary of the results is given in Table 7-1, Table 7-2 and Table 7-3. An estimate is also made of the operating costs for 20 years based on an inflation rate of 12% per annum for the electrical costs.

It should be noted that this is well below the anticipated increased noted in section 1. These values are then discounted at 7% per annum to achieve an effective present cost.

7.2 SUMMARY OF RESULTS

7.2.1 Bunton Shapes

Table 7-1: CFD simulation for piping placement

Item	Description	Shaft P_{Loss}	Estimated total annualised cost	% Differences	Estimated capital cost	Estimated current annual savings	Savings over 20 years
1.01	Airflow buntions	822	R3,908,773	1.00 (Baseline)	R8 965 440	–	–
1.02	Streamlined buntions	774	R3,716,566	0.95	R8 965 440	R192 206	-R 5 738 460
1.03	Square buntions	1,608	R7,058,823	1.81	R8 229 640	R3 150 051	R94 046 991
1.04	I-beam buntions	1 324	R5,932,280	1.52	R7 471 200	R2 023 507	R60 413 237

Note : % Differences, this is a difference when compared to the option chosen as the baseline (this option is shown as (Baseline))

As can be seen from Table 7-1, a significant saving can be made through the judicious choice of the buntion shape. This varies from 52% to 81% of the fan power costs as a direct result of the resistance the shaft offers to the flow of air through it. A small decrease in these costs was also not for the Streamlined buntions of 5%.

7.2.2 Piping Arrangements

Table 7-2: CFD simulation for piping arrangements

Item	Description	Shaft P _{Loss}	Estimated total annualised cost	% Differences	Estimated current annual savings	Savings over 20 years
2.01	Piping along shaft edge	856.7	R4 047 589	1.11	R405 769	R12 114 528
2.02	Piping away from shaft edge	819.3	R3 898 095	1.07	R 256 275	R7 651 281
2.03	Piping distributed around shaft	755.3	R3 641 819	1.00 (Baseline)	–	R -
2.04	Distributed piping with flange	866.7	R4 087 632	1.12	R445 812	R13 310 040

Note : % Differences, this is a difference when compared to the option chosen as the baseline (this option is shown as (Baseline))

This result shows that the judicious placement of the piping in the shaft can have a significant effect on the resistance in the shaft. This saving can be between 7% and 12% of the total resistance experienced in the shaft. The results also show that, once the most efficient position has been chosen for the piping, the use of flanges to join the pipes can increase the cost of supplying air to the mine by approximately 12%.

7.2.3 Coefficient of Fill and Cage Configurations

Table 7-3: CFD simulation for varying cage fill factors

Item	Description	Shaft P _{Loss}	Estimated total annualised cost	% Differences	Estimated current annual savings	Savings over 20 years
3.01	C _f = 10%	1 780.3	R7 746 095	0.31	R-17 197 073	R-513 430 817
3.02	C _f = 20%	3 293.3	R13 804 763	0.55	R-11 138 405	R-332 544 979
3.03	C _f = 30%	6 075.0	R24 943 168	1.00 (Baseline)	–	R -
3.04	C _f = 40%	11 966.0	R48 532 709	1.95	R23 589 540	R704 282 448
3.05	C _f = 50%	17 306.0	R69 915 639	2.80	R44 972 470	R1 342 684 978
3.06	C _f = 30% (fairings on top)	3 706.2	R15 458 139	1.00 (Baseline)	–	R -
3.07	C _f = 30% (fairings on bottom)	6 051.4	R24 848 827	1.63	R9 390 688	R280 365 636
3.08	C _f = 30% (fairings on top and bottom)	4 172.7	R17 325 986	1.13	R1 867 846	R55 765 881

Note : % Differences, this is a difference when compared to the option chosen as the baseline (this option is shown as (Baseline))

Although the overall savings here seem to be significant when the coefficient of fill of the cage decreases, it must be remembered from the previous conclusions that these losses can be avoided by the judicious design of level take-off configurations since the pressure losses shown here are most apparent when the cage is blocking the shaft. However, these data will give guidance as to the overall effect that could occur should this not be the case.

The most significant results of this analysis are the savings that can be achieved by the addition of fairings on the cage (of the order to 30%). This potential saving is not sufficient in itself to justify

wholesale changes in the design of conveyances. However, if such a change is required for safety reasons, it provides a way in which this can be achieved while also achieving savings. This safety concern arises from the possibility that falling objects in the shaft may penetrate the roof of the cage; a fairing of this nature will help to deflect such objects.

It can also be seen that these results are broadly consistent with those noted by Ruglen and Wilson (Ruglen and Wilson, 1978). The negligible reduction of the calculated pressure losses of the conveyance as a result of the bottom fairing was also discussed in this paper. This is as a result of the fact that these would have to be excessively long to affect the streamlines apparent with fully developed flow. The effect of the small fairing could however have the effect of increasing the effective length of the conveyance, thus increasing the total resistance offered by the conveyance. However it is important to note that conveyance will move up and down, so the fact that this fairing does not indeed add to the overall resistance is important to note.

7.3 SUMMARY AND CONCLUSIONS

The following specific points can be made from the collation of all the economic data.

- 1 The shape of the buntons is important in meeting the requirement to reduce the pressure drop in the shaft as much as is possible.
- 2 The placement of the piping in the shaft and the use of flanged piping can have a significant deleterious effect on the pressure drops in the shaft.
- 3 The addition of fairings to a cage can have a positive effect on the pressure drops that are apparent in a shaft. However, although this effect may be significant, it must be borne in mind that the overall effect of the cage on shaft pressure drops arises from the blockage it applies to the shaft. This can be mitigated more effectively by designing conveyance stop points to ensure that the ventilation air can flow around the cage with ease.

CHAPTER 8 SUMMARY, CONCLUSIONS AND RECOMMENDATIONS

8.1 SUMMARY

As a result of the rising electrical energy costs in South Africa, a method was sought to reduce the overall electrical consumption of typical shaft systems. To achieve this, the first step was to analyse a typical shaft system and to determine what areas required the most energy to operate.

A typical shaft configuration was analysed and the primary energy consumers were identified. The ventilation fans for this system were found to consume a total of 15% of the total energy of the shaft system. It was calculated that more than 50% of this energy is consumed by the shaft itself, more specifically by the pressure losses that occur in the shaft as the ventilation air passes through it. This area was deemed worthy of additional evaluation. To complete this evaluation, the following steps were undertaken:

- 1 Literature study
- 2 Definition of the objectives
- 3 Evaluation of current shaft configurations
- 4 Detailed analysis
- 5 CFD simulation of the shaft system
- 6 Economic evaluation

A comprehensive search was done to find literature on the evaluation of shaft resistances. The literature review in Chapter 2 discussed the manner in which the shafts have been designed and provided invaluable information with respect to the way the current shaft configurations have been achieved.

In this regard, it is interesting to note that the driver for understanding and then reducing the resistance that the shaft offers to ventilation air was the need to get ventilation air underground. Most of this work was completed circa 1960 and it is during this period that the most useful work was done. Very little has been done in this area since then. McPherson (1987) formalised the approach for designing shafts to reduce resistances but did not undertake further research. A number of papers discussing tests that had been conducted on shaft systems were evaluated. These provided the basis for the methodology used here in measuring the shaft systems under

consideration in this work.

Some CFD work was completed by Anglo American (Craig, 2001), but the driver for this was to find ways to optimise the design of the shaft steelwork. Interest in this work has more recently picked up again as the cost of electrical energy has increased and this is apparent in the papers published more recently.

Once the literature study had been completed and the work that has been done was understood, the next phase was to conduct some measurements on existing shafts. A number of shafts were evaluated at Impala Platinum. All these shafts were more than 10 years old. Although this was not ideal, it could not be avoided as none of the new-generation shafts had been commissioned at the time of writing.

These shafts did, however, provide a good spectrum against which to complete the initial tests. The following shafts were tested:

- 1 Impala 14 shaft
- 2 Impala 11 shaft
- 3 Impala 1 shaft
- 4 Impala 11C shaft
- 5 Impala 12N shaft

These shafts were all subjected to the testing described in Chapter 3. These tests consisted of placing data loggers in the shafts to take the environmental measurements. The results were collated against the measurements obtained from equipment placed on the winders of the shaft. The combination of these measurements showed the pressure drops in the shaft in relation to the movement of the conveyances within the shaft.

The testing of the shafts was completed over approximately 2 years. This long period was a result of various problems with the equipment being used and the availability of the shafts. The Impala Platinum ventilation personnel and the engineers on the various shafts were very helpful in this regard.

Once the data had been gathered and collated, they were all graphed against the same time scale such that the movement of the conveyance could be compared against the various pressure drops. These results were collated and the results tabulated in graphs which can be found in Appendices D, E, F, G and H.

Once this testing had been completed, the results were compared with those from a detailed theoretical analysis using the currently available techniques.

The detailed analysis and the measurements were then compared with the results obtained from CFD simulations. These simulations were completed using the STAR CCM+ computational fluid dynamics software.

One of the advantages of this sort of simulation was that the simulation models could be built and run incrementally. This allowed the evaluation of the various components within the shaft with respect to their contribution to the overall pressure losses experienced by the shaft.

The initial evaluation of the cost of sinking a shaft with respect to its diameter is shown in Figure 1-11. Discussions with mine personnel and shaft-sinking professionals resulted in the installation and maintenance costs not being included in this analysis. This is because these costs are considered to be the same no matter what bunton shape is used.

Shaft maintenance generally occurs during the weekly shaft inspections and is the same no matter which buntons are chosen. The only potential difference is the face that is presented to the ventilation airflow, as this is the face on which muck and other deleterious material collect. The use of a flat bunton could, if the shaft is not maintained correctly, give rise to more corrosion as the material does not naturally flow off this as would happen with the rounded face. This difference is not considered sufficient to result in any cost differential, assuming that the maintenance is done consistently.

The installation time for buntons depends primarily on the work that is done to provide accurately jugged and connected buntons at the installation stage. These operations take as long to do for any bunton shape and will therefore also not result in a cost differential between the options.

The operating costs are evaluated as the electricity required to operate the ventilation fans. These costs are also evaluated over a 20-year cycle. The capital cost is added to this amount to provide an overall cost of ownership.

The installation and maintenance cost for the piping is not considered a cost differential here and is therefore not included in the analysis. This includes the flanges and/or other pipe connectors that could be used.

8.2 CONCLUSIONS

8.2.1 Conclusions from Perusal of the Test Data

The following conclusions can be drawn from a perusal of the measured data:

- 1 There is little or no pressure loss associated with the movement of the cages. There was a small pressure increase in the tests for 1, 11 and 11C shafts. These pressure spikes were of short duration and lagged the passing of cages. The tests for 14 Shaft showed a general

increase in the resistance seen in the shaft during the periods when the skips were moving consistently between the shaft top and bottom. Neither of these findings was consistent with the theory.

- 2 There was also a significant difference between the measured pressures and the calculated pressures for the shafts, this was discussed in Section 6.2. The 12N shaft data were, however, so different as not to be useful. This difference is attributed to the placement of the pressure measurement devices in the shaft and will not be considered further here.
- 3 There was little congruence between the current theory and the and the measured data. The calculation of the pressure drop associated with the buntons using this theory is dependent on the availability of accurate data to define the coefficient of drag (C_d) of the buntons. As has been shown above, the buntons contribute the most significant portion of the overall pressure losses in a shaft system. The drag coefficient's (C_d) of the buntons as listed by McPherson have been calculated from various data associated with measurement of pressure losses in shafts (as listed in the right hand column of Table 3-1). The specific conclusion deriving from this analysis in conjunction with the CFD analysis is discussed in section 8.2.2.
- 4 The effects of a cage moving in the shaft can be ignored unless
 - i the constant movement of conveyances in the shaft is sufficiently regular such that the blockage in the shaft needs be considered. (This is mostly apparent in long shafts where the ventilation is introduced only in the lower level.)
 - ii the coefficient of fill (C_f) in a shaft of the cage is close to 30% of the free-flow area in the shaft. (The exact C_f at which this occurs is not known. This cross-over point should be evaluated using CFD analysis.)

One of the issues that should be considered in evaluating these data is that, should any of the conveyances remain stationary at a particular level for a length of time, the overall resistance seen in the shaft will increase. This emphasises the need to ensure that the stations are designed in such a way as to allow the ventilation air to bypass the conveyance without a significant pressure loss occurring.

8.2.2 General Conclusions from the Analysis

All the shaft configurations discussed were analysed with respect to the current theory available for the evaluation of the shaft system, as well as the being subjected to a detailed CFD analysis.

In order to break down the various contributors to the overall shaft resistance, both the theory and

the CFD model were used to analyse the shaft as it was built up. This analysis started with the bare shaft cross-section and sequentially included the complete bunton and piping sets and, finally, each of the conveyances. At each step of this process, it is possible to subtract the values obtained for the resistance offered by the wall or the buntions and thus to calculate specific figures for the resistance of individual sets. This approach to the overall evaluation yielded some interesting results.

1 The current theory does not provide sufficiently accuracy to design new shafts which differ from the current shaft configuration. It has been shown that this theory is does not provide the necessary definition to allow the shaft parameters to be varied and to provide accurate results based on these variations. In addition, the calculation of the pressure drop associated with the buntions using this theory is dependent on the availability of accurate data to define the coefficient of drag (C_d) of the buntions. If this is not the case, differences between the measured values and the calculated values are to be expected. This conclusion is valid only if it is assumed that the interference factor used for the calculation of the shaft resistance is accurate.

- i As the shaft was built up and the buntions and pipes were added, there was little correlation between the theoretical pressure losses and those predicted by the CFD analysis. This continued until a point was reached, as the piping was being added in its various configurations, when the resistance predicted by the CFD analysis equalled that of the theoretical analysis. The conclusion that was reached was that the inter-related nature of the equipment in the shaft increased the total resistance of the shaft by some 30%. This finding has two specific outcomes:
- ii The theoretical approach to the evaluation of shaft resistances, which consists of arithmetic adding the Chezy-Darcy friction factors for the various items in the shaft and then using the total Chezy-Darcy friction factor to calculate the shaft resistance, is incorrect. Although the final values for the theory and the CFD analysis agree to within 5–15%, the actual make up of the shaft resistance is not as the theory predicts. This conclusion was alluded to by Martinson (1957), however the data gathered was not sufficient to allow for a meaningful comparison.
- iii The inter-related effect of the fittings in the shaft is stronger than was initially anticipated. In order that shaft be designed in a manner which will limit the shaft resistance, the dynamic consideration of the shaft with respect to the turbulent ventilation flow needs to be considered in detail. Should the current theory be used without this consideration being taken in to account, changes

could be made to reduce the shaft resistance that are either incorrect or could not have as significant an effect as was originally thought. The emphasis should rather be placed on creating free-flowing channels and using buntion spaces and pipe configurations that facilitate flow and limit turbulence as far as is practically possible.

- 2 One of the areas that was considered worthy of further investigation was the manner in which the resistance of piping in the shaft was calculated. The piping was therefore modelled, initially at its pipe diameter, then at the flange diameter, as is required by the theory, and finally at the pipe diameter with flanges, which has not been done before. There was not a significant increase between resistances calculated by the CFD simulations using the piping at each of the diameters (less than 1%). However, when the piping was introduced with flanges there was a significant increase in the resistance (the piping in a bare shaft showed an increase of 20%, while the piping in a shaft with the buntions showed an increase of 10%). This is a significant increase and more than sufficient to warrant avoiding the use of flanges in a shaft and avoiding any discontinuities in the piping as far as practically possible.
- 3 The drag coefficient (C_D) calculated from the CFD analysis for comparison with the theory showed little agreement. The CFD-derived drag coefficient was significantly lower than that used in the available literature. This discrepancy reduced considerably when the interference factor was included in the calculation. Chasteau (1961) noted that the measured drag coefficient was different depending on the surrounding turbulence in the shaft. This was found to be correct. This does also give rise to some concern about the approach of the current theory as it seems that the appropriate drag coefficient for each shaft could differ depending on its configuration and velocity.
- 4 In addition, for the initial simulations in 11 shaft and 12N shaft (i.e. the simulations that considered only the pipe in the shaft at the pipe diameter), a small decrease in the shaft resistance was noted. This decrease was commented on by Bromilov (1960), but it did disappear when the pipe was made larger and the flanges introduced. This shows that perhaps the piping does having a smoothing effect on the ventilation flow.
- 5 In the even that more detail work is required for the evaluation of the resistance of shaft, both for the more detailed analysis of current shaft configurations as well as the analysis of future shaft. In this instance it is recommended that the configurations be evaluated using CFD techniques.

8.2.3 Conclusions from the Economic Evaluation

8.2.3.1 Buntons

Various buntion shapes were evaluated, with the following conclusions:

- i Aerofoil buntion shape (most cost-effective buntion shape to use based on the electrical consumption of the ventilation fans)
- ii Airflow buntion shape (+5% (from aerofoil shape))
- iii I-section buntions (+57% (from aerofoil shape))
- iv Rectangular buntions (+86% (from aerofoil shape))

It should be noted that the capital costs for the aerofoil and airflow buntions are approximately equal, while the I-beam buntion is 17% more costs effective than the aerofoil and the rectangular buntion is 8% more cost effective.

8.2.3.2 Pipes

Three pipe positions were evaluated: first pipes placed along the side of the shaft, then placed near the shaft centre and finally dispersed around the shaft. The final costs were evaluated with the best option chosen from these three positions (i.e. the option that results in the least resistance to flow), and flanges were added.

The overall finding from cheapest to the most expensive is:

- i Piping distributed around the shaft
- ii Piping aligned in the middle of the shaft (+7% from distributed option)
- iii Piping aligned at the shaft edge (+11% from distributed option)

Finally, should the piping be distributed around the shaft, but with flanges used as the pipe connection, the cost is +12% from the distributed option.

8.2.3.3 Cages

As can be seen from Table 7-2, the relationship between shaft resistance as a result of the size of the cage and the coefficient of fill for the cage is exponential.

Although the overall savings here seem to be significant, it must be remembered from the previous conclusions that these losses can be avoided by the judicious design of level take-off configuration. However, these data will provide a guide as to the overall effect that could occur should this not be the case ($C_f = 30\%$ (0), $C_f = 50\%$ (280% higher than $C_f = 30\%$). It is also interesting to note that

inclusion of fairings does have an effect on the resistance offered by the cage (39%).

The most significant results of this analysis are the savings that can be achieved by the addition of fairings on the cage. This potential saving is not sufficient in itself to justify wholesale changes in the design of conveyances. However, if such a change is required for safety reasons, it provides a way in which this can be achieved while also achieving savings. This safety concern arises from the possibility that falling objects in the shaft may penetrate the roof of conveyance; a fairing of this nature will help to deflect such objects.

8.3 SUGGESTIONS FOR FURTHER WORK

No work of this nature would be complete without considering the deficiencies of the results presented and the suggested direction for future work.

One of the more concerning and recurring themes of this work is the consistent reference to empirical data obtained more than 50 years ago. Of most concern are the values defined for the drag coefficient. It is suggested that the pertinent bunton shapes be subjected to a detailed experimental and CFD analysis to confirm this data..

The significant difference between the measurement results from the physical tests and those calculated from both the theory and the CFD analysis is a cause for concern. The best way to resolve this would be to find a shaft with a shorter section that could be properly surveyed and then subject it to tests similar to those described above. The technology for such a survey is available but there should be strong emphasis on the need to install instrumentation in the shaft itself to minimise potential losses. A way should also be found to consistently measure the ventilation velocity of the shaft over the same period in which the tests are completed.

CHAPTER 9

REFERENCES

- Barenbrug AWT, 1961. The economic aspect of reducing shaft resistance. *Journal of the South Africa Institute of Mining and Metallurgy*, October.
- Barenbrug WT, 1962. Contribution to discussion analysis of airflow in downcast shafts with reference to the trailing hose method of resistance measurement. *Journal of the Mine Ventilation Society of South Africa*, April.
- Bareza M and Martinson MJ, 1961. Ventilation resistance of some vertical downcast shafts in the Rand Mine Group. *Journal of the South African Institute of Mining and Metallurgy*, October.
- Berkoe JM and Lane DM, 2000. Putting computational fluid dynamics to work on the mining and minerals project. SME Annual Meeting, February.
- Biffi M, Stanton D, Rose H and Pienaar D, 2006. Ventilation strategies to meet future needs of the South African platinum industry. The Southern African Institute of Mining and Metallurgy, Johannesburg.
- Botha BJR and Taussig SG, 1961. The effect of equipment changes in existing shafts. *Journal of the South African Institute of Mining and Metallurgy*, October.
- Bromilov JG, 1960. The estimation and the reduction of the aerodynamic resistance of mine shafts. *Transactions of the Institution of Mining Engineers*, May.
- Brunner DJ, Miclea PC, McKinney D and Marthur S, 1995. Examples of the application of computational fluid dynamics simulation to mine and tunnel ventilation. Proceedings of the 7th US Mine Ventilation Symposium, June.
- Casati JAL and Martinson J, 1962. Scale model test on No. 4 Shaft Coty Deep Limited. *Journal of the South Africa Institute of Mining and Metallurgy*, March.
- Chamber of Mines of South Africa, 2010. *Annual Report 2009–2010*, Mining, 2010, p 31.
- Chasteau VAL. 1959. Investigation into the resistance to airflow of the Pioneer

Shafts at Buffelsfontein Gold Mining Co, Ltd (Part II). *Journal of the Mine Ventilation Society of South Africa*, June.

— Chasteau VAL, 1961. Investigation into the resistance to air flow of No. 1 Shaft, Vaal Reefs Exploration and Mining Company (Paper II). *Journal of the Mine Ventilation Society of South Africa*, January.

— Chasteau VAL, 1962. Equipment and techniques used for scale model investigations of mine shaft resistance to air flow in the CSIR laboratories. *Journal of the Mine Ventilation Society of South Africa*, May.

— Chasteau VAL, 1989. Fundamentals of fluid flow. In: *Environmental Engineering in South African Mines*, Chapter 1. Johannesburg: The Mine Ventilation Society of South Africa.

— Chasteau VAL and Kemp JE, 1962. Further results of scale model measurements of mine shaft resistance to airflow by the CSIR. *Journal of the Mine Ventilation Society of South Africa*, June.

— Deen, JB, 1991. Field verification of shaft resistance equations. Proceedings of the 5th Mine Ventilation Symposium, June, pp 647–655.

— Du Plessis AG, Wymer DG and Joughin NC, 1989. Equipment alternatives for stoping in gold mines. *Journal for the South African Institute of Mining and Metallurgy*, 89(12).

— Du Plessis JIL and Marx WM, 2007. Main fan power control. Presented at the Conference of the Mine Ventilation Society of South Africa, May.

— Eskom Holdings Limited, 2009. *Annual Report 2008*.

— Eskom Holdings Limited, 2010. *Annual Report 2009*.

— Eskom Holdings Limited, 2011. *Annual Report 2010*.

— Eskom, 2011. *Tariff Book*.

— Fraser P and Le Roux D, 2007. Three-chamber pump systems for DSM, *Energize*, December.

- Fytas K and Gagnon C, 2008. A database of ventilation friction factor for Quebec underground mines. Presented at the 12th North American Mine Ventilation Symposium, October.
- Graig K, 2001. Report on CFD analysis of bunton sections. Report prepared for Anglo Operation Limited, November.
- Graves DFH, 1961. Research into shaft resistance. *Journal of the Mine Ventilation Society of South Africa*, September.
- Graves DFH, 1962. Airflow resistance in downcast shafts equipped with streamlined buntons. *Journal of the South African Institute of Mining and Metallurgy*, June.
- Hartman HL, Mutmanský JM, RV Ramani and Wang YJ. 1997. *Mine Ventilation and Air Conditioning*, 3rd edition. New York: Wiley.
- Hemp R, 1975. Density patterns in some vertical downcast shafts. Proceedings of the International Mine Ventilation Congress, Johannesburg.
- Hemp R, 1979. A method for analysing pressure survey measurements. *Journal of the Mine Ventilation Society of South Africa*, 32: 1.
- Hemp R, 1989. Pressure surveys. In: *Environmental Engineering in South African Mines*, Chapter 6. Johannesburg: The Mine Ventilation Society of South Africa.
- Hustrulid WA and Bullock RL, 2001. Underground mining methods – Engineering fundamentals and international case studies. Littleton, Colorado: Society for Mining, Metallurgy, and Exploration.
- Jade RK and Sastry BS, 2008. An experimental and numerical study of two-way splits and junctions in mine airways. Presented at the 12th North American Mine Ventilation Symposium.
- Deen BD, 1991. Field verification of shaft resistance equation. Proceedings of the 5th Mine Ventilation Symposium, June.
- Kemp JF, 1962. Analysis of the air flow in downcast shafts with reference to the trailing-hose method of resistance measurement. *Journal of the Mine*

Ventilation Society of South Africa, January.

- Krishna R, 1992. Research on the economic design of mine ventilation systems. Proceedings of the 6th Mine Ventilation Symposium.
- Lambrechts, JdeV and Deacon TE, 1962. Improvements in ventilation capacity by smooth lining of upcast shafts. *Journal of the South Africa Institute of Mining and Metallurgy*, February.
- Lloyd F, 1989. Main ventilation practice. In: *Environmental Engineering in South African Mines*, Chapter 10. Johannesburg: The Mine Ventilation Society of South Africa.
- Macfarlane AS, 2005. Establishing a new metric for mineral resource management. Proceedings of the First International Seminar on Strategic versus Tactical Approaches in Mining. Johannesburg: The South African Institute of Mining and Metallurgy, September.
- Martinson MJ, 1957. Determining the friction factors of Nos 2 and 3 Shafts, Harmony Gold Mining Co, by means of scale models. *Journal of the Mine Ventilation Society of South Africa*, March.
- Martinson MJ, 1962. Contribution to discussion on airflow resistance in downcast shafts equipped with streamlined buntons. *Journal of the South African Institute of Mining and Metallurgy*, June.
- Marx WM, Von Glehn FH and Wilson RW, 2008. Design of energy efficient mine ventilation and cooling systems. Proceedings of the Mine Ventilation Society Annual Conference, Pretoria, May.
- McPherson MJ, 1971. The metrication and rationalisation of mine ventilation calculations. *Mining Engineer (UK)*, 130(131: 729–738.
- McPherson MJ, 1987. The resistance to airflow of mine shafts. Proceedings of the 3rd Mine Ventilation Symposium, October.
- McPherson MJ, 1993. *Subsurface Ventilation and Environmental Engineering*, 2nd edition. Clovis, CA, US: MVS Engineering, pp 9–23.

- Meyer JP and Marx WM, 1993. The minimising of pressure losses in a fan drift-mine shaft intersection, using computational fluid dynamics. *R&D Journal*, 9(3).
- Musingwini C, Minnitt RCA and Woodhall M, 2006. Technical operating flexibility in the analysis of mine layouts and schedules. Proceedings of the International Platinum Conference “Platinum Surges Ahead”, South African Institute of Mining and Metallurgy, Johannesburg, October.
- NERSA (National Energy Regulator of South Africa), 2010. Multi-year price determination 2010/11 to 2012/13. Report MYPD 2, Pretoria: NERSA.
- Pankhurst, RC. 1964. *Introductory Survey. Dimensional Analysis and Scale Factors*. London: Chapman and Hall, pp 13–19, 53–55.
- Petit PJ, 2006. Electric rock drilling system for in stope mining in platinum operations. Proceedings of the International Platinum Conference “Platinum surges Ahead”, South African Institute of Mining and Metallurgy, Johannesburg, October.
- Prince LJ, 1961. Contributions for discussion for the economic aspect of reducing shaft resistance. *Journal of the South Africa Institute of Mining and Metallurgy*, December.
- Quilliam JH, Finn PJ, Graves DFH and Martinson MJ, 1961. Investigation into the resistance to air flow of No. 1 Shaft, Vaal Reefs Exploration and Mining Company (Paper I). *Journal of the Mine Ventilation Society of South Africa*, January.
- Ruglen N, Wilson PH, 1978. Aerodynamic Studies of Shaft / Airway Intersection Losses and Mine Cage Resistance. The Australian Institute of Mining and Minerals Conference, North Queensland, September.
- Seeber HC, 2002. Ventilation – Understanding the factors affecting air resistance and their implications on mine operating and capital costs. Presented at the SME Annual Meeting, February.
- Statistics South Africa, 2011a. Mining: Production and Sales. Statistical Release P2041, May, p 10.
- Statistics South Africa, 2011a. Electricity Generated and Available for

Distribution. Statistical Release P4141, March.

- Statistics South Africa, 2011c. Gross Domestic Product, Fourth Quarter 2010. Statistical Release P0441, February, p 9.
- Stevenson A, 1956. Mine ventilation investigation. Shaft pressure losses due to cages. Unpublished thesis, Royal College of Science and Technology, Glasgow. Also as: The estimation and the reduction of the aerodynamic resistance of mine shafts. *Transactions of the Institution of Mining Engineers*, Glasgow.
- The Mine Ventilation Society of South Africa. 1989. Johannesburg: *Environmental Engineering in South African Mines*.
- Uhlmann HLB , 1961. Economic value in fluid flow. *South African Mechanical Engineer*, October: 105–106.
- Unsted AD and Benecke KC, 1978. Some observations on the effects of a large cage in a downcast shaft. *Journal of the Mine Ventilation Society of South Africa*, March.
- Van Wyk CFB, 1961. A review of progress in the design of shaft equipment aimed at a reduction in shaft resistance. *The South African Mechanical Engineer*, August.
- Wala A, Yingling JC, Zhang J and Ray R, 1997. Validation study of computational fluid dynamics as a tool for mine ventilation design. Proceedings of the 6th International Mine Ventilation Congress, May.
- Wala A, Vytla S, Taylor C and Huang G, 2007. Mine face ventilation: A comparison of CFD results against benchmark experiments for the CFD Code validation. US: National Institute for Occupational Safety and Health (NIOSH).
- Wallace KG and Rogers GK, 1987. Airflow in ventilation and hoisting shafts. Proceedings of the 3rd Mine Ventilation Symposium, October.
- Wells, HM, 1973. Influence of economics on the design of mine shaft systems. *Journal of The South African Institute of Mining and Metallurgy*, 73(10): 325–338.
- White FM, 1986. *Fluid Mechanics*, 2nd edition. New York: McGraw-Hill, pp 308–

314.

- Wills J, 2008. Hydropower and stope drilling systems – An energy saving perspective. Proceedings of the Narrow Vein and Reef Conference, South African Institute of Mining and Metallurgy, Johannesburg, October.
- Wilson RW, Bluhm SJ, Smit H and Funnel RC, 2003. Surface bulk air cooler concepts producing ultra-cold air and utilising ice thermal storage. Proceedings of the Mine Ventilation Society Annual Conference, “Managing the Basics”, Pretoria, February.



Appendices

All of the appendices are contained in separate files.



APPENDIX A:
CALCULATIONS FOR THE 'MODEL' MINE

See Separate Files



APPENDIX B:
INITIAL TEST METHODOLOGIES

See Separate Files



APPENDIX C:
VERIFICATION OF RESULTS OF THE QUOTED PAPERS

See Separate Files



APPENDIX D:
RESULTS OF TESTS FOR 14 SHAFT

See Separate Files



APPENDIX E:
RESULTS OF TESTS FOR 11 SHAFT

See Separate Files



APPENDIX F:
RESULTS OF TESTS FOR 11C SHAFT

See Separate Files



**APPENDIX G:
RESULTS OF TESTS FOR 1 SHAFT**

See Separate Files



**APPENDIX H:
RESULTS OF TESTS FOR 12N SHAFT**

See Separate Files
